Characterization of Draxin as a potential secreted Netrin-1 modulator in vertebrate neural development

Dissertation

der Mathematisch-Naturwissenschaftlichen Fakultät

der Eberhard Karls Universität Tübingen

zur Erlangung des Grades eines

Doktors der Naturwissenschaften

(Dr. rer. nat.)

vorgelegt von

Xuefan Gao

aus Beijing (P. R. China)

Tübingen
2015

To my parents

Abstract

Axon guidance cues are crucial signals for neurons to build complex networks during early developmental stages. Netrin is one of the main guidance cues that in most cases attracts neurons to their destinations. Distinct Netrins and Netrin receptors have been identified to carry out the guidance function. However, no direct Netrin modulator has been described yet. In this study, we used AVEXIS (Avidity based Extracellular Interaction Screen), a large-scale protein-protein interaction screen assay, to identify novel binding partners for Netrin proteins, and zebrafish as model organism to study the function of the newly identified interactions.

We found Draxin, a secreted axon guidance protein, to directly interact with Netrin. The novel interaction is conserved for the orthologous human proteins. Furthermore, Draxin is able to outcompete Netrin receptors for Netrin-1 binding in a biochemical competition assay. The binding of Netrin receptors to Netrin-1 is reduced or even abolished in the presence of Draxin, indicating an inhibitory function of Draxin by breaking the communication between Netrin and its receptors. By generating Netrin truncations, I narrowed down the interaction interface to the third EGF domain of Netrin-1, the domain described to be necessary for Netrin-Netrin receptor interactions. I further narrowed down the interaction interface to a highly conserved 22 amino acid fragment within Draxin. This Draxin 22 amino acid fragment is sufficient for binding to Netrin-1 and the protein sequence is conserved across vertebrate species including chick, mouse and human. Furthermore, the 22 amino acid peptide fused to the Fc protein (the constant region of an immunoglobulin molecule) is able to outcompete Netrin receptors for Netrin binding.

Expression analysis in zebrafish embryos shows that both *draxin* and *netrin* mRNAs are expressed in the neural tube. They are co-expressed in regions surrounding the forebrain commissures. In the spinal cord, *draxin* is mainly expressed dorsally whereas *netrin* is located ventrally. Since both Draxin and Netrin are secreted proteins and have been reported to act as long-range guidance cues, the expression patterns suggests that reciprocal gradients of active Draxin and Netrin proteins can form along the dorsal-ventral axis of the developing spinal cord to regulate the correct formation of spinal cord commissures. Two independent embryonic binding assays revealed that Draxin and Netrin are able to interact in zebrafish embryos.

Thus, we propose a model in which Draxin functions as a secreted Netrin signaling modulator influencing vertebrate axon pathfinding. Draxin might shape the functional extracellular Netrin gradient by sequestering Netrin proteins. Since human Netrin-1 serves as a survival factor for specific tumors, Draxin—or the Netrin binding fragment of Draxin—could be potentially used to activate cell death in human cancer cells.

Key words:

Draxin, Netrin, DCC, UNC5, AVEXIS, protein-protein interaction, axon guidance, neural development, neural wiring, commissures, zebrafish (*danio rerio*)

Zusammenfassung

Axonale Lenkungsmoleküle (engl.:Axon guidance cues) sind wichtige Signalstoffe, ohne die Nervenzellen während der frühen Embryonalentwicklung keine komplexen Netzwerke etablieren könnten. Netrin ist eines dieser wichtigen Signalproteine und lockt/zieht Axone allermeistens hin zu ihren Zielgebieten. Verschiedene Netrine und Netrin-Rezeptoren wurden in unterschiedlichen Geweben beschrieben. Komponenten, die direkt im extrazellulären Bereich auf Netrin wirken sind bisher unbekannt. In der vorliegenden Arbeit wurde ein sogenannter ‚Avidity based Extracellular interaction Screen' (AVEXIS: Protein-Protein-Interaktionsscreen) benutzt, um neue Partner für Netrin-Proteine zu identifizieren. Die neu gefundenen Interaktionspartner wurden im Zebrafisch auf ihre *in vivo* Funktionen hin untersucht.

Wir identifizierten Draxin, ein sezerniertes Protein, das an der Axonführung beteiligt ist, als direkten Bindungspartner von Netrin. Diese, bislang noch nicht beschriebene Interaktion, kann auch für die menschlichen Orthologe nachgewiesen werden. Im biochemischen Kompetitions-Assay hemmt Draxin die Bindung von Netrin-1 an den entsprechenden Rezeptor. Dabei wird die Bindung von Netrin-1 an den Rezeptor stark abgeschwächt oder gänzlich aufgehoben. Indem das Protein die Kommunikation zwischen Netrinen und den entsprechenden Rezeptoren hemmt kann Draxin eine inhibitorische Funktion zugeschrieben werden. Durch gezielte Verkürzungen des Proteins konnte ich zeigen, dass die Interaktion mit Draxin über die dritte EGF-Domäne von Netrin-1 stattfindet. Diese Domäne ist ebenfalls für die Interaktion mit dem Netrin-Rezeptor notwendig. Ich identifizierte außerdem ein hoch-konserviertes 22 Aminosäuren umfassendes Peptid in Draxin, das an der Interaktion mit Netrin beteiligt ist. Dieses Peptid ist ausreichend für eine Bindung an Netrin-1 und die Aminosäuresequenz ist hochkonserviert innerhalb der Wirbeltiere,

einschließlich Huhn, Maus und Mensch. Zudem kann dieses Peptid, als Fusion mit dem Fc Protein (der konstanten Region eines Antikörpermoleküls), die Bindung von Netrin an den Rezeptor hemmen.

Eine Expressionsanalyse in Zebrafischembryonen zeigt sowohl *netrin* als auch *draxin* mRNAs werden im Neuralrohr exprimiert. In den Arealen nahe der Vorderhirn-Kommissur sind beide Gene ko-exprimiert, wohingegen im Rückenmark *draxin* hauptsächlich dorsal lokalisiert, *netrin* hingegen ventral. Sowohl Netrin als auch Draxin werden sezerniert, und beide Proteine sind über längere Distanzen hinweg als Signalmoleküle aktiv. Somit legen die Expressionsmuster nahe, dass die aktiven Proteine möglicherweise reziproke Gradienten entlang der dorso-ventralen Achse des sich entwickelnden Rückenmarks bilden, anhand derer die richtige Bildung der Kommissuren reguliert wird. In zwei unabhängigen Tests wurde gezeigt, dass Draxin und Netrin in vivo in Zebrafisch-Embryonen miteinander interagieren können.

Wir schlagen ein Modell vor, bei dem Draxin als sezernierter Modulator die Funktion von Netrin bei der Steuerung der axonalen Zielfindung beeinflusst indem es extrazelluläres Netrin komplexiert, seine Bindung an den Rezeptor verhindert und so die Form des aktiven Netrin-Gradienten negativ verändert. Da Netrin-1 bei bestimmten menschlichen Tumoren als Überlebenssignal dient könnte Draxin– oder das identifizierte Fragment, das an Netrin bindet – eine Möglichkeit bieten Zelltod in menschlichen Tumorzellen auszulösen.

Contents

Contributions

CV

Acknowledgements

List of Figures

List of Tables

List of Abbreviations

aa: amino acid

alb: zebrafish *albino* mutant

AP-MS: Affinity Purification-Mass Spectrometry

AVEXIS: <u>AV</u>idity-based <u>EX</u>tracellular <u>I</u>nteraction <u>S</u>creen

BCIP: 5-bromo-4-chloro-3-indoyl-phosphate

BMP: bone morphogenetic proteins

bp: base pair

BSA: bovine serum albumin

c.elegans: Caenorhabditis elegans

CAM: cell adhesion molecule

cAMP: cyclic Adenosine monophosphate

Cdc42: cell division control protein 42 homolog

Co-IP: Co-Immunoprecipitation

COMP domain: Cartilage Oligomeric Matrix Protein

D.melanogaster: Drosophila melanogaster

DB: Dcc-binding domain

Dcc: Deleted in colorectal carcinoma (Netrin receptor)

DD: death domain

DIG: Digoxigenin

Dkk: Dickkopf

DNA: deoxyribonucleic acid

dpf: days post fertilization

DSCAM: Down Syndrome Cell Adhesion Molecule (Netrin receptor)

E. coli: Escherichia coli

ECD: ectodomain (extracellular domain of a protein)

EGF domain: epidermal growth factor-like domain

ELISA: Enzyme-Linked Immuno-sorbant Assays

ExPASy: Expert Protein Analysis System

FBS: fetal bovine serum

FCS: Fluorescence correlation spectroscopy

Fgf: Fibroblast growth factor

FISH: Fluorescence In Situ Hybridization

FN III domain: fibronectin type III domain

FRET: fluorescence resonance energy transfer

Fz: Frizzled (Wnt receptor)

GAG: glycosaminoglycan

GFP: green fluorencent protein

GPI: glycosylphosphatidylinositol

GRASP: GFP Reconstitution Across Synaptic Partners

GTP: guanosine triphosphate

GTPase: hydrolase enzymes that can bind and hydrolyze GTP

HBS: HEPES-buffered saline

HEK cells: Human Embryonic Kidney cell

hFc: fragment crystallizable region of human IgG protein

His-tag: Affinity purification tag Histidine

Hpf: hours post fertilization

HRP: horseradish peroxidase

IC$_{50}$: Inhibitor concentration at 50 % inhibition

Ig domain: immunoglobulin domain

ISH: *In situ* hybridization

KD: knockdown

KO: knockout animal

LRP6 receptor: LDL receptor – related protein 6

LRR: leucine-rich repeat domain

Matn4: Matrilin-4

memRFP: membrane RFP

MESAB: ethyl -m-aminobenzoate methanesulfonate

min: minute

MeOH: Methanol

MO: morpholino

Morphant: animal that injected with morpholinos

mRNA: messenger RNA

NBT: 4-nitro blue tetrazolium

Neo: Neogenin (Netrin receptor)

NGL: The ligand of Netrin-G proteins

NGS: normal goat serum

nm: nanometer

nM: nanomolar

Ntn: Netrin

P0: postnatal day 0

P1, P2 and P3: conserved regions in the cytoplasmic domain of DCC

PBS: phosphate buffer saline

PCR: polymerase chain reaction

PEI: polyethylenimine

PFA: paraformaldehyde

PKA: protein kinase A

pNPP: para-Nitrophenylphosphate

PTU: 1-phenyl 2-thiourea

RFP: red fluorencent protein

RGM: repulsive guidance molecule

RNA: Ribonucleic acid

Robo: Roundabout, receptor of axon guidance cues from the Slit family

RT: room temperature

s.d.: standard deviation

sfGFP: superfolder GFP

shh: *sonic hedgehog*

SMART: Simple Modular Architecture Research Tool

SP: signal peptide

SPR: surface plasmon resonance

SST: signal sequence trap

TSA: Tyramide Signal Amplification TSA

TSP: thrombospondin domain

Unc5s: Netrin receptor Uncoordinated locomotion-5

vs.: versus

WT: wild type

Y2H: Yeast two Hybrid

ZU5: zona occludens 5 domain

μM: micomolar

Neuroanatomy:

AC: anterior commissure

CC: corpus callosum

CNS: central nervous system

di: diencephalon

DVDT: dorsalventral diencephalic tract

FB: forebrain

HB: hindbrain

HC: hippocampal commissure

MB: mindbrain

MDB: mibrain-diencephalon boundary

MHB: midbrain-hindbrain boundary

NC: notochord

PC: posterior commissure

PNS: peripheral nervous system

POC: postoptic commissure

SC: spinal cord

SOT: supraoptic tract

tel: telencephalon

Chapter 1
Introduction

1.1 Molecular mechanisms of neural wiring

The nervous system is composed of billions of neurons in vertebrates. How this large number of cells build complicated networks during development still remains a key question in neurobiology. Ramón y Cajal, the pioneer Spanish neuroanatomist, first approached this question. He studied the commissural neurons in the developing chick spinal cord and discovered the axonal growth cone as "the distal tip of all growing nerve fibers" that navigates the path for nerve cells (1890). From his observation that the growth cone changed its shape according to the environment, he proposed the "neurotropic theory" (Sotelo, 2004):

> "*The target cells were able to secrete inducing or attracting substances, and that growth cones are provided with chemotactic sensitivity or chemically elicited ameboidism……*"   --Ramón y Cajal, 1892 (translated)

This neurotropic theory was under debate for several decades until Sperry elaborated it as "chemoaffinity theory" in 1963 (Sperry, 1963). According to the observation of axon pathfinding in the frog retina, Sperry hypothesized a chemical tag on each single neuron in the retina that "preferentially selects" its pathway to the target region.

The chemoaffinity theory has not been generally accepted until the 1980s, after Bonhoeffer and Huf developed a new explant tissue culture method (Bonhoeffer and Huf, 1980, 1982). With this method, the primary neurons can be cultured *in vitro* under finely controlled conditions, this allowed to obtain direct experimental evidence for the chemoaffinity theory. Using this method, Lumsden and Davies co-cultured embryonic mouse sensory neurons with their targets and other tissues in collagen gels, and found an unknown factor involved in attracting neurons directly to their innate targets (Lumsden & Davies, 1983). A few years later, Marc Tessier-Lavigne and his coworkers improved the explant method and found the spinal cord floor plate to secret diffusible factor(s) that attract the spinal cord commissural axons (Tessier-Lavigne et al., 1988). After several years of hard work, his group purified Netrin-1, the first attractive substance, by combining the explant method with biochemical purification from floor plate tissue (Serafini et al., 1994). This approach helped to identify the diffusible guidance cue that Ramón y Cajal predicted one-hundred years earlier.

Thanks to the fast-developing era of modern molecular biology and genetics, scientists greatly expanded the molecular vocabulary of neural wiring. Four groups of

evolutionary highly conserved axon guidance cues and their receptors have been found in the 1990s (Guan & Rao, 2003; Kolodkin & Tessier-Laigne, 2011): Netrin-DCC/Unc5b (Hedgecock et al., 1990; Kennedy et al., 1994; Serafini et al., 1994; Keino-Masu et al., 1996), Slit-Robo (Rothberg et al., 1988; Brose et al., 1999; Kidd et al., 1999; Li et al., 1999; Wang et al., 1999; Kidd et al., 1998), Ephrins-Eph receptors (Holzman et al., 1990; Cheng & Flanagan, 1994) and Semaphorins-Plexins/ Neuropilin (Kolodkin et al., 1992; Luo et al., 1993; Takahashi et al., 1999; Tamagnone et al., 1999; Pasterkamp & Kolodkin, 2003). Besides these diffusible cues, cell adhesion molecules (CAMs) also play an irreplaceable role in the guidance process. Altogether, axon guidance cues direct a variety of different groups of neurons to their respective targets and work in combination with each other to ensure proper development of the nervous system.

A basic understanding of the molecular wiring code and how it is acting *in vivo* was summarized by Marc Tessier-Lavigne and Corey Goodman (Tessier-lavigne et al., 1996). Basically, the known molecules can be categorized according to four types of mechanisms based on their mode of action: chemoattraction, chemorepulsion, contact attraction and contact repulsion (Fig. 1.1)
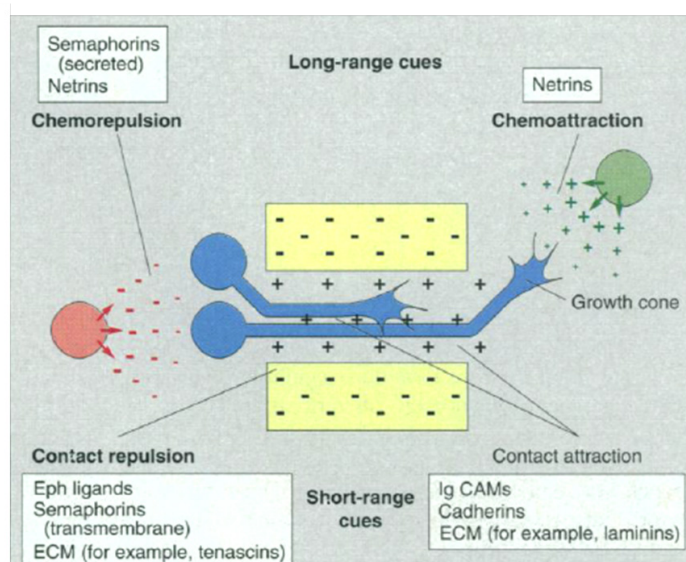
Figure 1.1   Molecular mechanism of axon guidance

Cartoon shows four types of axon guidance mechanisms: chemoattraction, chemorepulsion, contact attraction and contact repulsion. The main groups of guidance cues are shown according to the four working mechanisms. (From Tessier-lavigne et al., 1996)

1.2 Building brain and spinal cord commissures during vertebrate neural development

Forebrain commissures

The forebrain commissures connect the two cerebral hemispheres in vertebrate brains. The forebrain commissural neurons project their axons far away from their soma following axon guidance cues; they develop in a highly stereotyped sequence. They are ideal models for studying axon guidance *in vivo*. The architecture of major forebrain commissures is highly conserved between vertebrates. Figure 1.2 A shows mouse and zebrafish forebrain commissures at stages when the first axonal bundles are settled. Mouse and fish display similar commissures such as anterior and posterior commissures as well as the postoptic commissure.

Spinal cord commissures

A classical model for studying axon guidance is the midline crossing behavior of the spinal cord commissural neurons. Commissural neurons extend axon across the midline, forming sensory and motor connections between the left and right side of the body (Dickson and Zou, 2010). These commissural neurons are born in the dorsal spinal cord. They first extend axons towards the ventral midline—the floor plate. Once reaching the floor plate, they cross the midline, and then join to form posterior projecting longitude tracts. Figure 1.2 B shows the pathfinding of commissure neurons in transverse sections of the spinal cord. Figure 1.2 B (a) is the original drawings of Ramón y Cajal showing the Golgi staining of neurons in E4 stage chick spinal cord. Ramón y Cajal described the diverse shapes of the commissural axon growth cones and correctly predicted the position of the floor plate. Figure 1.2 B (b) shows commissure axons visualized by the TAG-1 antibody in E11.5 mouse (Dickson and Zou, 2010).

The spinal cord midline is composed of ependymal cells including gliacytes. Multiple guidance cues derived from both dorsal and ventral midline cells direct the trajection of pathfinding commissural axons (Fig. 1.2 B (c)). Netrin-1 and Shh expressed by floor plate cells attract the precrossing commissural axons whereas Draxin and BMPs derived from roof plate cells repel these axons (Placzek & Briscoe, 2005; Dickson & Zou, 2010).
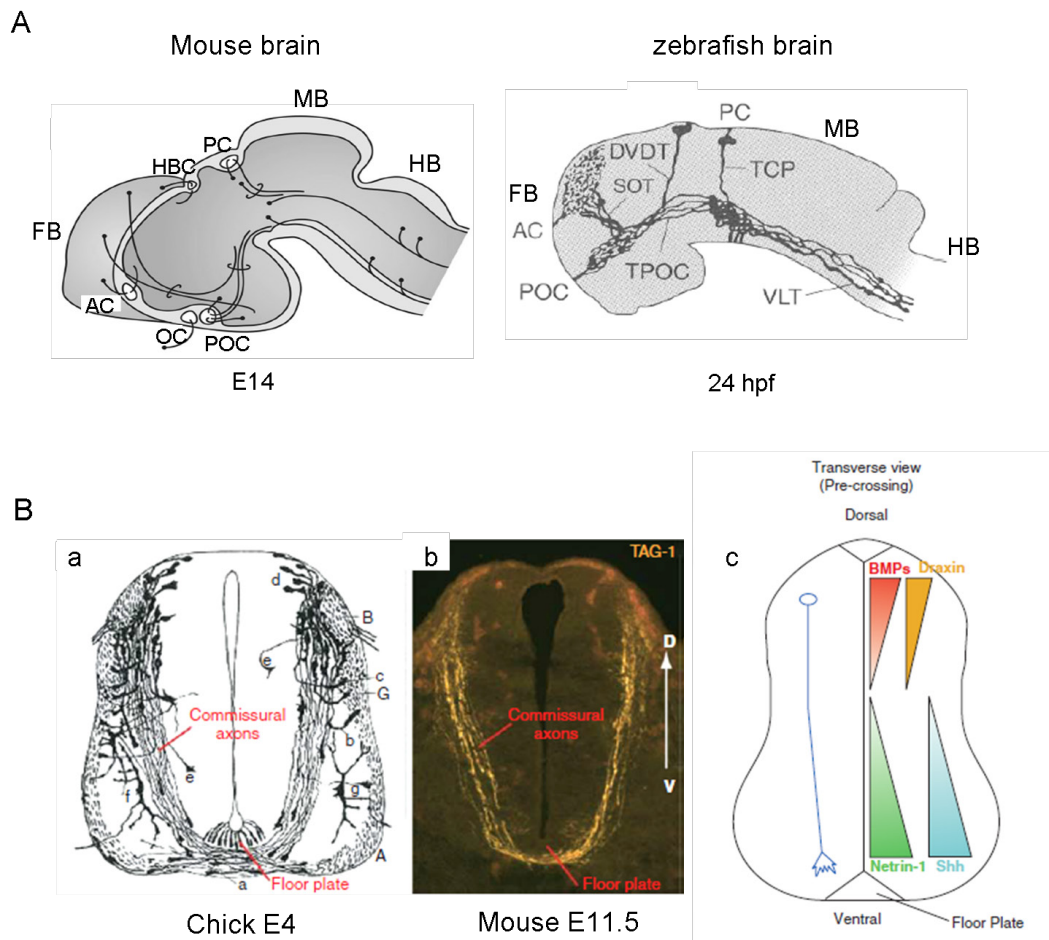
Figure 1.2   Models for commissural axon midline crossing

(A) Forebrain commissures in E14 mouse and 24 hpf zebrafish embryos. The embryonic stages corresponding to the time point when first axonal bundles are settled. Mouse and zebrafish share highly conserved forebrain commissures. The picture shows the lateral view with anterior left. FB: forebrain, MB: midbrain, HB: hindbrain; AC: anterior commissure, PC: posterior commissure, OC: optic chiasm, POC: postoptic commissure, HBC: habenular commissure, TPOC: tract of postoptic commissure, SOT: supraoptic tract, DVDT: dorsoventral diencephalic tract, TPC: tract of posterior commissure, VLT: ventral longitudinal tract. (adapted from Suárez et al., 2014; Raper & Mason, 2010, fish figure originally from Ross et al, 1992) (B) Pathfinding of the spinal cord commissural axons in chick and mouse (transverse section). a) Drawing by Ramón y Cajal shows the Golgi staining of E4 chick spinal cord. b) Spinal cord commissural axons are labeled by the TAG-1 antibody in E11.5 mouse. c) Multiple guidance cues control the pathfinding of spinal cord commissural axons. (Adapted from Dickson & Zou, 2010)

1.3 Netrin signaling in embryonic nervous system

1.3.1 Members of Netrin and Netrin receptor families

Netrin family members

Netrins are present in both invertebrates and vertebrates. They are highly conserved molecules across a variety of species and can be found even in leeches and the sea anemone *Nematostella vectensis* (Fig. 1.3 A). The vertebrate Netrin family includes secreted Netrins (Netrin 1, 2, 3, 4, and 5) and GPI-anchored membrane proteins (Netrin-Gs) (Moore et al., 2007).

All Netrins are composed of roughly 600 amino acids and are related to the Laminin proteins, extracellular matrix components which form heterotrimers consisting of α, β and γ subunits (Miner and Yurchenco, 2004). Netrins have three distinct protein domains: domain VI (so called N-terminal domain), domain V (contains three EGF domains) and domain C (C-terminal domain). The Netrin N-terminal domain plus three EGF domains are homologous to the N-terminus of Laminin protein. Based on sequence similarity, the Netrin family is divided into three groups: The Netrin-1, 2, 3, 5 group, the Netrin-4 group and the Netrin-G group. Netrin-1, 2, 3, 5 are evolutionarily closer to the γ-chain of Laminin whereas Netrin-4 is related to the laminin β-chain. Netrin-Gs are GPI anchored Netrins, they are more distantly related to the secreted Netrins (Fig. 1.4 A, Koch et al., 2000; Leclère & Rentzsch, 2012). The expression patterns as well as the receptors are quite distinct for each Netrin group. Figure 1.3 B lists the members of all three groups of Netrins in several vertebrate species.

Netrin receptor members

In vertebrates, receptors for Netrin-1, 2, 3, 5 are Deleted in colorectal carcinoma (DCC), Neogenin (Neo, a DCC paralogue), Uncoordinated locomotion-5 (Unc5s) and Down Syndrome Cell Adhesion Molecule (DSCAM). All these Netrin-receptors are type-I receptors (single-pass transmembrane proteins), which belong to the immunoglobulin superfamily. NGLs are the ligands for the membrane associated Netrin-G group (Fig. 1.3 B and Fig. 1.4 B) (Sun et al., 2011).

Other Netrin binding partners

Besides the classical Netrin receptors summarized above, there are two additional groups of binding partners for Netrin-1: Integrins and Heparins. Integrins are transmembrane receptors that act as mediators bridging cell-cell and cell-environment interactions. Integrin α6β4 and α3β1 were reported to bind to Netrin-1. These interactions were suggested to regulate epithelial cell migration and adhesion (Yebra et al., 2003). Heparin, a sulfated glycosaminoglycan, is another extracellular matrix component. Heparin binds to Netrin-1 with high affinity (Kappler et al., 2000). It was used to purify Netrin from membrane associate components in the initial discovery of Netrin (Serafini et al., 1994). Both Intergrins and Heparins bind to the C-terminal domain of Netrin, and are involved in regulating the association of Netrin with extracellular matrix components.

A Evolutionary tree of Netrins

Rat, mouse & human:
Netrin-1
Netrin-3 (NTN2L)
Netrin-4 (β-netrin)
Netrin-G1 (Laminet-1)
Netrin-G2 (Laminet-2)

Fruit fly:
Netrin-A
Netrin-B

Zebrafish:
Netrin-1a
Netrin-1b
Netrin-2
Netrin-4
Netrin-G1
Netrin-G2

Purple sea urchin:
Netrin-1a
Netrin-1b

C. elegans:
UNC-6

S. mediterranea:
Smed-netrin1
Smed-netrin2

Leech:
Netrin

N. vectensis:
NvNetrin

Mammals
Vertebrates
Echinoderms
Deuterostomes
Arthropods
Nematodes
Flatworms
Annelids
Protostomes
Cnidarians
Comb jellies
Bilateral symmetry
Radial symmetry
Sponges
Colonial protists

B Members of Netrins and their receptors in vertebrates

Species	Netrin	Netrin receptor
Human	Netrin-1	Neogenin
	Netrin-3	DCC
	Netrin-4	UNC5A
	Netrin-5	UNC5B
	Netrin-G1	UNC5C
	Netrin-G2	UNC5D
Mouse	Netrin-1	Neogenin
	Netrin-3	DCC
	Netrin-4	UNC5A
	Netrin-5	UNC5B
	Netrin-G1	UNC5C
	Netrin-G2	UNC5D
Chicken	Netrin-1	Neogenin
	Netrin-2 (-3)	UNC5B
		UNC5C
Zebrafish	Netrin1a	Neogenin
	Netrin1b	Dcc
	Netrin-2 (-3)	Unc5b
	Netrin-4	
	Netrin-G1	
	Netrin-G2	

Figure 1.3   Netrins and Netrin receptors in various organisms

(A) An evolutionary tree of Netrin homolgs in variety of animals with bilateral symmetry. (B) Members of Netrin and their receptors in human, mouse, chick and zebrafish. The list for Netrin receptors includes receptors only for Netrin-1, 2, 3, and 5, but not for Netrin-4 and Netrin-G families. (A from Moore et al., 2007; B summarizes published data from Sun et al., 2011; Leclère & Rentzsch, 2012)
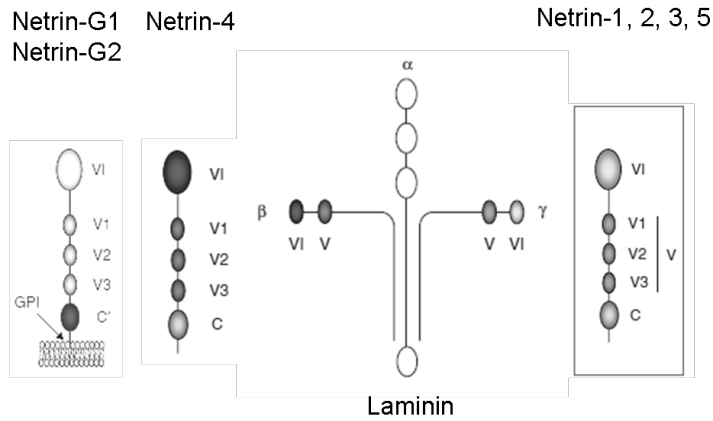
Figure 1.4   Molecular domain structure of Netrins and Netrin receptors

(A) Netrins are members of the Laminin superfamily. The N-terminal domains (domain VI) and the EGF domains (domain V 1-3) are homologous to the N-terminal part of Laminin protein. Netrin-1, 2, 3, 5 (in the square frame) are evolutionary related to the γ-chain of laminin whereas Netrin-4 is more closely related to the laminin β-chain. Netrin-Gs are only distantly related to the rest of the Netrins. (B) Netrin receptors of Netrin-1 and Netrin-G including DCC, Neogenin, Unc5s, DSCAM and NGL. GPI: Glycosylphosphatidylinositol; Ig: immunoglobulin domain; FNIII: fibronectin type III domain; P1, P2 and P3: conserved regions in the cytoplasmic domain of DCC; TSP: thrombospondin domain; ZU5: zona occludens 5 (ZU-5) domain; DB: DCC-binding domain; DD: death domain; LRR: leucine-rich repeat domain. (adapted from Bernet & Fitamant, 2008; Sun et al., 2011)

1.3.2 Netrin signaling mechanisms

Ligand-receptor binding sites

The receptor binding domains in Netrin-1 are within the N-terminal regions: domain VI plus V (N-terminal domain plus the three EGF domains) (Serafini et al., 1994). Two recent structural studies showed that the third EGF domain (V3) in Netrin-1 binds to the Netrin receptor DCC. The N-terminal domain (VI) and the first EGF domain (V1) might also contribute to the binding (Finci et al., 2014; Xu et al., 2014). Although the two studies have a different opinion on the second binding site in Netrin-1, they both propose that DCC forms a homodimer upon binding to Netrin-1. The second EGF domain (V2) in Netrin-1 has been suggested to be involved in Netrin-Netrin homodimer formation in the 2:2 ligand-receptor complex (Xu et al., 2014).

Netrin-1 binds to the extracellular domains of Netrin recepotrs. The Netrin binding sites were mapped to FN III 4-5 domains in DCC and Ig 1-2 domains in Unc5 (see Fig. 1.4 B for Netrin receptor domain organization, Kruger et al., 2004). The fifth FN III domain in DCC was confirmed to be involved in the formation of Netrin-Netrin receptor crystal complex in the recent structural studies (Finci et al., 2014; Xu et al., 2014). There are indications for a second Netrin binding site in the DCC FN III domains, however, further studies are required to determine which FN III domain(s) contribute to the second binding site.

Attraction vs. repulsion: different roles of Netrin receptors DCC and Unc5

Netrin-1 has conserved axon guidance functions in both invertebrate and vertebrate species. The main function is chemoattraction through its receptor DCC (Keino-Masu et al., 1996; Kolodziej et al., 1996). Netrin also functions as a chemorepulsive cue through another receptor—Unc5 (Hong et al., 1999).

It is possible to distinguish between long- and short-range repulsion, which result from different Netrin receptor combinations. Unc5 alone mediates short-range repulsion, whereas long-range repulsion needs DCC as a co-receptor for Unc5. The intracellular DCC binding domain ("DB") of Unc5 is required for signal transduction in long-range repulsion through DCC (Hong et al., 1999; Keleman and Dickson, 2001).

Netrin intracellular signaling

The Netrin signaling cascade from extracellular ligand-receptor binding to the response of pathfinding neurons goes through several steps. The signal transduction starts when Netrin activates its receptors on the growth cone membrane. Growth cones are the leading tips of growing neurons, they are highly dynamic, actin- and microtubule- supported extensions of developing neurites. The activated Netrin receptor triggers the regulation of small GTPases inside the cell. Cdc42, Rac and Rho are the three main GTPases that directly regulate the dynamics of actin and microtubules. The Netrin receptor DCC can activate Cdc42 and Rac as well as indirectly Rho, thus inducing actin reorganization (Huber et al., 2003). In summary, during axon outgrowth, Netrin signaling converges on GTPases that reorganize the cytoskeleton and therefore controls the directions of growing growth cones.

Regulation of Netrin signaling

The Netrin receptors are the crucial factors for Netrin signaling regulation. Netrin signaling can be silenced by activation of Robo, a Slit receptor. The cytoplasmic domain of Robo directly binds to the Netrin receptor DCC causing silencing of the attraction but not affecting the growth-stimulation by Netrin-1. The silencing of Netrin-mediated attraction prevents spinal cord commissural axons from re-crossing the midline (Stein and Tessier-Lavigne, 2001). In addition, there is evidence showing that DCC can be regulated at translational and post-translational levels. Protein kinase A (PKA) activation promotes membrane insertion of DCC enhancing the attraction through Netrin-1 (Bouchard et al., 2004). Local DCC synthesis within the growth cone was also suggested to enhance the response to Netrin-1 (Huber et al., 2003).

Netrin signaling can also be regulated on downstream converging steps such as intracellular small GTPases. cAMP concentration and PKA activation negatively regulate Rho, a small GTPase, thus regulating the sensitivity of chemoattraction to Netrin-1 (Huber et al., 2003; Moore and Kennedy, 2006). Factors that directly regulate cytoskeletal organization can also influence the output of Netrin signaling.

So far, no Netrin modulator acting directly on the ligand has been found.

1.3.3 Netrin expression patterns and function

Netrin-1 expression in vertebrates

netrin-1 mRNA is highly expressed in the floor plate region during the developmental stages when commissural axons navigate in mouse, chick and zebrafish embryos (Fig. 1.5). Mouse *netrin-1* is not only highly expressed in the floor plate cells, in addition, the expression spans roughly two thirds into the spinal cord. It is also highly expressed in the somites of E9.5 embryos (Fig. 1.5 A and E, (Filosa et al., 1997; Serafini et al., 1996). Chick *netrin-1* is expressed at high levels in the floor plate of the hindbrain, midbrain, caudal diencephalon and the spinal cord. At early stages (st.15), the expression domains are slightly broader. At this stage, chick *netrin-1* was also detected in the developing optic cup and stalk as well as in somites outside the CNS. Chick *netrin-2* is not expressed by the floor plate; instead, it is expressed throughout two thirds of the ventral spinal cord however with lower levels compared to *netrin-1* (Fig. 1.5 B, G, I; Kennedy et al., 1994; Kennedy et al., 2006). Similarly, zebrafish *netrin1a* and *netrin1b* are expressed in large areas of the ventral CNS with dynamic patterns. At 24 hpf, *netrin1a* is expressed in the ventral midbrain, the midline of the hindbrain and the ventral half of the spinal cord (Fig. 1.5 K, L, M; Lauderdale et al., 1997). The expression of *netrin1b* in the spinal cord is slightly different from *netrin1a*. It is only expressed in the floor plate region (arrowheads in Fig. 1.5 N; Strähle et al., 1997).

The Netrin protein is secreted and highly diffusible. In E9.5 mouse and stage 17 chick embryos, Netrin-1 proteins were detected far away from their sources forming a gradient towards the dorsal spinal cord (Fig. 1.5 F and H; Kennedy et al., 2006).

Netrin-1 knockout mice phenotypes

netrin-1 knockout mice have severe defects in forebrain commissures and spinal cord commissures. The *netrin-1* mutants lack the corpus callosum (CC), the hippocampal commissure (HC) and the anterior commissure (AC). Only very few commissural axons cross the floor plate in the spinal cord (Fig. 1.6) and the ventral commissure is much thinner than in wild types (Serafini et al., 1996).

Netrin functions besides axon guidance

In the last ten years, Netrins were shown to be involved in diverse processes outside neuronal tissues. It has been reported that Netrins elicit the migration and support the survival of neurons in the CNS (Bloch-Gallego et al.,1999). This function is maintained in other tissues such as the olfactory bulb and intestinal tract. Besides, Netrins are also regulating cell adhesion and branching morphogenesis in terminal end buds of the mammary glands, during lung development and in angiogenesis (Yebra et al., 2007; Sun et al., 2011). Netrins and their receptors also participated in tumor formation (Mehlen et al., 2011).
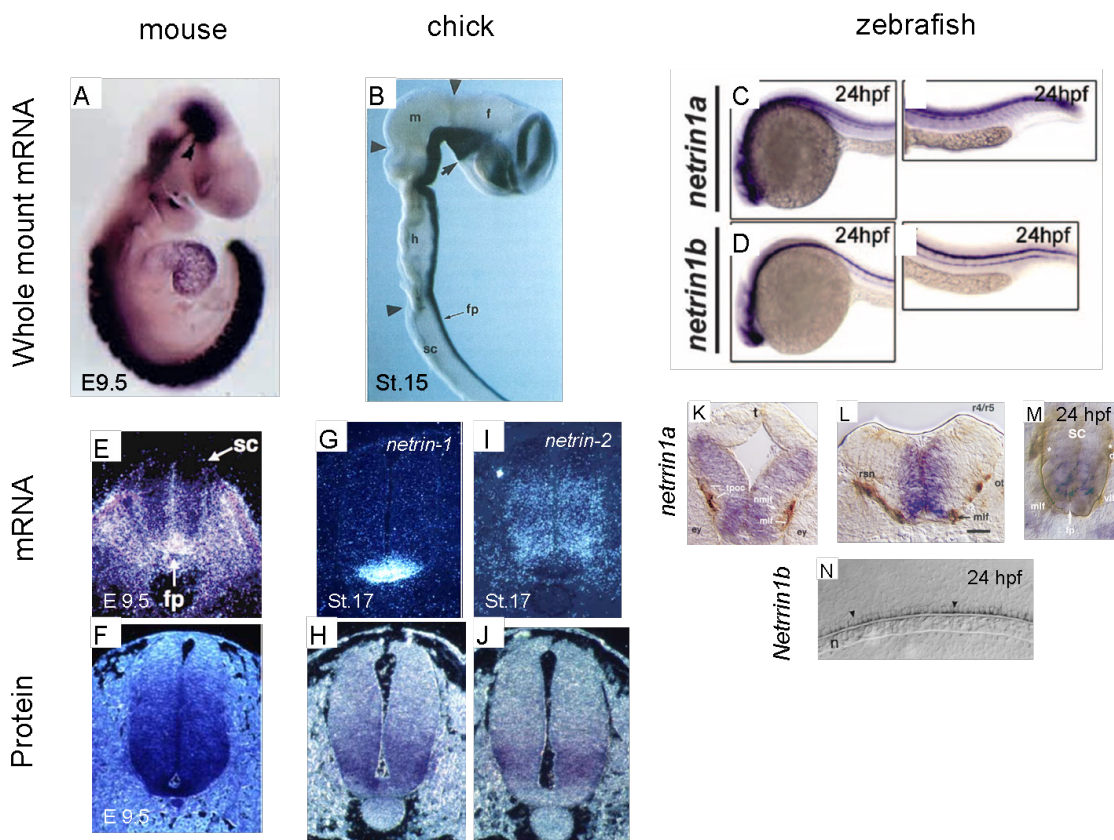
Figure 1.5   Netrin expression patterns in mouse, chick and zebrafish embryos
Expression of Nerin transcripts and distribution of Netrin proteins in mouse (A, E, F), chick (B, G-J, with B, G, H Netirn-1 and I, J Netrin-2) and zebrafish (C, D, K-N) at indicated stages. Whole mount embryos: A-D; spinal cord transverse sections: E-J, M; midbrain (K) and hindbrain (L) transverse sections; spinal cord lateral view: N. f: forebrain; m: midbrain; h:hindbrain; fp: floor plate; sc: spinal cord. t: tectum. (rearranged: Filosa et al., 1997 (A), Kennedy et al., 1994 (B), Park et al., 2008 (C,D), Serafini et al., 1996 (E), Kennedy et al., 2006(F, G-J), Lauderdale et al., 1997 (K, L, M), Strähle et al., 1997 (N))

	Forebrain commissures	Spinal cord commissures
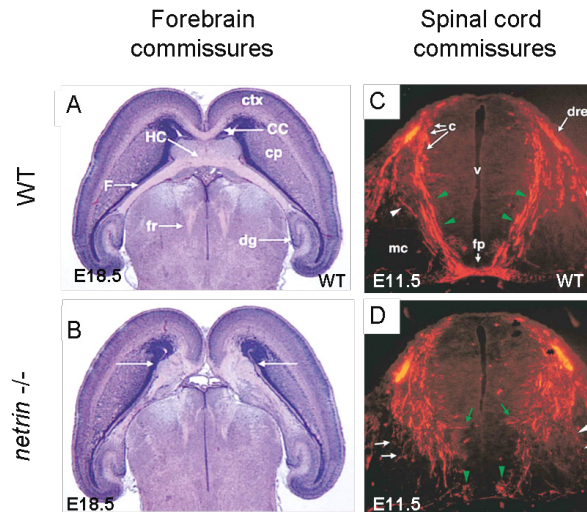
Figure 1.6 Phenotypes of *netrin* knockout mice in the central nervous system

Defects of *netrin-1* KO mouse compared to wt siblings in forebrain commissures (A, B, coronal sections) and spinal cord commissures (C, D, transverse sections, commissural axons are visualized with the TAG-1 antibody). Compared to wild type animals, *netrin-1* mutant mice lack forebrain commissures CC and HC. Their spinal cord commissural axons are disorganized and only few axons reach the floor plate. The majority of commissural axons can not cross the floor plate. Arrows show the defects in the mutants (B, D). CC: corpus callosum, HC: hippocampal commissure; ctx: cerebral cortex; cp: caudo-putamen; dg: dentate gyrus; fr: fasciculus retroflexus; c: commissural neurons and their axons; d: dorsal root ganglion; drez: dorsal root entry zone; fp: floor plate; mc: motor column; v: ventricle. (rearranged: Serafini et al., 1996)

1.4 Draxin in embryonic neural development

1.4.1 Draxin protein family

Draxin (<u>D</u>orsal <u>r</u>epulsive <u>ax</u>on guidance prote<u>in</u>) has been identified in a screen searching for novel axon guidance proteins (Islam et al., 2009). In this screen, the signal sequence trap (SST) method was used to identify secreted and membrane-anchored proteins (Shirozu et al., 1996). Draxin was found in a chick embryonic cDNA library enriched for floor plate, roof plate and motor neuron transcripts. Draxin was reported to inhibit or repel neurite outgrowth (Islam et al., 2009). Thus, Draxin was defined as a novel chemorepulsive axon guidance cue.

The *draxin* gene can be found in vertebrate genomes such as chick, mouse and human, but not in invertebrates. Mouse and human Draxin proteins are highly similar, they share 76 % sequence identity (Miyake et al., 2009). Draxin has a signal peptide at the N-terminus, but no membrane association sequence, confirming that it is a secreted protein (Islam et al., 2009). A cysteine-rich domain is present in the C-terminal region of Draxin, and the spacing of the 10 cysteine residues in this domain is similar to the position of cysteines found in Dickkopf (Dkk) family members (Miyake et al., 2009), suggesting a potential similar function between Draxin and Dickkopf family proteins.

2.4.2 Draxin expression patterns

Previous studies revealed that Draxin is highly expressed in developing mouse, chick and zebrafish embryos (Fig.1.7, Islam et al., 2009; Miyake et al., 2012). In mouse, during early embryonic stages, *draxin* mRNA was observed in the dorsal part of the brain and in regions surrounding the forebrain commissures as well as in the dorsal spinal cord (Fig.1.7 A and E). The expression was also detected at postnatal day 0 (P0) in the olfactory bulb, the cortex, midbrain, cerebellum and pontine nuclei (Islam et al., 2009). In chick, *draxin* mRNA was detected in a similar spatiotemporal distribution. *draxin* is strongly expressed in dorsal regions of the CNS, including the roof plate, as well as the dorsal lip of the dermomyotome (Fig.1.7 B and G) (Islam et al., 2009). In zebrafish, *draxin* is expressed in the telencephalon, diencephalon, dorsal tectum and in lateral regions of the hindbrain in 24 hpf embryos. The CNS expression is maintained until 36 hpf (Fig.1.7 C, D, I and J). Strong spinal cord expression is

observed during segmentation stages (arrows in Fig.1.7 C, D and K) and maintained until at least 36 hpf. The *draxin* expression pattern in zebrafish is consistent with that of *draxin* in mouse (Miyake et al., 2012).

Long range diffusibility of Draxin protein was detected in the mouse and chick spinal cord. In mouse E10.5 embryos, Draxin protein was detected along the basement membrane of the spinal cord. A similar discribution was detected within chick stage 19 embryos. Compared to the region of mRNA expression, Draxin protein diffused far away from its source (Fig. 1.7 F and H; Islam et al., 2009).

1.4.3 Proposed functions of Draxin

Draxin is a repulsive axon guidance cue. *In vitro* experiments showed that Draxin repelled neurites from spinal cord commissural neurons. Along the same direction, *draxin* knockout (KO) mice showed absence of forebrain commissures, including the commissures AC, CC and HC. Abnormal fasciculation of spinal cord commissural axons was also observed in the KO animals (Fig. 1.8, Islam et al., 2009). Thus, this data highlights the function of Draxin in commissure formation. Since Draxin and DCC (a classic Netrin receptor) KO mice share similar phenotypes in commissural axon pathfinding, Draxin was proposed to directly associate with Netrin signaling. Subsequently, Ahmed and his colleagues reported that Draxin directly binds to a structurally diverse set of Netrin receptors (DCC/Neo1, Unc5 and Dscam) (Ahmed et al., 2011). This is further support for a direct involvement of Draxin in Netrin signaling.

Besides the function in axon guidance, Draxin was proposed to have an inhibitory function on Wnt signaling (Miyake et al., 2009). Draxin was shown to bind to the LRP6 receptor (LDL receptor – related protein 6) with its cysteine-rich domain in a pull down assay. The LRP6 receptor is a co-receptor of the Wnt receptor Frizzled (Fz). In an *in vitro* assay, the induction of intracellular signaling by Wnt (beta-catenin) was reduced through the LRP6-Draxin interaction. This indicates Draxin might be a Wnt antagonist by preventing the formation of the LRP6-Fz receptor complex with its cysteine-rich domain, similar as reported for Dkk family proteins.
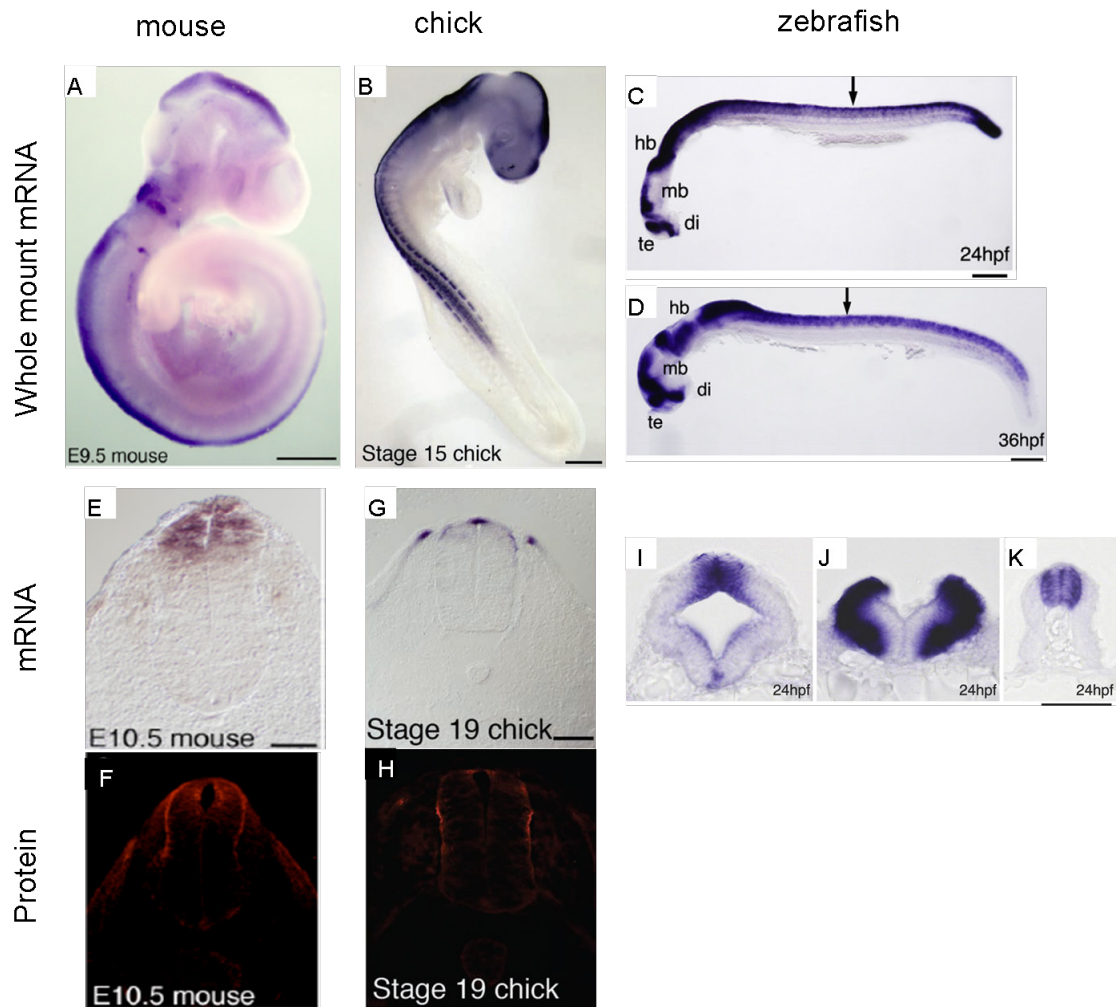
Figure 1.7   Draxin expression patterns in mouse, chick and zebrafish embryos

Expression of Draxin transcripts and distribution of Draxin proteins in mouse (A, E, F), chick (B, G, H) and zebrafish (C, D, I, J, K) at indicated stages. Whole mount embryos: A, B, C and D; Spinal cord transverse sections: E, F, G, H and K; midbrain (I) and hindbrain (J) transverse sections. mb: midbrain, hb: hindbrain, te: telencephalon (in cerebrum), di: diencephalon (interbrain). The arrows in (C) and (D) indicate the spinal cord. Scale bar: 500 µm in (A), 1000 µm in (B), 100 µm in (C) and (D), 100 µm in (E) and (G), 50 µm in (K). (rearranged: Islam et al., 2009; Miyake et al., 2012)

Forebrain commissures — Spinal cord commissures
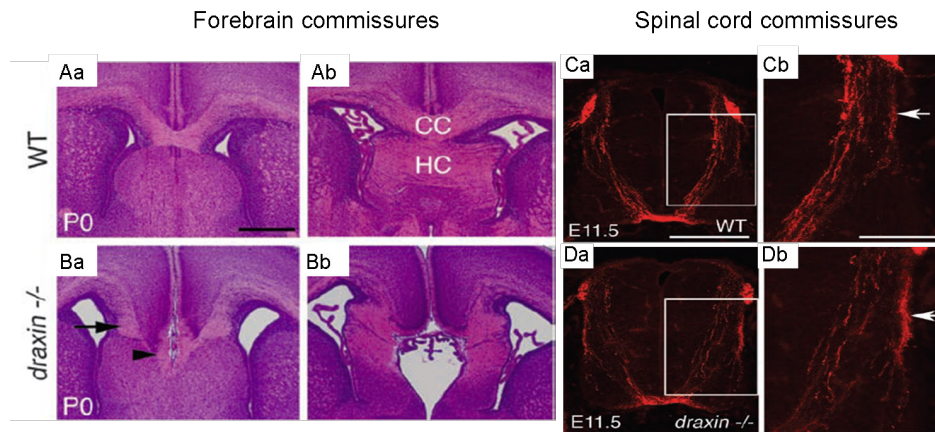
Figure 1.8   Phenotypes of *draxin* knockout mice in the central nervous system

Abnormal projections of forebrain commissures (Aa to Bb, coronal sections) and if spinal cord commissural axons (Ca to Db, transverse sections) in Draxin knockout mice. Arrows and arrowhead in (Ba) indicate tangled and misprojecting CC axons. Arrows in (Cb) and (Db) indicate Tag-1 labeled axon bundles of the spinal cord commissures. CC: corpus callosum, HC: hippocampal commissure. Scale bar: 500 µm in (Aa), 200µm in (Ca) and 100 in (Cb). (rearranged: Islam et al., 2009)

18

1.5 Using AVEXIS as method to discover novel protein-protein interactions in neural wiring

Searching for novel extracellular interactions

So far, the majority of known axon guidance cues have been discovered either by elaborate biochemical purification, or by genetic screens using *Caenorhabditis elegans* (*C.elegans*) or *Drosophila melanogaster (D.melanogaster)*. Surprisingly, a large number of protein-coding genes in the genomes are predicted to encode cell surface receptors or secreted proteins (Diehn et al., 2006; Liu & Rost, 2001). However, the interactions and the functions of these proteins in the developing nervous system are strongly underrepresented (Özkan et al., 2013; Söllner & Wright, 2009).This makes it likely that additional protein-protein interactions from these proteins remain to be uncovered. The starting point of our research was to perform a biochemical protein-protein interaction screen to identify novel extracellular interactions.

1.5.1 Advantages of AVEXIS

The <u>AV</u>idity-based <u>EX</u>tracellular <u>I</u>nteraction <u>S</u>creen (AVEXIS) is a biochemical screening assay recently developed to detect extracellular protein-protein interactions on a large scale (Bushell et al., 2008; Kerr & Wright, 2012). It has several advantages for studying interactions involved in neural wiring.

First, AVEXIS targets extracellular proteins, such as cell surface proteins and secreted proteins, which are centrally involved in neuron-neuron and neuron-environment communications. These proteins are biochemically difficult to work with since many of them contain hydrophobic transmembrane regions which make the proteins insoluble. Often they also contain structurally important posttranslational modifications such as glycosylation and disulfide bonds, which are not properly created in prokaryotic expression systems. By expressing the whole ectodomain of these proteins as soluble recombinant protein in mammalian cells, the AVEXIS assay overcomes the biochemical intractability of extracellular proteins.

Second, AVEXIS can be used for large-scale high throughput screening. This is due to the fact that cell culture supernatants can be used directly, avoiding extensive purification. Furthermore, proteins are normalized to detect interactions with a low false-positive rate. Therefore, large numbers of different protein fragments can be screened and interactions between uncharacterized proteins, as well as unknown interactions among known proteins can be reliably detected.

Third, AVEXIS can be applied to screen for protein-protein interactions in different species of metazoans. This advantage enables to test orthologous interactions thus allowing to compare such interactions among different species.

Finally, AVEXIS can detect low affinity interactions. Among extracellular proteins required for neural wiring, weak interactions between cell surface proteins, such as interactions between cell adhesion molecules, are common. In AVEXIS, prey proteins are pentamerized leading to an increase in the local concentration of the protein of interest, thus, increasing the avidity of the interaction. This enables the detection of very transient interactions with half-lives of less than 0.1 seconds.

Therefore, since AVEXIS is able to detect transient extracellular interactions on a large scale without system-specific limitations, it is suitable for studying interactions involved in neural wiring.

1.5.2 How AVEXIS works

Basically, AVEXIS is an ELISA-style binding assay (Fig. 1.9 A). Normalized bait proteins are captured on streptavidin-coated microtiter plates. After washes with buffer, normalized recombinant prey proteins containing an enzyme activity are incubated with bait proteins on the plates. An enzyme substrate is added after brief washes. Positive interactions are detected by the enzyme activity of the captured prey measured by a color change from yellow to red (Absorbance at 486 nm).

Libraries of proteins of interest are prepared by recombinant expression of the entire extracellular domains (ectodomains) of these proteins. (Fig. 1.9 B). The insoluble transmembrane regions are removed while the extracellular binding function is retained; therefore, single-pass transmembrane proteins, such as type I and type II proteins as well as GPI-linked cell surface receptors and secreted proteins, are suitable for constructing the library. The recombinant proteins are produced in mammalian

expression systems (HEK293E cells), taking advantage of the glycosylation machinery in these cells and the oxidizing environment of the secretory pathway to ease the production of functional extracellular proteins.

The ectodomains of the proteins of interest are designed in two different forms: monomeric captured "bait" and pentameric detected "prey" (Fig. 1.9 B). The bait proteins contain C-terminal in-frame fusions of rat CD4 domains 3 and 4, followed by a 17 amino acid peptide with a single biotinylation site (Schatz, 1993; Brown et al., 1998). The CD4 tag allows determining the protein concentrations of the recombinant proteins independently of the ectodomains by standard ELISA techniques. The biotinylation peptide can be modified by the *Escherichia coli* (*E. coli*) biotin ligase BirA. The biotinylated tail allows capturing of the proteins on streptavidin-coated microtitre plates with the ectodomain facing outward. The prey proteins also contain an in-frame fusion of rat CD4 domains 3 and 4, followed by the pentamerization domain derived from the rat cartilaginous oligomeric matrix protein (COMP) (Tomschy et al, 1996) and the beta-lactamase protein from *E.coli* at the C-terminus. Prey pentamers are formed via the coiled-coil COMP pentamerization domain and detected through the beta-lactamase enzyme activity.

Since it has been reported that the expression levels of recombinant proteins in cell culture supernatants can differ by up to 3 to 4 orders of magnitude (Bushell et al., 2008; Özkan et al., 2013), it is essential that the protein concentrations can be normalized to predetermined levels prior to the AVEXIS binding test. The normalization step is crucial to reduce the number of false positive and false negative interactions. The concentrations of bait proteins captured on streptavidin-coated microtitre plates are determined by ELISA using anti-rat CD4 antibody. Bait protein concentrations are normalized to the level that the baits saturate the biotin binding sites on the plates. Prey protein concentrations are normalized by colorimetric detection of hydrolysis of nitrocefin by beta-lactamase. Protein concentrations are adjusted using spin concentrators or dilution with conditioned cell culture supernatant.
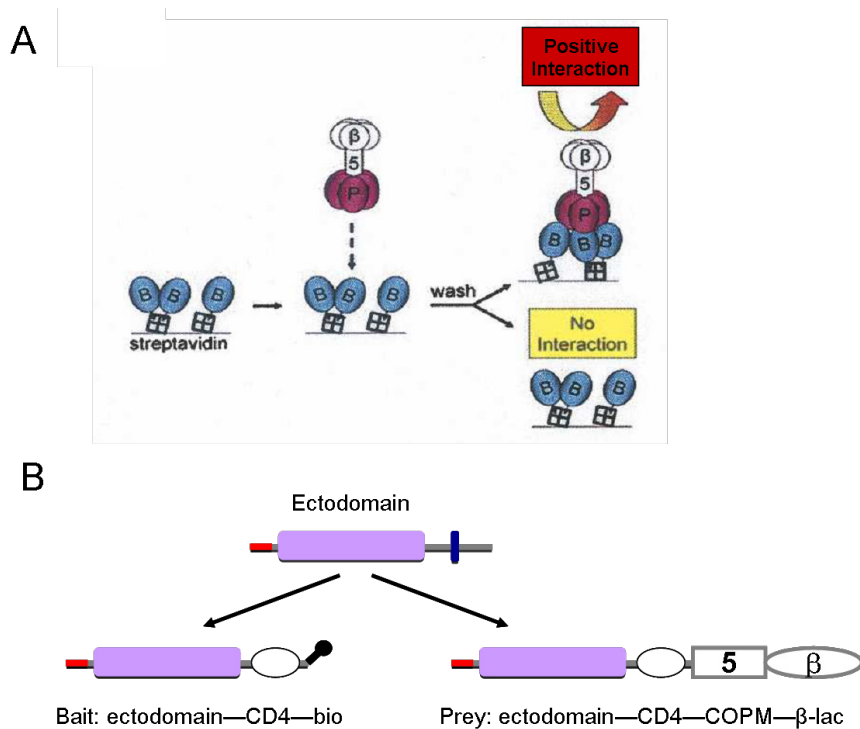
Figure 1.9   How AVEXIS works

(A) Schematic illustration of AVEXIS. Biotinylated monomeric bait proteins (blue) are captured on a streptavidin-coated plate and probed against pentameric beta-lactamase tagged prey proteins (pink). Positive interactions are detected by the turnover of the enzyme substrate from yellow to red. (B) Domain architecture of bait and prey proteins. The entire extracellular domains of the proteins of interest (purple rectangle) are cloned in bait and prey. The bait proteins contain C-terminal in-frame fusion with rat CD4 domains 3+4 (white circle) followed by a biotinylation peptide (bar with a dot). The prey proteins contain an in-frame fusion of rat CD4 domain 3+4 (white circle) followed by a pentamerization domain of rat COMP ("5" in white rectangle) and beta-lactamase ("β" in white ellipse) in the C-terminus. (adapted: Bushell et al. 2008; Soellner et al. 2009)

1.5.3 Comparison of AVEXIS with other high throughput screening methods

AVEXIS is not the only high throughput protein-protein interaction screening method. The yeast two-hybrid (Y2H) assay is a standard method for screening intracellular interactions. However, since the proteins are targeted to the nucleus for detection, it is unlikely to produce properly folded and posttranslationally modified extracellular proteins. Another high-throughput screening method is affinity purification followed by mass spectrometry (AP-MS). Since it depends on co-purification of interaction partners, weak interactions and interactions involving membrane proteins cannot be reliably detected.

Recently, several high throughput screening methods including AVEXIS have been developed to target extracellular protein-protein interactions. All of them are based on the expression of soluble ectodomain fragments. These approaches have several disadvantages as compared to the AVEXIS assay used in this study.

The ELISA-based binding assay (Wojtowicz et al., 2007) is the first reported high throughput screening assay designed to determine the binding specificity of the vast number of splice variants of the fruit fly Dscam protein. This assay is based on bait-prey detection with separate tags: the ectodomain fused to alkaline phosphatase (AP) as bait ("receptor") and the ectodomain fused to the Fc region of human IgG1 as prey ("ligand"). Bait-AP proteins are coated on the plate using an anti-AP antibody and the prey-Fc proteins are detected by an anti-Fc antibody conjugated to horseradish peroxidase (HRP). Binding is measured by HRP activity. As in AVEXIS, this method applies oligomerization to increase the avidity of the binding. Instead of prey pentamers, dimers of both prey and bait proteins are used. The main difference between this assay and AVEXIS is that additional steps are involved. First, the bait is indirectly bound to microtitre plates using antibodies; therefore, the captured bait protein concentration is difficult to monitor. Second, the HPR enzyme is not directly conjugated to the prey protein, thus adding another level of potential inaccuracy.

Another high throughput screening method is the so-called extracellular interactome assay (ECIA) (Özkan et al., 2013). It also specifically targets weak extracellular interactions using the oligomerization principle. Dimers of bait proteins containing the Fc region of human IgG1 and pentamers of prey proteins containing the COMP

and AP domains are used. The Fc region is captured directly on protein-A coated plates and the AP activity of the prey proteins is measured to detect the interactions. As in AVEXIS, prey protein concentrations are easily determined by AP enzyme activity and the concentrations of captured bait proteins can be determined by standard ELISA. However, in contrast to AVEXIS, the ECIA method focuses on post experimental data analysis to rule out false positive and false negative interactions while AVEXIS focuses on normalizing protein concentrations in the first place to get better original data. This difference in the strategy results in different quality of data.

A protein microarray (Ramani et al., 2012) has been specially designed for detecting interactions between secreted proteins and receptors by using multivalent protein-coated beads. Very small amounts of proteins are needed for each sample, which makes this method especially suitable for genome-wide screening. Though it is a high throughput method, purification of both bait and prey protein is needed. Also, since the signal is derived directly from the fluorescence of the recombinant proteins, the detection signal is not amplified. This differs from AVEXIS and other ELISA-style binding assays and makes this assay less sensitive.

Since none of these alternative methods provide substantial advantages, the AVEXIS assay was used to study the interactions of neuronal extracellular proteins to get a better understanding of the molecular mechanism of zebrafish neural development.

1.6 AVEXIS detected a direct interaction between Draxin and Netrin

To systematically identify new molecules involved in neural wiring, the AVEXIS assay was used to screen for novel interactions (Söllner and Wright, 2009). Signals potentially occurring between neurons and their microenvironment were of great interest for studying neural wiring. A library has been generated, which contains several hundreds of zebrafish secreted proteins and ectodomains of cell-surface receptors expressed mainly in neural tissues in early zebrafish embryos. The protein library has been screened for novel interactions within cell-surface receptors and secreted proteins.

The novel interaction between Netrin and Draxin was detected in the Tübingen discovery screen by Dr. Christian Söllner (Gao et al., 2015). The Draxin prey protein bound to members of the Netrin family. Within 158 bait proteins, zebrafish Netrin1a and Nerin-2 were the only positive hits besides the positive control (Matn4) (Fig 1.10).
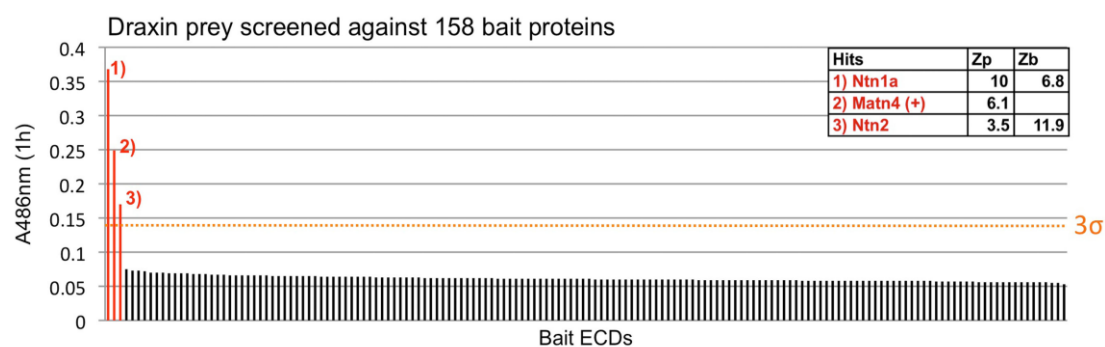
Figure 1.10   AVEXIS identified a physical interaction between Netrin and Draxin
Bar chart figure depicting the screening results for the Draxin prey in the discovery screen. Three hits were detected: Netrin1a, the positive control Matn4, and Netrin2. The positive signals had a Z-score >3, that is, the signals were >3 standard deviations above the mean. The Z-scores of the hits are indicated (see Tab 4.4 for the protein identities). ECD: ectodomain. Ntn1a: Netrin1a, Ntn2: Netrin2.

1.7 Goals of this study

Netrin and Draxin are both known diffusible axon guidance molecules expressed in the developing CNS in vertebrates. Both *Netrin-1* and *Draxin* knockout mice were reported to have defects in commissural neuron projections in the embryonic brain and spinal cord (Kennedy et al., 1994; Serafini et al., 1994; Islam et al., 2009). The large scale extracellular protein-protein interaction screen detected a novel direct interaction between these two guidance cues. This indicates Netrin-1 and Draxin function in the same biological process and/or same signaling pathway. Draxin might be a very interesting candidate for a potential Netrin modulator and could help to uncover a novel regulatory mechanism of Netrin signaling regulation.

The specific goals of this study are:

1) To analyze the interactions between Draxin and Netrin *in vitro*: examine binding specificity and define binding networks between known Draxin and Netrin family members

2) To explore the binding mechanisms of the Draxin-Netrin interaction

3) To test the function of the binding between Draxin and Netrin *in vitro*

4) To characterize the potential function of the interaction *in vivo* in zebrafish embryos

Chapter 2

Results

2.1 Biochemical analysis of the Draxin-Netrin interaction *in vitro*

My first goal was to confirm the initial finding of a Netrin/Draxin interaction in the Tübingen AVEXIS screen (Fig. 1.10). I also aimed to characterize the interaction between the two secreted proteins in greater detail. To this end, I used an extracellular protein-protein interaction assay and addressed specifically each of the following questions:

1) Is the interaction between Draxin and Netrin conserved within vertebrates?
2) What would be the potential function of this interaction in the context of Netrin signaling?
3) Does the direct binding of Draxin to Netrin influence Netrin/Netrin receptor interactions?
4) What are the kinetic parameters of the Draxin-Netrin interaction?

2.1.1 Conservation of the binding specificity of Draxins to Netrins

2.1.1.1 Adaptation of AVEXIS for small-scale interaction screening

The AVEXIS method was designed for large-scale, protein-protein-interaction screening. Thus, several modifications were implemented to optimize this method in order to assay in detail binding events between Draxin and Netrin at a smaller scale.

The original AVEXIS method was designed to detect infrequent interactions among a large number of proteins. False negative signals—due to very weak protein-protein-interactions, low protein concentrations or misfolded proteins—were tolerated. In this apporch, all prey proteins were normalized using β-lactamase enzymatic activity (Bushell et al., 2008). However, this may potentially cause an overestimation of the levels of prey proteins, since free β-lactamase in solution—which cannot bind to captured bait proteins in this assay—also can convert substrat. In my small-scale assay, it was crucial to detect all positive interactions. Therefore, an additional internal control was needed to normalize prey protein concentrations more accurately. Matrilin-4 (Matn4) had been shown to bind to the pentamerization domain of Cartilage Oligomeric Matrix Protein (COMP) (Mann et al., 2004), which is designed in prey proteins. In each experiment, we add Matn4 bait protein as an internal contral to monitor prey protein concentrations. In this way, we can normalize prey protein concentrations accoding to the amount of captured prey proteins. This helps to increase the sensitivity of this assay.

The identification of what is called a "positive interaction" ("hit") was also adapted to a small-scale assay. AVEXIS was developed to identify novel interactions by screening a large-scale protein library. The identification of "hits" was, therefore, based on assumed normal distribution of the detected binding values. A signal was considered as a "hit" if the intensity was above the absorbance mean value by a defined number of standard devitions (Z-score). In the large-scale AVEXIS, the hit rate is between 0.4 % and 0.6 % of defined positive interactions among all of the tested interactions (Bushell et al., 2008). However, in a targeted small-scale screen with low sample numbers, the hit rate is expected to be substantially higher. Thus I replaced the Z-score based standard for calling hits with a combined hit definition, computing absolute binding value overal background level. Absobance values that were 1.5 fold above background level were defined positive interactions.

2.1.1.2 Binding specificity of zebrafish Draxins and Netrins

To explore the interaction between Draxin and Netrin in detail, I wanted to know whether the interaction occurs among all members of their respective protein families, or between a few specific members. Thus, I examined all known zebrafish Draxin and Netrin proteins for binding specificity using AVEXIS.

As a first step, I cloned the *draxin* paralog (gene name: *si:dkey-1c11.1*) and the annotated diffusible *netrin* genes including *netrin1b, netrin-2* and *netrin-4* (Fig. 1.4). For all of the cloned *netrin* genes, truncated constructs were generated which contained the Netrin N-terminal domain and three EGF domains. The C-terminal domain of Netrin was excluded because it binds to components of the extracellular matrix (e.g. heparins) (Serafini et al., 1994). Removing the Netrin C-terminal domain does not affect receptor binding (Geisbrecht et al., 2003; Xu, Wu et al., 2014). In fact, expressing truncated versions of Netrin in eukaryotic cell cultures result higher protein yields (Serafini et al., 1994; Özkan et al., 2013). The expression level of Netrin-2 was low even after the removal of C-terminal domain, so that Netrin-2 was not included in further experiments.

As shown in Figure 2.1 A_1, Netrin1a bound strongly to both Draxin and the Draxin paralog (*si:dkey-1c11.1*), weakly to itself and to Netrin1b. Figure 2.1 A_2 shows that Draxin bound strongly to both Netrin1a and Netrin1b, but not to Netrin-4. For all bait/prey pairs, reciprocal pairs (e.g. A-bait to B-prey and B-bait to A-prey) were tested. The results are summarized in Figure 2.1 B. Reciprocal tests confirmed the initial observation that both Draxin and the Draxin paralog bound strongly to Netrin1a and Netrin1b, whereas Netrin1a and Netrin1b showed homophilic binding as well as heterophilic binding to each other. Netrin-4 did not bind to any of the tested proteins.

Figure 2.1 C summarizes the result of the AVEXIS binding test for zebrafish Netrins and Draxins. It confirms the initial result that was obtained for Draxin and Netrin1a in the large-scale AVEXIS screen. Interestingly, both Draxin paralogs bound to the tested Netrin members belonging to Laminin γ-chain derived Netrins (Netrin1a, Netrin1b), but not to Laminin β-chain derived Netrins (Netrin-4). Not all of the Netrins bound to Draxin, which suggests that Draxin is a selective binder of Laminin γ-chain derived Netrins.
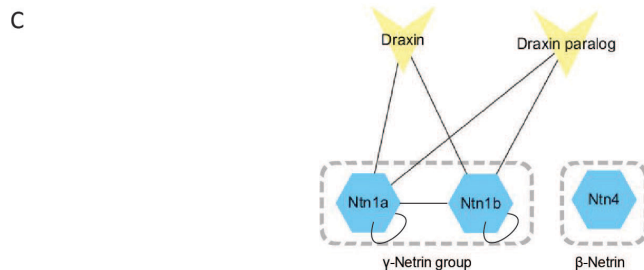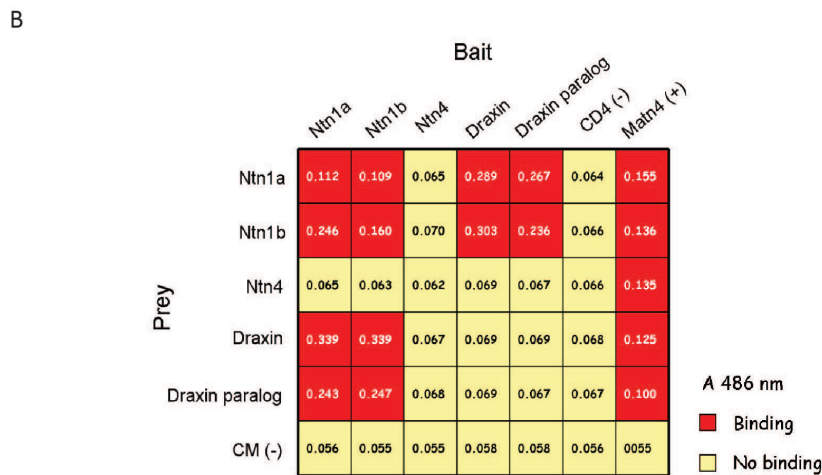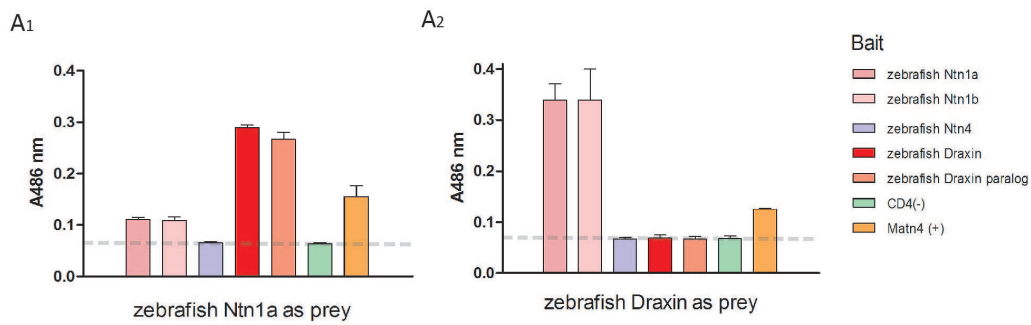
Figure 2.1   Zebrafish Draxin-Netrin interactions

(A) AVEXIS pair wise binding results for zebrafish Netrin-Draxin binding experiments. A$_1$) zebrafish Netrin1a as prey. A$_2$) zebrafish Draxin as prey. The values show absorbance reads of substrate turnover at 486 nm, mean ± SD, n=3. The dashed line shows the absorbance of the negative control (a construct containing only the CD4 tag as bait) and corresponds to the background level. The screen was performed in both bait-prey orientations using pentameric prey proteins. (B) Heatmap view of the results. Values show 486 nm absorbance means of triplicates. Red: binding (binding value/background >1.5), yellow: no binding (binding value/background <1.5). (C) Network view of the results. The dashed line indicates two different groups of Netrin proteins: Laminin γ-chain derived Netrins (γ-Netrin group) and β-chain derived Netrin (β-Netrin). Ntn: Netrin.

2.1.1.3 Conservation of the Netrin-Draxin interaction in human orthologs

Since both Draxin and Netrin are present in a wide range of vertebrate genomes (Fig. 1.3 A), I wondered whether the interactions between zebrafish Draxin and Netrin are conserved to human. To test for binding conservation, I examined the binding of different human Draxin and Netrin orthologs. Clones of human Netrin-1, Netrin-3, Netrin-4, Netrin-G1 and Netrin-G2 as well as Draxin protein were generated and expressed. Just as we did for the zebrafish Netrin proteins, we generated truncated versions for all human Netrins, which contained the Laminin domain and the EGF domains (domain VI+V).

As seen in Figure 2.2 A_1, human Draxin bound to human Netrin-1. Draxin strongly bound to Netrin-1 and weakly to Netrin-3 (Fig. 2.2 A_2). Netrin-4, Netrin-G1 and Netrin-G2 did not bind to any of the tested proteins. The reciprocal bait/prey tests confirm the binding results (Fig. 2.2 B). In sum, the interactions between Draxins and Netrins observed in zebrafish are conserved for the human orthologs (Fig. 2.2 C). Human Draxin bound to Netrin-1 and Netrin-3, both of these proteins are members of Laminin γ-chain derived Netrins, and Draxin did not bind to all of the Netrins. These findings are in agreement with the binding specificity that was observed within zebrafish proteins.

2.1.1.4 Cross-species interactions between zebrafish and human proteins

Since the binding between Draxin and Netrin is conserved among zebrafish paralogs and human orthologs, I further asked whether the binding interface is conserved across species. To this end, I carried out cross-species interaction experiments. I tested the binding specificity of human Draxin to zebrafish Netrin as well as human Netrin to zebrafish Draxin.

As shown in Figure 2.3 A, I detected strong binding between human Draxin bait and zebrafish Netrin1a prey. The signal strength was comparable to the signal that was observed when zebrafish Netrin bound to zebrafish Draxin. Similarly, I observed strong binding when the human Netrin-1 prey bound to the zebrafish Draxin bait (Fig. 2.3 B). These results show cross-species interactions. Thus, the interaction interfaces between Draxin and Netrin are most likely highly conserved.
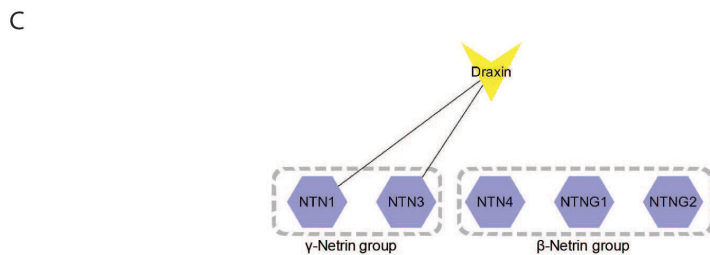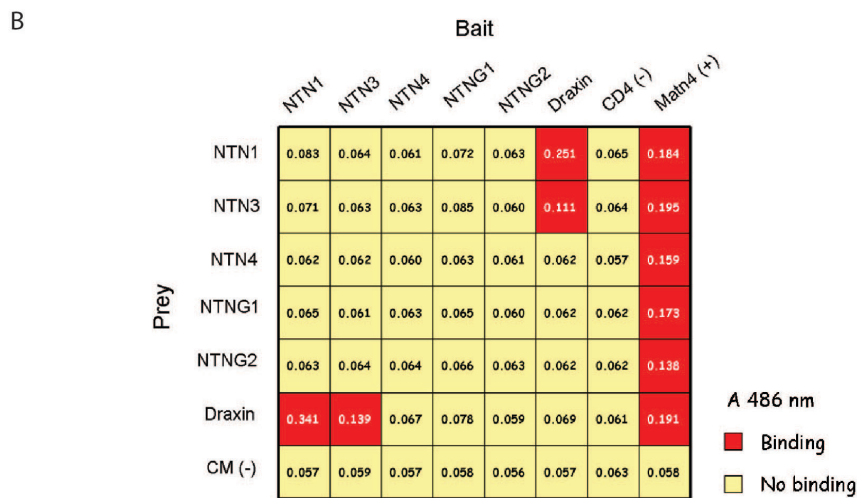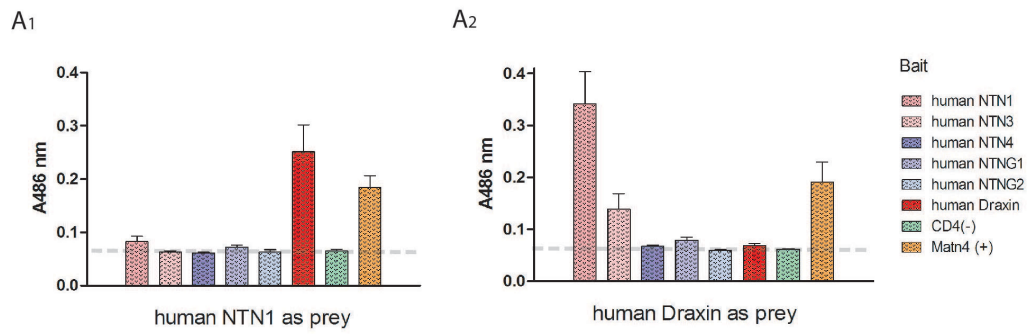
Figure 2.2 Human Draxin-Netrin interactions

A) AVEXIS pairwise binding results of human Netrin-Draxin interactions. A_1) human Netrin-1 as prey. A_2) human Draxin as prey. The values show absorbance of the substrate at 486 nm, mean ± SD, n=3. The dashed lines show the absorbance of the negative control (construct with CD4 tag as bait), indicating the background level. The screen has been performed in both bait-prey orientations using pentameric prey proteins. B) Heatmap view of the results. The values show the 486 nm absorbance means of triplicates. Red: binding, yellow: no binding. C) Network view of the results. The dashed line indicates two different groups of human Netrin. NTN: Netrin

A

A486 nm (zebrafish Ntn1a as prey)

B

A486 nm (human NTN1 as prey)

Bait:
- zebrafish Draxin
- human Draxin
- CD4 (-)
- Matn4 (+)
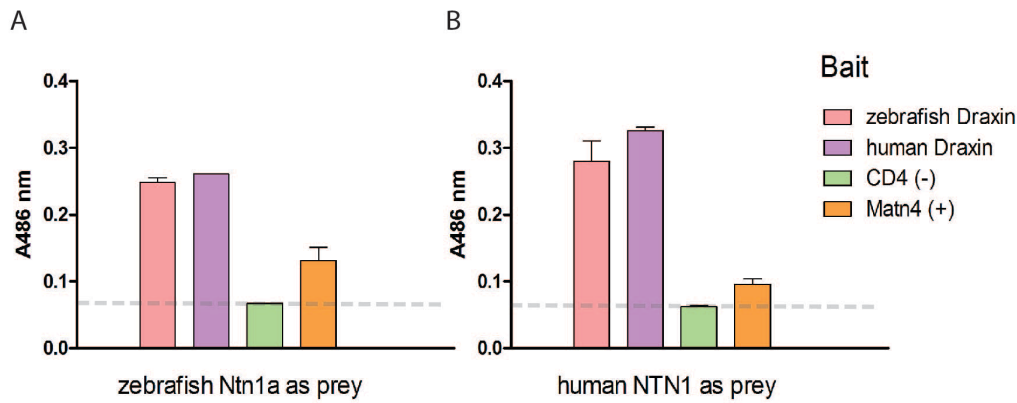
Figure 2.3   Zebrafish and human Draxin-Netrin cross-species interactions

AVEXIS screen results: (A) zebrafish Netrin1a as prey and (B) human Netrin1 as prey. The values show absorbance of the substrate at 486 nm, mean ± SD, n=3. The dashed line corresponds to the absorbance read from the negative control (CD4 tag as bait), and this corresponds to the background level. NTN: Netrin.

A — zebrafish

		Ntn1a	Ntn1b	Ntn4	Draxin	Draxin paralog	CM (-)	CD4 (-)	Matn4 (+)
Prey	CM (-)	0.058	0.056	0.056	0.059	0.059	/	0.058	0.056
	Dcc	0.188	0.126	0.069	0.074	0.070	/	0.068	0.130
	Neo1	0.307	0.220	0.064	0.067	0.063	/	0.059	0.123
	Unc5b	0.153	0.103	0.073	0.077	0.072	/	0.070	0.128
Bait	Dcc	0.155	0.178	0.065	0.067	0.067	0.057	/	/
	Neo1	0.266	0.302	0.065	0.071	0.066	0.061	/	/
	Unc5b	0.280	0.285	0.072	0.068	0.070	0.061	/	/
	CD4 (-)	0.064	0.066	0.066	0.068	0.067	0.056	/	/
	Matn4 (+)	0.155	0.136	0.135	0.125	0.100	0.055	/	/

B — human

		NTN1	NTN3	NTN4	NTNG1	NTNG2	Draxin	CM (-)	CD4 (-)	Matn4 (+)
Prey	CM (-)	0.057	0.059	0.057	0.058	0.056	0.057	/	0.063	0.058
	DCC	0.342	0.065	0.062	0.069	0.059	0.060	/	0.062	0.185
	UNC5B	0.116	0.062	0.061	0.068	0.063	0.069	/	0.065	0.124
Bait	DCC	0.233	0.067	0.064	0.063	0.062	0.065	0.057	/	/
	UNC5B	0.138	0.062	0.059	0.060	0.060	0.067	0.057	/	/
	CD4 (-)	0.065	0.064	0.057	0.062	0.062	0.061	0.063	/	/
	Matn4 (+)	0.184	0.195	0.159	0.173	0.138	0.191	0.058	/	/

A486 nm — ■ Binding (Red)   ■ No binding (Yellow)

Figure 2.4   Netrin-Netrin receptor and Draxin-Netrin receptor interactions

Targeted AVEXIS screen results for zebrafish (A) and human (B) Netrin-Netrin receptor and Draxin-Netrin receptor binding experiments. The values show 486 nm absorbance means of triplicates. Both bait-prey orientations are indicated. Red: binding, yellow: no binding. Zebrafish Draxin paralog: *si:dkey-1c11.1*. "/": not tested; Ntn or NTN: Netrin.

2.1.2 Draxin binds to Netrin, but not to Netrin receptors

Draxin and Netrin are both secreted proteins of similar size; they are both axon guidance cues; and Netrin is a known ligand of several receptors. This brings up an interesting question: how does the direct interaction between Draxin and Netrin proteins influence their respective functions?

As Draxin is reported to bind to all Netrin receptors (Ahmed et al., 2011), the first hypothesis was that the binding of Draxin to Netrin might influence the interaction between Draxin and Netrin receptors. In order to test this, I first studied the direct interactions between various Netrins, Draxins and Netrin receptors using AVEXIS.

I focused on Netrin-1 and receptors of Netrin-1 for several reasons: 1) Draxin appears to specifically interact with Laminin γ-chain derived Netrins, and Netrin-1 is the major and the best studied Netrin in this group. 2) The receptors of Netrin-1, DCC and Unc5, are also the best studied Netrin receptors. The functions of these receptors are known, which enables the follow-up functional studies of the interactions. All of the Netrin-1 receptors were cloned for the binding tests, including Dcc, Neogenin, Unc5b and Dscam. Dscam was excluded from the binding tests because of low protein expression level.

Figure 2.4 shows the protein binding results. The three tested zebrafish Netrin-1 receptors bound to both Netrin1a and Netrin1b; they did not bind to Netrin-4. Interestingly, I did not detect binding of any of the three Netrin receptors to Draxins. I observed similar results in the reciprocal prey/bait orientation. On the other hand, the human Netrin receptors DCC and UNC5B specifically bound to Netrin-1, but not to any other of the tested Netrins, including Netrin-3, Netrin-4 and two Netrin-G proteins. Neither of these human Netrin receptors interacts with Draxin, similarly to the results obtained using zebrafish proteins.

In summary, all of the tested Netrin receptors, from both zebrafish and human, were able to directly bind to Netrin but not to Draxin. These findings give a different view from the previous observations in which Draxin directly bound to all of the Netrin receptors.

2.1.3 *In vitro* competition between Draxin and Netrin receptors for Netrin binding

The second hypothesis addressing the function of the interaction between Draxin and Netrin was that Draxin might compete with Netrin receptors for Netrin binding. I developed a competition assay to test this hypothesis.

2.1.3.1 Establishment of an AVEXIS-based competition assay

The competition assay was designed as a modification of the AVEXIS assay (Fig. 2.5). In this competition assay, Netrin-1 was used as bait, and the extracellular domains of Netrin receptors were used as prey proteins. The binding between Netrin-1 bait and Netrin receptor prey proteins was challenged by addition of increasing concentrations of purified soluble Draxin (the potential competitor). By design, this assay is able to distinguish among three different possibilities: (i) an increase in the substrate turnover rate (deriving from Netrin-Netrin receptor binding) would indicate that Draxin facilitates the interaction between Netrin and Netrin receptors; (ii) no change in the substrate turnover rate would suggest that Draxin has no effect on binding; (iii) a decrease in the substrate turnover rate (even to a rate of zero) would indicate that Draxin inhibits the binding of Netrin to Netrin receptors, quanlifying as a novel negative regulator of Netrin signaling.

I modified the AVEXIS assay to measure competition by introducing a new way of normalizing prey protein concentrations. To exclude any possibility of signal saturation and to avoid a too low signal baseline that may interfere with the detection of the inhibition, prey proteins were normalized to absorbance values 2 to 5 fold above the background level within the reaction incubation time.

The percentage of binding was calculated as:

$$\% \text{ binding} = \left(\frac{binding\ with\ inhibitor}{binding\ without\ inhibitor} \right) * 100\%$$

Background levels (the average binding value using BSA) were subtracted from all of the binding values prior to the calculation. The percentage of binding reflects the competition effect.
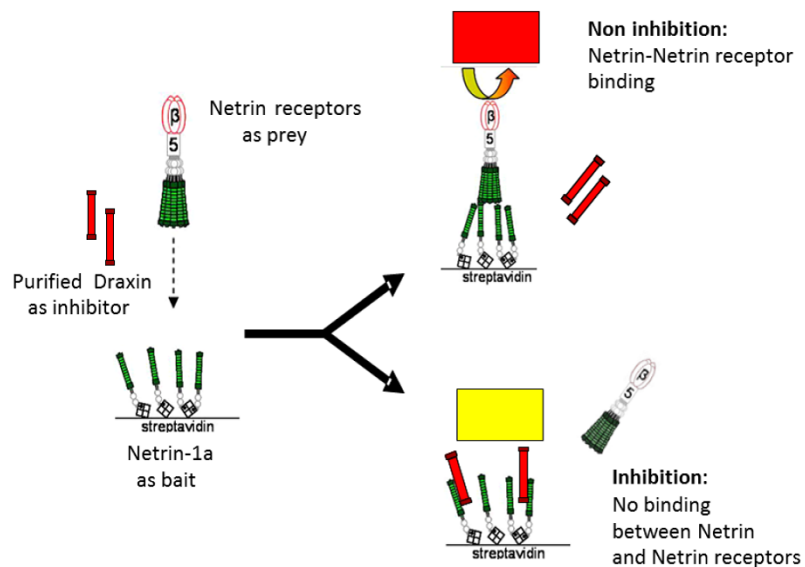
Figure 2.5   Schematic representation of the AVEXIS-based competition assay

Netrin1a (green, monomer) is used as bait protein, Netrin receptors (green, pentarmer) are used as prey proteins probed together with purified Draxin (red, monomer) as the tested inhibitor. This assay is able to distinguish among three different possibilities: (i) Draxin facilitates the interaction between Netrin to Netrin receptors; (ii) Draxin has no effect on binding; (iii) Draxin inhibits the binding of Netrin to Netrin receptors. The Draxin construct contained rat CD4 and histine tag: N' Draxin-CD4 d3+4-6XHis-stop C'. (adapted: Söllner et.al., 2009)

2.1.3.2 Results of the competition assay

Using the competition assay, I tested whether Draxin is able to compete with Netrin receptors for Netrin binding. Figure 2.6 shows the raw data from one of the experiments. Concentrations of Draxin between 100 nM and 1 μM are able to outcompete all the tested Netrin receptors from Netrin binding. The inhibition effect of Draxin is variable among different Netrin receptor-Netrin pairs. Unc5b-Netrin interaction is most sensitive to the Draxin-dependent inhibition among all of the tested binding pairs.

In order to quantitate the inhibitory effect, I used purified Draxin in the competition assay. Figure 2.7 A shows that purified Draxin is able to reduce the binding between Netrin1a and Dcc. Draxin concentrations higher than 1 μM completely abolished binding. Similarly, the interaction between Netrin1a and Unc5b was inhibited by addition of Draxin (Figure 2.7 B). The concentration of Netrin at which 50 % inhibition was observed (IC_{50}), measured 50 nM (Netrin1a-Dcc interaction) and 10 nM (Netrin1a-Unc5b interaction). In addition, Draxin interfered with the Netrin1a-Neo1 interaction, although it appears that higher concentrations of Draxin are required to trigger this effect (red line in Fig. 2.7 C). Since the competition effect of Draxin to Netrin1a-Neo1 is not as strong as the effect seen with Netrin1a-Dcc or Netrin1a-Unc5b, I wanted to rule out the possibility of a non-specific result. Figure 2.7 C shows that equal amounts of BSA did not interfere with the binding between Netrin1a and Neo1 (dotted black line). Thus, the capability of Draxin to interfere with the interaction between Netrin and its receptors is a specific property of Draxin in my analysis.

To further test whether Netrin is a specific target of Draxin, Netrin was replaced with another ligand in the competition test. The Netrin receptor Neo1 has other known ligands belonging to the membrane-bound repulsive guidance molecule (RGM) protein family (Rajagopalan et al., 2004). RGMc (Hfe2) is one of these RGMs. As shown in Figure 2.7 D, high concentrations of Draxin were not able to influence Hfe2-Neo1 binding. These data indicate that the inhibitory effect of Draxin is specific to Netrin1a and does not affect the binding of Hfe2 to Neo1.

Finally, to test how efficiently Draxin is able to disrupt Netrin-Netrin receptor interactions, I designed an experiment including different initial ratios of Netrin / Netrin receptor subjected to competion (Fig. 2.8 A). After Netrin-1 bait proteins were

immobilized, Netrin receptor preys were either added before, together with, or after the addition of Draxin. In the first condition, the Netrin-Netrin receptor complex formed before the presence of the inhibitor. Figure 2.8 B shows the results of this competition experiments. The Netrin1a-Dcc binding level was reduced in response to increasing concentrations of Draxin in all three conditions. The inhibition effect of Draxin to preformed Netrin-Netrin receptor complexes was similar to the other two competition conditions. This indicates that Draxin is able to outcompete Netrin receptors, disrupting preformed Netrin-Netrin receptor complex.

In conclusion, Draxin specifically interferes with the interaction between Netrin and Netrin receptors *in vitro*, thereby, confirming the second hypothesis.
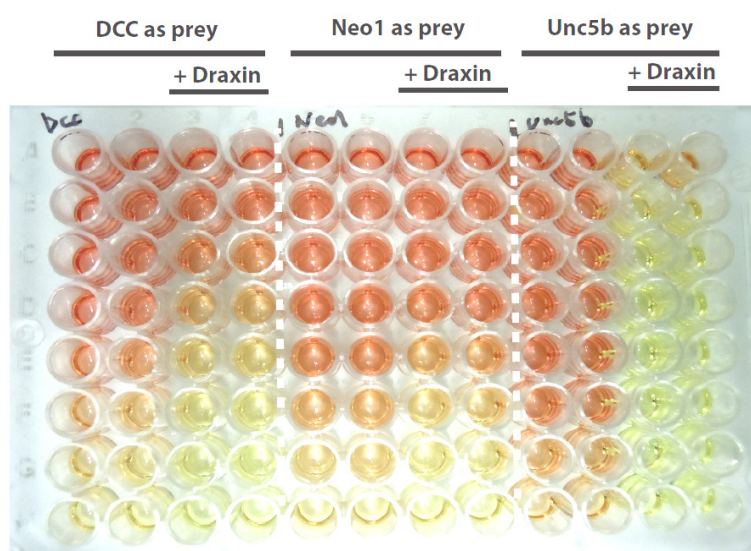
Figure 2.6   Draxin is able to outcompete Netrin receptors for Netrin binding (raw data)

Raw data of the AVEXIS-based competition assay. Netrin1a was used as bait and the indicated Netrin receptors were used as prey proteins. Two-fold dilution series of prey proteins are displayed from top to botton. For each group, the two columns on the left show binding without Draxin, the two right colunns show binding with Draxin. Red wells show the colorimetric enzyme reactions indicating binding events, yellow wells indicate no binding. Equal concentrations of Draxin were added as inhibitor. A Netrin1a version containing the Laminin N-terminal domain plus 3xEGF domains (Netrin VI+V) was used as bait protein; complete ectodomains of Netrin receptors were used as prey proteins; Monomeric Draxin (with the concentration between 100 nM and 1 µM) is harvested from tissue culture medium.
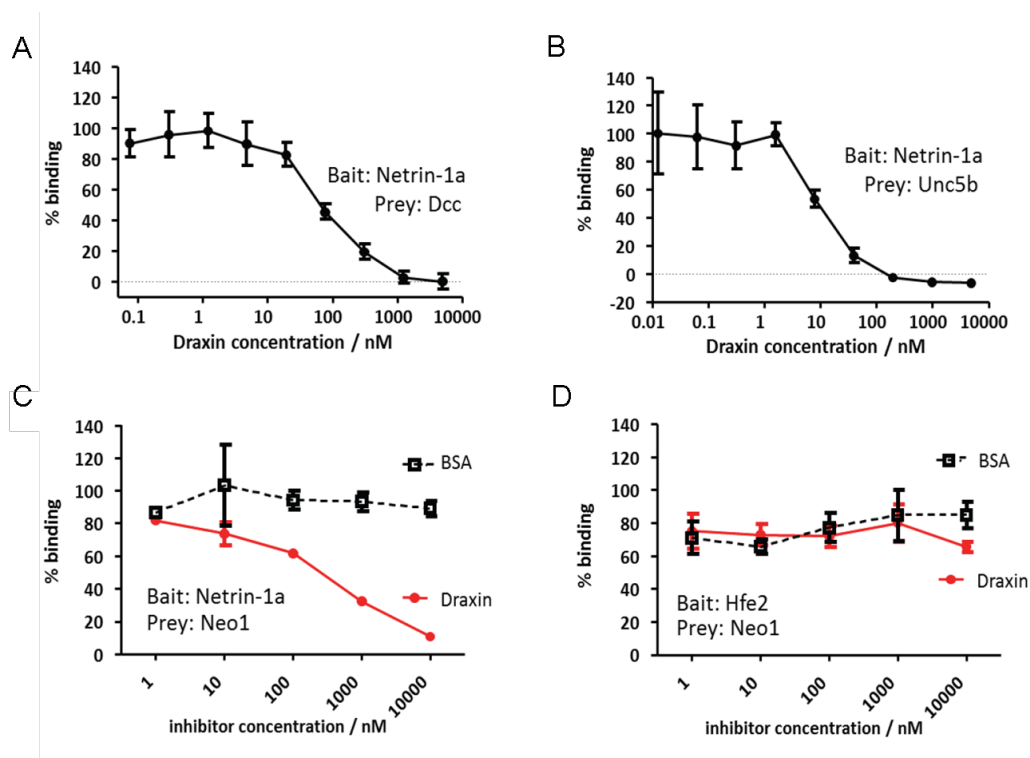
Figure 2.7   Draxin inhibits the binding of Netrin to Netrin receptors *in vitro*

(A) Binding curve of Netrin1a-Netrin receptor Dcc interaction challenged by Draxin. The binding value from Netrin1a to Dcc is reduced with increasing concentrations of Draxin. This effect is also observed for other Netrin receptors Unc5b (B) and Neo1 (C, indicated with red line). Equal amounts of BSA were not able to compete for Netrin1a-Neo1 binding (C, indicated with dashed black line). (D) Draxin is not able to interfere with the binding of Neo1 to Hfe2 (RGMc), another known Neo1 ligand. Zebrafish proteins were used in this assay. A Netrin1a version containing the Laminin N-terminal domain plus 3xEGF domains (Netrin VI+V) was used as bait protein; complete extracellular regions of Netrin receptors were used as prey proteins; His$_6$-tagged full length Draxin in frame fusion with rat CD4 domain3+4 was used as the potential inhibitor; binding reads were taken within 1-2 hours at room temperature. % binding: (binding with inhibitor / binding without inhibitor) X100 %. Error bars indicate mean±s.d; n=4. Similar results were obtained three times independently, and with monomeric prey proteins of Dcc and Unc5b.
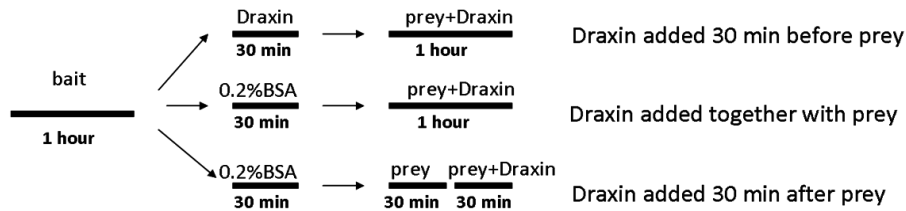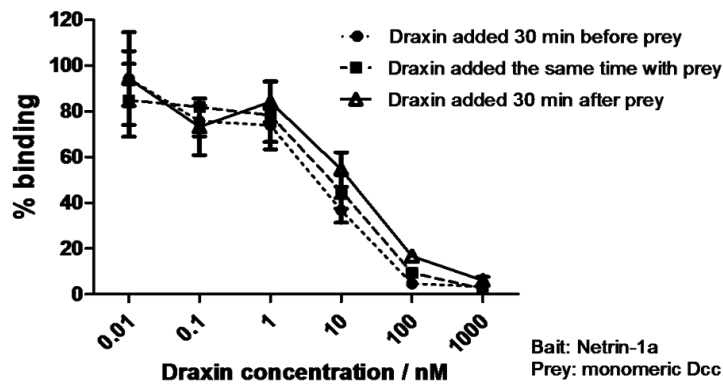
Figure 2.8   Draxin outcompetes the binding of Netrin to Netrin receptor

(A) Schematic illustration of the assay.   After 1 hour incubation with bait proteins, Draxin was added 30 min before, together with or 30 min after addition of prey proteins. (B) The competition curves of three different conditions. In all of the cases, the binding of Dcc to Netrin is reduced with increasing concentrations of Draxin. Zebrafish proteins were used in this assay. Netrin1a containing Laminin N-terminal plus 3xEGF domains (Netrin VI+V) was used as the bait protein; extracellular region of Dcc was used as monomoeric prey protein; full-length His_6- tagged Draxin fused to rat CD4 domain3+4 was used as potential inhibitor. A486nm 1 hour reads were taken. % binding: (binding with inhibitor / binding without inhibitor) X100 %, error bars indicate mean±s.d. n=4.

2.1.4 Kinetic analysis of the Draxin-Netrin interaction using SPR

To independently confirm the interaction between Draxin and Netrin detected using the AVEXIS assay, we performed surface plasmon resonance (SPR) experiments. SPR is a method to determine the kinetics of protein-protein interactions in real time. It can measure whether a binding event occurs, and allows to determine how strong and how fast the interaction is. SPR-based methods are currently the golden standard method to determine the kinetics of protein-protein interactions.

We injected serial dilutions of purified human Draxin (R&D systems, monomer) over immobilized C-terminal biotinalyated human Netrin-1 on a streptavidin-coated sensor chip and used Netrin-G1 as the reference. We also performed similar experiments with Draxin and the ectodomain of human Netrin receptors Unc5B and DCC immobilized on the chip.

As seen in Figure 2.9 A, we detected direct binding between Draxin and Netrin-1. The binding curve is not well fitted a simple 1:1 dissociation model but more closely fitted the heterogeneous ligand model (k_{a1} 2.12 10^{-6}; $M^{-1} s^{-1}$; k_{d1} 0.0212 s^{-1}; k_{a2} 5.03 $10^{-6} M^{-1} s^{-1}$; k_{d2} 6.19 $10^{-4} s^{-1}$). The binding dissociation constant (K_D) was 10 nM, which falls within the known range detected for Netrin-Netrin receptor interactions. These kinetic data support our previous conclusions showing that Draxin can disrupt Netrin binding to its receptors. No binding of Draxin to UNC5B and DCC was detected (Fig. 2.9 B and C), which confirmed the results we obtained using AVEXIS.
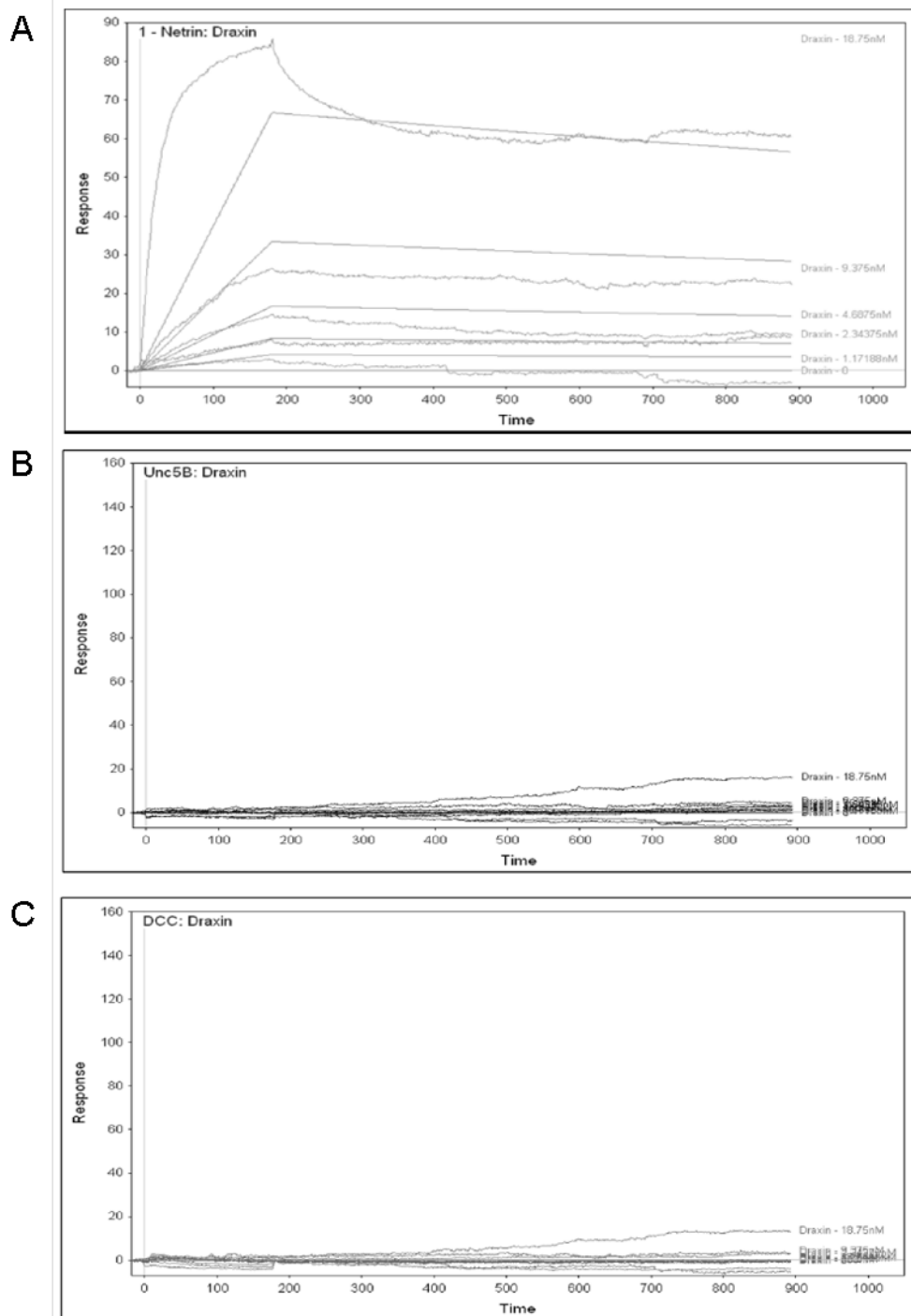
Figure 2.9   Surface Plasmon Resonance analysis of Draxin as analyte

Binding of Draxin to immobilized recombinant Netrin-1, UNC5B, and DCC was monitored using SPR experiments on a Biacore 3000 instrument. The binding curves are fitted with 1:1 dissociation model. Recombinant Netrin-G1 was used as a reference. Human proteins were used in the analysis.

2.2 Characterization of the binding sites for the interaction between Draxin and Netrin

In order to uncover the molecular mechanism of the interaction between Draxin and Netrin, my next goal was to characterize the protein regions that mediate the Draxin-Netrin interaction. By using orthologous protein alignment and protein feature analysis, I designed a series of constructs encoding different protein versions. These protein contained deletions or were truncated, allowing the mapping of zebrafish Draxin and Netrin1a binding interfaces. The AVEXIS assay was used for the mapping.

I asked the following specific questions:

1) Where is the binding interface of Draxin and Netrin when they interacting?
2) Are the binding sites in both proteins specific to the Draxin-Netrin interaction?
3) The Draxin-Netrin interactions is conserved from zebrafish to human, is the binding site formed by conserved protein sequence?

2.2.1 The Draxin binding interface to Netrin is mapped to a highly conserved 22 aa peptide

2.2.1.1 Protein domain analysis of zebrafish Draxin

Since no structural or domain prediction data was available for Draxin, I aligned protein sequences of Draxin orthologs from different species in order to identify conserved regions of the protein. In addition, protein features were analyzed using the following online bioinformatics' tools: SMART (Simple Modular Architecture Research Tool) for protein domain annotation; SignalP 4.0 for signal-peptide prediction; HHpred (from the Tuebingen Bioinformatics Toolkit) for homologous protein detection and protein structure prediction; NetNGlyc 1.0 and other prediction programs in ExPASy (Expert Protein Analysis System) for the identification of protein-sugar binding regions.

Figure 2.10 shows the alignment of human, mouse, chick and zebrafish Draxin proteins as well as the protein feature analysis. The N-terminal half of Draxin is poorly conserved, whereas a highly conserved region is recognizable from the middle of zebrafish Draxin onwards (aa 209, indicated by the arrowhead in Fig. 2.10). This region includes a highly conserved 22 aa stretch (zebrafish Draxin 231-252 aa, underlined in red) followed by a 10-cysteines containing region (zebrafish Draxin 284-360 aa, underlined in magenta). The amino acid cysteine is highly conserved within proteins that share similar functions, because the cysteines form disulfide bridges that play essential roles in both the stabilization of protein structure and the preservation of biological function. The 10-cysteines containing region in Draxin is known as Dickkopf (Dkk)-like domain, and contains a similar number and spacing of cysteines as found in Dkk proteins (Miyake et al., 2009). By HHpred analysis, I was able to characterize the starting point of the Dkk-like domain (zebrafish Draxin aa 275, underlined in blue). In addition, a positively charged motif was detected (zebrafish Draxin 260-268 aa, KRKDKRRSK, underlined in yellow), which likely binds to negatively charged glycosaminoglycans (sugars). I used these properties to design mapping constructs for the Draxin protein.
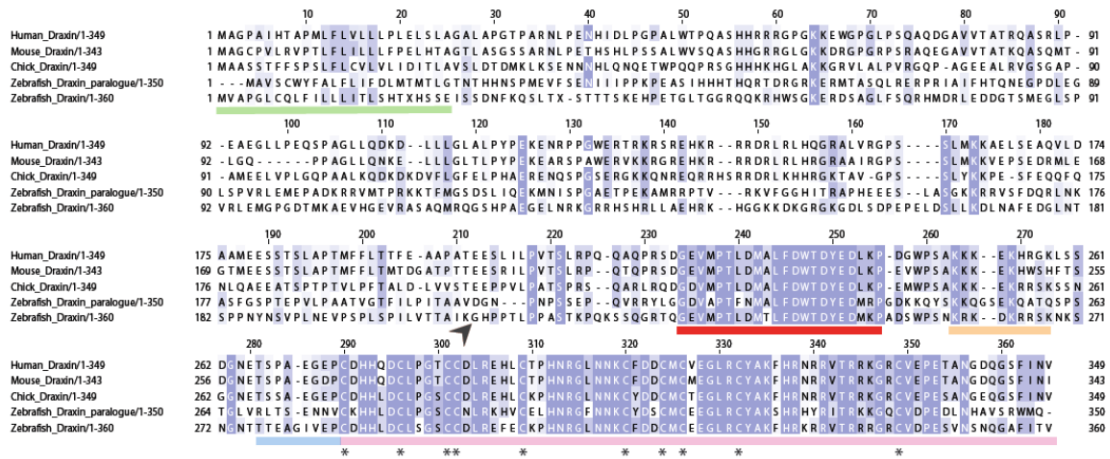
Figure 2.10 Draxin protein alignment and analysis

ClustalW alignment of human, mouse, chick, and zebrafish Draxin proteins. Draxin display high conservation from a central region (zebrafish Draxin 231-252 aa, red line). In the C-terminus of the protein, a conserved domain (magenta line, Dkk-like domain) containing 10-cysteines is recognizable. By HHpred analysis, this domain is identified from 275 aa to 360 aa of zebrafish Draxin (blue line). The signal peptide in zebrafish Draxin is underlined in green, and a positively charged sequence is underlined in yellow. The name of the zebrafish Draxin paralog is *si:dkey-1c11.1*.

2.2.1.2 Mapping the Netrin-binding-interface in Draxin to a 22 aa motif

In order to map the Netrin-binding-interface in Draxin, I first generated a series of 25 different zebrafish Draxin protein truncations. These truncations were tested against Netrin for binding activity using the AVEXIS assay.

Several considerations were taken into account to adapt the AVEXIS assay for the mapping experiments. Draxin prey proteins were normalized to concentrations yielding a signal 2-5 fold above background level in the binding assay. This expedient provided an increase in the detection sensitivity of the binding test. To reduce the non-specific binding signal, a monomeric Netrin1a prey protein lacking the COMP domain (pentamerization domain) was generated. For monomeric prey proteins, the avidity effect generated by pentermerized prey proteins does not apply (Bushell et al., 2008). Hence, using the monomeric prey protein versions helped to reduce signals derived from weak and transient interactions, whereas strong binding events were still detectable. Similar to the binding experiments mentioned in the Results, section 2.1, a zebrafish Netrin1a protein consisting the domain VI (Netrin N-terminal domain) and domain V (the three EGF domains) was used in the mapping experiments.

Figure 2.11 shows the mapping result of the Netrin-binding-interface in Draxin. All constructs comprising a 22 aa protein motif (zebrafish Draxin 231-252 aa) bound to Netrin1a (Fig. 2.11 A); the positive binding signals were higher than 5-fold above background level, indicating that truncated Draxin protein have the same binding activity as full-length Draxin (Fig. 2.11 B). Interestingly, the 22 aa peptide alone (Draxin 231-252 aa) is sufficient for binding. Removal of the 22 aa motif from full-length Draxin (Draxin $\triangle$209-284 aa and Draxin $\triangle$231-252 aa) completely abolished the binding ability. These results emphasize the requirement of the 22 aa motif in Draxin for successful binding to Netrin1a. Furthermore, shortening this motif by 5 aa from C-terminus (Draxin 209-247 aa, 226-247 aa) resulted in weak binding to Netrin1a. The binding signal was less than 1.5 fold above background level.

In conclusion, the binding region of Draixn to Netrin1a was mapped to a 22 aa motif (zebrafish Draxin 231-252 aa). The identified peptide is both necessary and sufficient to mediate the interaction between Draxin and Netrin1a.
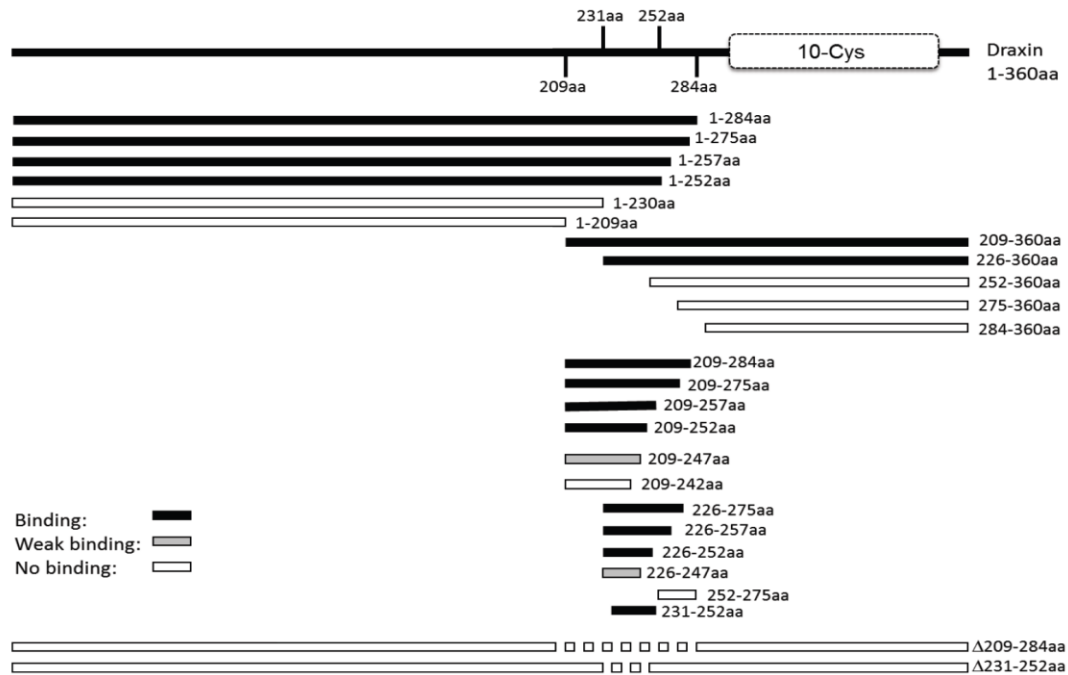
Figure 2.11   A Draxin-derived 22 aa fragment is sufficient for binding to Netrin1a

(A) AVEXIS binding results from a set of Draxin protein fragments tested against Netrin1a.
Binding is indicated in black, weak binding in grey, and no-binding in white.

B

Draxin prey					Draxin bait
AA of Draxin	Netrin-1a bait	Matn4 (+)	BSA (-)	Netrin-1a prey	BSA (-)	AA of Draxin
1-360	0.321	0.178	0.055	0.393	0.059	1-360
1-284	0.383	0.153	0.059	/	/	1-284
1-275	0.391	0.134	0.059	0.413	0.061	1-275
1-257	0.342	0.132	0.058	0.382	0.061	1-257
1-252	0.344	0.173	0.058	0.362	0.062	1-252
1-230	0.055	0.144	/	0.062	0.059	1-230
1-209	0.059	0.254	0.059	0.059	0.058	1-209
209-360	0.387	0.143	0.058	0.485	0.06	209-360
226-360	0.416	0.129	0.06	0.457	0.059	226-360
252-360	0.063	0.142	0.06	0.059	0.059	252-360
275-360	0.062	0.125	0.061	0.06	0.058	275-360
284-360	0.062	0.138	0.072	0.059	0.058	284-360
209-284	0.39	0.143	0.059	0.284	0.06	209-284
209-275	0.399	0.169	0.058	0.348	0.056	209-275
209-252	0.357	0.142	0.058	0.384	0.055	209-252
209-247	0.102	0.179	0.056	0.075	0.063	209-247
209-242	0.099	0.101	/	0.063	0.058	209-242
226-275	0.404	0.147	0.06	0.412	0.057	226-275
226-257	0.416	0.123	0.058	0.412	0.058	226-257
226-252	0.413	0.149	0.063	0.431	0.064	226-252
226-247	0.094	0.11	0.057	0.093	0.058	226-247
252-275	0.058	0.158	0.058	0.062	0.072	252-275
231-252	0.381	0.111	0.057	0.464	0.058	231-252
△76aa	0.064	0.136	0.059	0.06	0.057	△76aa
△22aa	0.075	0.13	0.061	0.062	0.056	△22aa

Binding: ■
Weak binding: ▤
No binding: ☐

Figure 2.11　A Draxin-derived 22 aa fragment is sufficient for binding to Netrin1a (continued)

(B) Original data of the mapping experiments. The prey proteins were normalized to substrate turnover levels 2-5 fold above background by using the Matn4 bait as positive control; 2 % BSA serves as negative control. The average of duplicates is shown. "/": not tested.

2.2.1.3 Binding specificity of the Draxin-derived 22 aa peptide (library screen)

Next, I determined whether the Draxin-derived 22 aa peptide specifically binds to Netrin. To this end, I took advantage of the AVEXIS method and the large extracellular protein library generated by our group. In these experiments, the Draxin 22 aa peptide was screened against a diverse set of cell surface and secreted proteins including 132 bait and 172 prey proteins (see Tab. 4.4 for protein identities).

As shown in Figure 2.12, one strong hit corresponding to Netrin1a was detected in both bait and prey orientations. The binding value of the Draxin-derived peptide to the rest of the library was within background level. This result demonstrates that the binding between the Draxin-derived 22 aa peptide and Netrin1a is highly selective among a diverse set of protein families.

2.2.1.4 The 22 aa motif of Draxin is highly conserved within vertebrate Draxins

I was interested in the protein features of the Draxin 22 aa peptide sequence because of its binding selectivity to Netrin1a. BLAST (Basic Local Alignmnet Search Tool) searches detected similar motifs only within vertebrate Draxin homologos. Figure 2.13 shows the protein alignment of Draxins from human, mouse, rat, cow, pig, chimpanzee, chick, frog, puffer fish and zebrafish. This alignment shows that the 22 aa motif from zebrafish Draxin is highly conserved between distant vertebrate species.

Together, these results from section 2.2.1.3 and 2.2.1.4 indicate that the identified 22 aa peptide in Draxin selectively binds to Netrin1a and is uniquetly found in the vertebrate Draxin protein family.
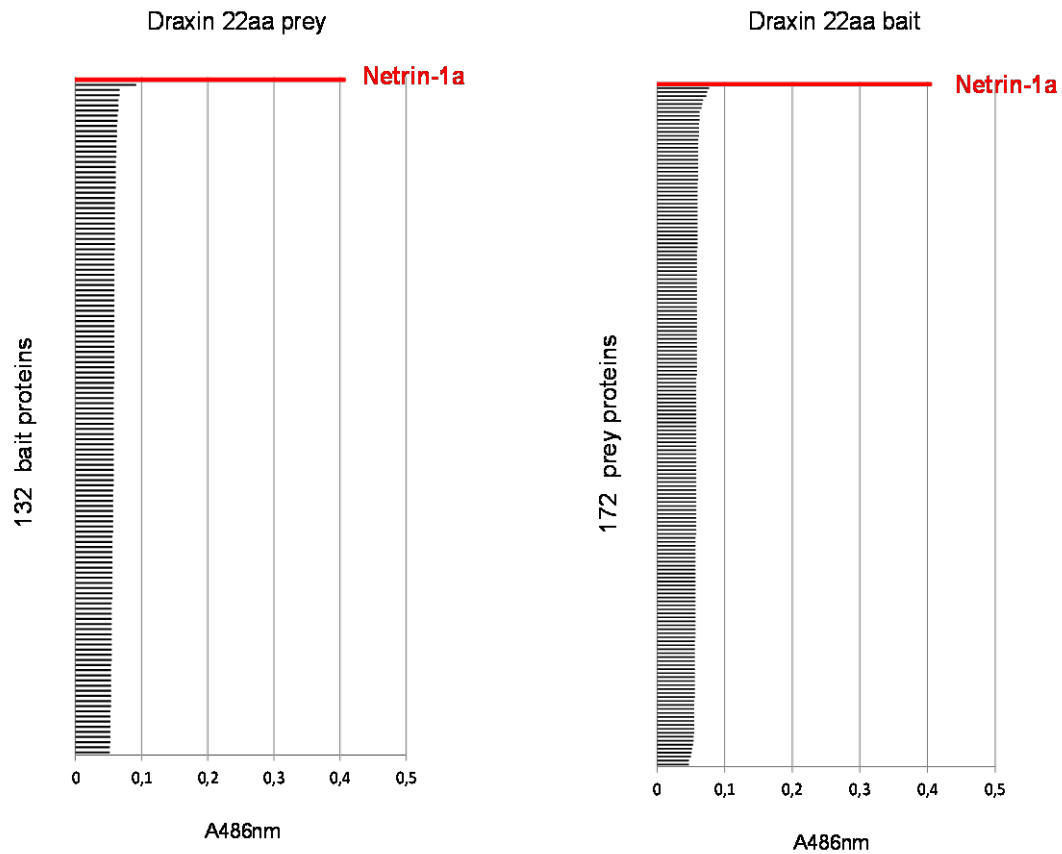
Figure 2.12 Binding selectivity of the 22 aa Draxin-derived peptide

The 22 aa Draxin-derived peptide was screened against 132 different bait proteins and 172 prey proteins from a variety of protein families (see Tab. 4.4 for protein identities). 486 nm absorbance values were obtained after a two-hour incubation of the substrate.
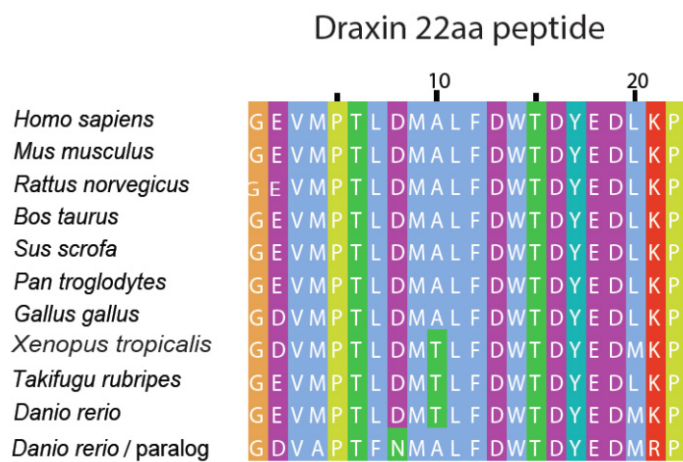
Figure 2.13 Conservation of the Netrin-binding motif in Draxin homologs

2.2.1.5 The 22 aa Draxin peptide (fused to the Fc region of IgG) is sufficient to compete with Netrin receptors for Netrin binding

Since the 22 aa Draxin motif is sufficient for binding to Netrin1a, I next asked whether the same peptide was also able to block Netrin receptor-Netrin interactions in the same way as the full-length Draxin. The *in vitro* AVEXIS-based competition assay was used for this purpose. Here, the 22 aa Draxin peptide, the full-length Draxin, and a truncated Draxin version containing a deletion of the 22 aa motif (Draxin △22 aa) were fused to the Fc region of human IgG protein (hFc), which serves as a dimerization tag. I used the three fusion proteins above as "competitors" in the competition assay. Netrin receptor-Netrin binding was "challenged" by addition of Draxin fusion proteins in order to determine their inhibitory effect.

Figure 2.14 shows that the fusion protein containing Draxin 22 aa peptide (Draxin 231-252aa-hFc) was able to block Netrin1a-Dcc interactions. Furthermore, Draxin 231-252aa-hFc and dimeric full-length Draxin (Draxin-hFc) had a similar inhibitory capability. On the other hand, deletion-containing Draxin (Draxin Δ231-252aa-hFc) was unable to effectively influence the interaction beween Netrin and its receptors. These results show that the 22 aa Netrin-binding region of Draxin is required to outcompete Netrin receptors from Netrin binding, and the Draxin derived 22 aa peptide is sufficient for exert inhibition.

In order to further test whether the inhibitory effect is specific to Netrin-Netrin receptor interaction, I used the same set of Draxin-hFc to examine their effect on other interactions. Figure 2.15 B-D shows no detectable interference with Cntn1a-Ptprz1b (B), Vasna-Islr2 (C), or EphB4a-EphrinB2a (D). These results further demonstrate that Draxin specifically inhibits Netrin/Netrin receptor interaction via its conserved 22 aa peptide.

Figure 2.13 (preceding page)   Conservation of the Netrin-binding motif in Draxin homologs

Protein sequence alignment of the Draxin-derived 22 aa Netrin-binding peptide from different vertebrate species. The zebrafish (*Danio rerio*) Draxin paralog is *si:dkey-1c11.1*.
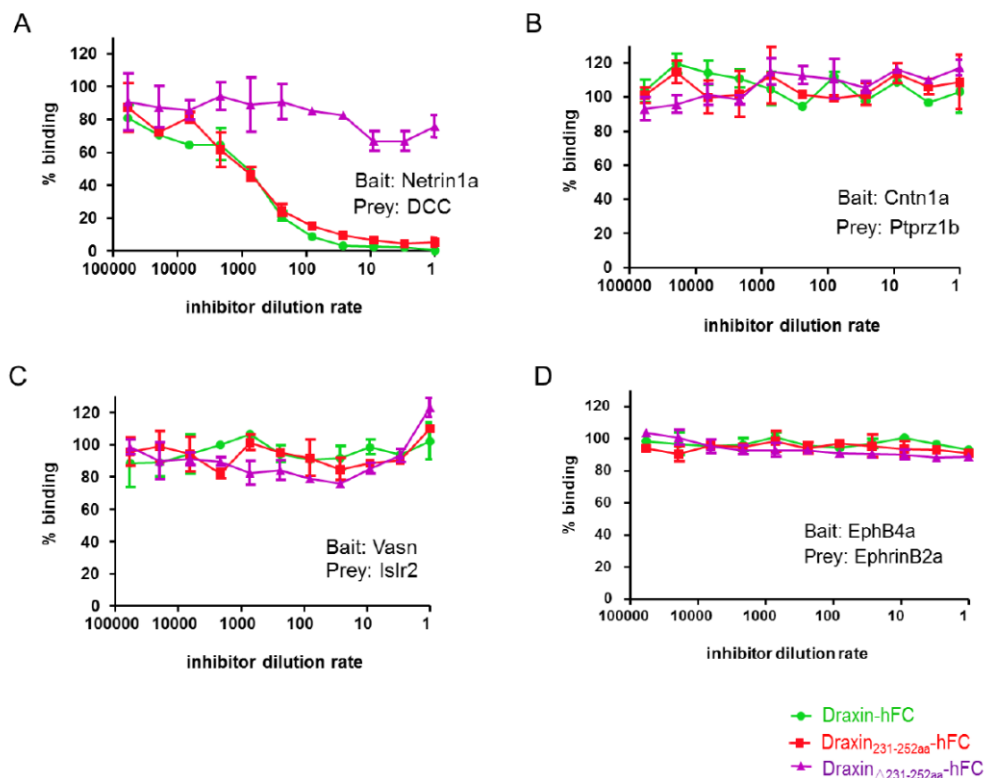
Figure 2.14 The Netrin-binding 22 aa peptide in Draxin is sufficient to compete with Netrin receptor for Netrin binding

AVEXIS-based competition assay using three different Draxin versions fused to the Fc region of the human IgG protein as potential competitors. (A) Full-length Draxin-hFc (green) and the Netrin-binding 22aa-hFc (red) proteins were able to outcompete Dcc for binding to Netrin1a. Full-length Draxin carrying a deletion of the Netrin-binding motif (△231-252 aa, magenta) was not able to compete with the Netrin receptor for binding to Netrin. (B-D) None of the three Draxin-hFc fusion proteins was able to block binding between other receptor-ligand pairs tested: Cntn1a-Ptprz1b (B), Vasna-Islr2 (C), and EphB4a-EphrinB2a (D). Concentration normalized Fc fusion proteins were used. % binding: binding with inhibitor / binding without inhibitor X100 %; error bars show mean ± s.d., n = 3; two repeats.

2.2.2 The 3rd EGF domain of Netrin1a is sufficient for binding to Draxin

2.2.2.1 Netrin1a domain boundary analysis and protein linker design

In order to dissect the functional units of Netrin for the Draxin-binding-region mapping experiments, I first analyzed the domains of the Netrin1a protein. Netrin1a contains multiple known domains (Fig. 1.4 A), however, the exact boundaries of each EGF domains remains unclear. The SMART program was used for predicting the boundaries of these EGF domains. The key element to define a typical EGF domain is the spacing of the 8 conserved cysteines. The cysteines produce disulphide bonds that preserve the tertiary protein structure. The structure of an EGF domain is shown in the following diagram, and the disulphide bonds are indicated:

```
         +-----------------------------+
    +----|----------------+            |        +--------------+    +--------------------------+
    |    |                |            |        |              |    |                          |
   xx Cx Cxxxxxxxxxxx C xxxxxx C xx C xxxxxGxx C xx C xxgaagxxxxxxxxxxx Cxx
```
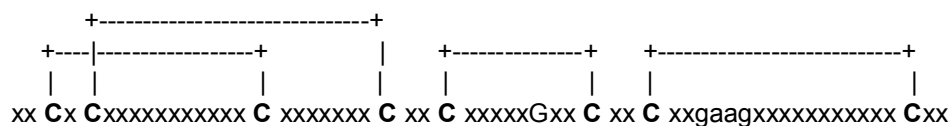
According to this prediction, aa 338 and aa 401 in zebrafish Netrin1a were proposed to correspond to the start of the 2nd EGF and the 3rd EGF domain.

Since the first cysteine is located near the beginning of the EGF domain, the structure of a truncated protein can be easily affected if the truncation site is not accurately designed. In order to increase the likelihood of producing properly folded proteins for individual EGF domains, I optimized the protein expression constructs by adding protein linkers between the signal peptide and the respective EGF domains. The following protein linkers were used:
a) SMFAAQTSPPDP (endogenous)
b) PASPASPAS
c) GSTGTT

2.2.2.2 Mapping the Draxin-binding-interface to the 3rd EGF domain of Netrin1a

To map the Draxin-binding-interface, I designed a set of Netrin1a constructs containing either individual domains or combinations of consecutive domains. These

truncated Netrin proteins were tested for binding activity against full-length Draxin. This set of truncated Netrins was also tested against Draxin △231-252 aa and Draxin 231-252 aa peptide, and compared with full-length Draxin.

Figure 2.15 A shows the result of the interaction screen using Netrin1a truncations against Draxin. The N-terminal domain and the C-terminal domain (C345C) of Netrin1a are not required for binding to Draxin. In contrast, the three-EGF domain (257-458 aa) in Netrin displayed strong binding. By screening individual EGF domains against Draxin, I was finally able to narrow down the Draxin-binding-region to the 3rd EGF domain of Netrin1a (401-458 aa).

Furthermore, I was able to show that truncated-Draxin (containing a deletion of the 22 aa motif) was unable to bind to any of the truncated Netrin1a constructs (Fig. 2.15 B). In contrast, the Draxin derived 22 aa peptide alone was able to bind to all of the truncated Netrin1a constructs which also bound to full-length Draxin (Fig. 2.15 B). Moreover, the binding activity of the 22 aa peptide to Netrin1a was similar to that of full-length Draxin. Interestingly, the 22 aa Draxin peptide was able to bind to the 3rd EGF domain of Netrin1a.

In conclusion, I resolved the binding region of Netrin1a to Draxin to the 3rd EGF domain (401-458 aa) in Netrin1a. The 231-252 aa Draxin peptide was able to bind to the 3rd EGF domain of Netrin1a.

A

LamNT   EGF1 EGF2 EGF3   c345c   Netrin-1a 1-603aa

257aa   338aa 401aa 458aa

1-458aa
1-402aa
1-339aa
257-458aa
338-458aa
401-458aa
338-402aa
257-402aa
450-603aa

Binding: —
No binding: ▭

B
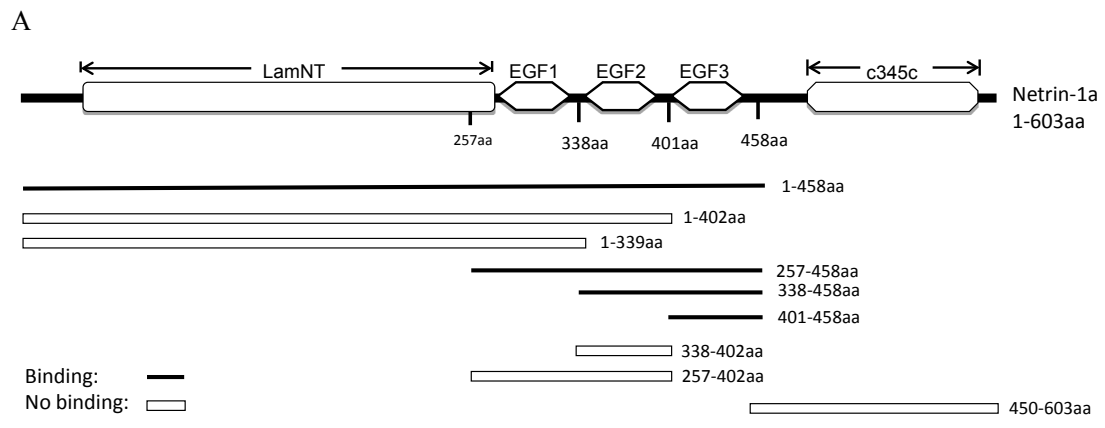
	Draxin	Draxin △22 aa	Draxin 22aa	Matn4 (+)	BSA (-)
Netrin-1a prey	aa of Netrin-1a				
1-458	0.144	0.057	0.148	0.135	0.053
1-402	0.052	0.051	0.053	0.135	0.051
1-339	0.052	0.051	0.054	0.19	0.051
257-458	0.091	0.054	0.135	0.146	0.052
338-458	0.095	0.065	0.16	0.13	0.054
401-458	0.159	0.052	0.216	0.192	0.052
338-402	0.059	0.056	0.053	0.167	0.054
257-402	0.077	0.075	0.053	0.151	0.05
450-603	*0.092	/	/	0.125	0.06
Netrin-1a bait					
1-458	0.305	0.057	0.298	/	0.052
1-402	0.052	0.056	0.05	/	0.051
1-339	0.052	0.05	0.05	/	0.053
257-458	0.289	0.056	0.292	/	0.051
338-458	0.197	0.051	0.201	/	0.05
401-458	0.252	0.056	0.303	/	0.053
338-402	0.05	0.052	0.051	/	0.05
257-402	0.054	0.053	0.051	/	0.054
450-603	0.057	/	/	/	/

Binding: ▰
Weak binding: ▱
No binding: ▭

Figure 2.15 Identification of the Draxin-binding domain in Netrin1a

2.2.2.3 Binding specificity of the 3rd EGF domain in Netrin1a (library screen)

To test whether the mapped binding domain in Netrin1a selectively interacts with Draxin, I screened the 3rd EGF domain of Netrin1a against a large set of proteins in our library. 88 bait proteins and 162 prey proteins were screened for protein-protein interactions using AVEXIS (see Tab. 4.4 for the protein identities).

Figure 2.16 shows that only a single strong hit corresponding to Draxin was detected in both bait/prey orientations. The binding values presented in the library against the 3rd EGF domain were below background threshold. This result demonstrates that the binding of the 3rd EGF domain in Netrin1a to Draxin is highly specific among a large set of proteins.

Figure 2.15 (preceding page) Identification of the Draxin-binding domain in Netrin1a (A) AVEXIS binding results obtained by screening a set of 9 different Netrin protein truncations against Draxin proteins. The Draxin-binding interface in Netrin1a was narrowed down to the 3rd EGF domain (401-458 aa). Binding is indicated in black, no-binding in white. (B) Original data from the mapping experiments. Data showing interactions tests between Netrin truncations and Draxin version includeing full-length Draxin, Draxin 22 aa peptide (231-252 aa), and Draxin 22 aa deletion (Δ231-252 aa). Prey proteins were normalized to binding values 2-5 fold above background level using Matn4 as a positive control; 2 % BSA is a negative control. The average of duplicates is shown. Comparable results were obtained in the reverse bait/prey orientation. "/": not tested; "*": the binding signal observed for the Netrin1a 450-603 aa prey protein might be derived from the known sugar-binding properties of this domain.
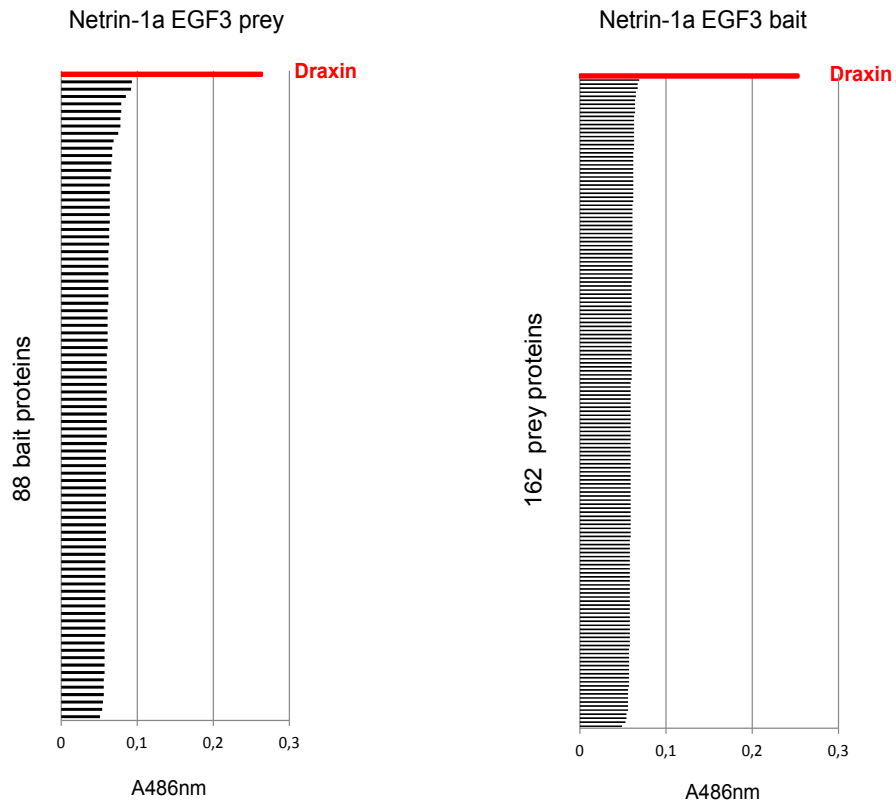
Figure 2.16   Binding selectivity of the 3rd EGF domain of Netrin1a

The 3rd EGF domain of Netrin1a was tested against 88 bait and 162 prey proteins (see
Tab. 4.4 for the list of the tested proteins). In both orientations, only one strong hit
highlighting Draxin was detectable. 486 nm absorbance values were obtained after a
two-hours' incubation.

2.2.2.4 The 3rd Netrin EGF domain is highly conserved within γ-Netrins

To determine the conservation of the mapped Draxin-binding-region in Netrin1a, I aligned the 3rd EGF domain from all known human and zebrafish Netrins. Figure 2.17 shows that the 3rd Netrin EGF domain is highly conserved among Laminin γ-chain derived Netrins (γ-Netrins). It shows lower conservation when compared with other Netrins (e.g. Netrin-4 and Netrin-G). Indeed, among the three EGF domains in Netrin-1, the 3rd EGF domain is the most highly conserved domain within γ-Netrins. For example, the protein sequences of the 3rd EGF domain from zebrafish Netrin1b and human Netrin-1 are completely identical, whereas the 2nd EGF and the 1st EGF have lower conservation rates (Fig. 2.18).

In summary, the binding interfaces of the Netrin-Draxin interaction were mapped to a 22 aa peptide in Draxin (231-252 aa) and to the 3rd EGF domain in Netrin. Both binding sites displayed high binding specificity. The 22 aa peptide in Draxin is highly conserved and can only be found in vertebrate Draxins. The 3rd EGF domain of Netrin is also highly conserved within γ-Netrins.

Collectively, my binding-site mapping experiments show that the interaction interfaces of both proteins are highly conserved among vertebrate Draxin and γ-Netrin proteins, which supports the cross-species binding results observed in the Results, section 2.1 in this dissertation.

Figure 2.17 The 3rd Netrin EGF domain is highly conserved within Laminin-γ-chain derived Netrins

Protein sequence alignment of the 3rd EGF domain from human and zebrafish Netrins. Dr, *Danio rerio*; Hs, *Homo sapiens*.

Figure 2.18   Pair wise protein sequence alignment of individual EGF domains from human and zebrafish Netrins

The amino acidic identity percentage is indicated. "\": not tested.

2.3 Characterization of the Draxin-Netrin interaction in zebrafish embryos

My results, so far, favor an inhibitory role of Draxin in the Netrin signaling pathway. These results include: a) the competition between Draxin and Netrin receptors for Netrin binding; b) the finding of conserved Draxin-Netrin interactions in both zebrafish and human; and c) the mapping of highly conserved binding regions in both proteins. These data suggests that Draxin operates as a Netrin antagonist by competing with Netrin receptors for Netrin binding in vertebrates.

In order to test the above hypothesis *in vivo*, I asked the following questions:

1) Does the protein-protein interaction between Draxin and Netrin occur *in vivo*?
2) Where are the two genes expressed in the embryo? Are there potential co-expression regions for the two secreted proteins?
3) Is it possible to detect the binding between Draxin and Netrin *in situ*?

2.3.1 *In vivo* detection of the Draxin-Netrin interaction in zebrafish embryos

2.3.1.1 Establishing an *in vivo* binding assay

To test whether Draxin and Netrin are able to bind to each other *in vivo*, I designed a novel *in vivo* binding assay (Fig. 2.19 A). This assay is based on the transient co-expression of fluorescently tagged proteins in zebrafish embryos. Draxin was fused to superfolder-GFP (Draxin-sfGFP), and Netrin1a was fused to either mCherry (Ntn1a-mCherry) or superfolder-GFP (Ntn1a-sfGFP). mRNAs encoding these fusion proteins were injected into one-cell stage zebrafish embryos. Upon translation, the tagged proteins were secreted to the extrocellular space, leaded by the endogenous signal peptide in the created constructs. The distribution of the corresponding fluorophore-tagged proteins was analyzed in zebrafish embryos at sphere stage (4 hours post fertilization, hpf). At this developmental stage, the amount of extracellular space between cells is very large, and therefore, it is ideally suited for visualizing the localization of secreted proteins.

2.3.1.2 Result of the *in vivo* binding analysis

Following mRNA injection, the signal of Draxin-sfGFP was evenly distributed throughout the extracellular milieu of 4 hpf zebrafish embryos (Fig. 2.19 B-a, a', a'', imaging plane is indicated in Fig. 2.19 A). In contrast, the distribution of Netrin1a-sfGFP was restricted to cell surface domains (Fig. 2.19 B-b, b' b''). When *draxin-sfGFP* mRNA was co-injected with *netrin1a-mCherry* mRNA, Draxin-sfGFP proteins relocated to membrane densities composed of Netrin1a fusion proteins (co-localization is indicated by arrowheads in Fig. 2.19 B-c, c', c''). This indicates that local Netrin1a-mCherry proteins are able to capture diffusible Draxin-sfGFP proteins.

In conclusion, exogenous mRNAs expression experiments show that Draxin and Netrin1a are able to interact with each other *in vivo* in zebrafish embryos.

Box 1: *In vivo* binding assay

(This method was adapted from Ries et al., 2009; Yu et al., 2009)

- The tested mRNAs were injected into zebrafish embryos at one-cell stage.

- The injected mRNAs were then translated into proteins in zebrafish embryos. The encoded secreted proteins distributed throughout the extracellular space.

- Distinct fluorophores were fused to proteins of interest to visualize protein distribution. The co-localization of fluorophore signals indicates detailed co-expression, a hint of binding events.

- Draxin and Netrin show different extracellular localization when separately expressed. This observation enables the analysis of binding events *in vivo*.
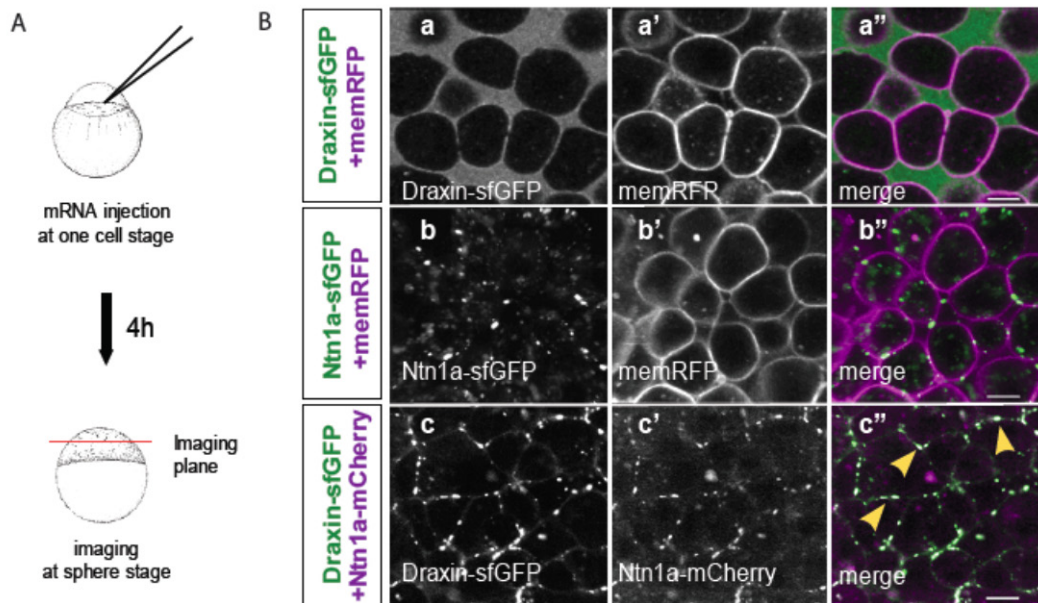
Figure 2.19 *in vivo* **detection of the Draxin-Netrin interaction in zebrafish embryos**
(A) Design of the *in vivo* binding assay. mRNAs encoding the indicated fluorophore-tagged proteins were injected into one-cell stage zebrafish embryos and imaged at blastula stages (4 hpf). The imaging plane corresponds to a region approximately 15 μm beneath the enveloping layer (dorsalmost layer) of the embryos. (B) Single optical section confocal images of sphere stage embryos. (B-a) Embryos injected with 100 pg Draxin-sfGFP mRNA displayed uniform protein distribution in the extracellular space. (B-b) Injection of 100 pg Ntn1a-sfGFP mRNA resulted in dense membrane associated speckles positive for Ntn1a-sfGFP protein. In (B-a') and (B-b') membrane RFP (memRFP) was used to label the cell surface. (B-c) Upon co-injection of 200 pg Draxin-sfGFP mRNA and 200 pg of Ntn1a-mCherry mRNA, Draxin-sfGFP and Ntn1a-mCherry proteins co-localized into membrane associated foci (arrowheads). Scale bars: 10 μm; n = 7.

2.3.2 *draxin* and *netrin* gene expression analysis in zebrafish

The functional importance of the Draxin-Netrin interaction strongly depends on whether and where the two proteins encounter each other in a living organism. Since there is no standard assay available to sensitively detect the endogenous binding events of secreted proteins *in vivo*, I first determined the expression of *draxin* mRNA by *in situ* hybridization. Subsquently, I performed double *in situ* hybridization detection of both *draxin* and *netrin* in the same embryo to identify potential regions of co-expression.

Box 2: Whole mount *in situ* hybridization in zebrafish embryos

- *In Situ* Hybridization (ISH) is a method that detects mRNA expression. Main steps include:
  1) Generation of antisense RNA probes
  2) Hybridization of RNA probes to endogenous mRNA in fixed zebrafish embryos
  3) Detection of hybridized RNA probes in zebrafish embryos

- Fluorescence *In Situ* Hybridization (FISH) uses fluorescent substrates to visualize RNA probes. This method enables the detection of multiple gene expression domains using different fluorophores in the same specimen.

- Double *in situ* hybridization was used in this study to detect the expression of *draxin* and *netrin* in the same embryo.

2.3.2.1 *draxin* mRNA expression analysis in zebrafish

The spatial and temporal patterns of *draxin* mRNA were detected by whole mount *in situ* hybridization in zebrafish embryos (Fig. 2.20). *draxin* mRNA is expressed in a dynamic manner in the nervous system, the somites and the tail bud.

In forebrain and hindbrain regions of 20 hpf embryos, the expression of *draxin* was detected in the telencephalon. Higher expression levels were detected in anterior and dorsal regions of the diencephalon as well as in the lateral hindbrain (Fig. 2.20 A and B). High expression within the diencephalon was associated with the post-optical commissure and the posterior commissure. At 24 hpf, there was strong expression along the border of telencephalon/diencephalon as well as in the lateral hindbrain (D and E). Strong expression was detected in these regions until at least 30 hpf (G and H). Starting from 48 hpf, the expression was restricted to the olfactory bulb in the telencephalon, and distinct regions within the hindbrain (J and K). By 76 hpf, strong expression was detected only in the regions of the olfactory bulb and lateral hindbrain (M and N).

In the spinal cord, *draxin* displayed a dynamic expression pattern shown in the right panel of Figure 2.20. The spinal cord (SC) and the notochord (NC) are separated by a short bar indicating the boundary between the two regions. At 20 hpf, *draxin* was basically expressed throughout the entire spinal cord (Fig. 2.20 C). At 24 hpf, the ventral spinal cord expression diminished. From 30 hpf (Fig. 2.20 I) to at least 48 hpf (Fig. 2.20 L), the expression of *draxin* was detected only in the dorsal third of the spinal cord. Starting from 76 hpf, *draxin* expression in the spinal cord was below detection limit (Fig. 2.20 O).

draxin expression was also detected in non-neuronal tissues. At 6.5 hpf, low levels of *draxin* mRNA were detected in the posterior part of the embryo. At segmentation stages (between 10.3 hpf and 24 hpf), strong *draxin* expression was detected along the trunk with the highest expression level located in the tail bud. In the embryonic trunk, *draxin* expression got restricted to posterior regions over time. At 24 hpf, non-neuronal expression was detected only in the tail bud.

In summary, *draxin* mRNA was dynamically expressed in the nervous system and in non-neuronal tissues. Within the brain, it was mainly expressed in the telencephalon, in the anterior and dorsal diencephalon and in the lateral hindbrain. At 20 hpf, *draxin* was expressed uniformly throughout the spinal cord. *draxin* expression restricted to the dorsal spinal cord at about 30 hpf and disappeared before 76 hpf. During

segmentation stages, *draxin* was highly expressed in the tail bud.
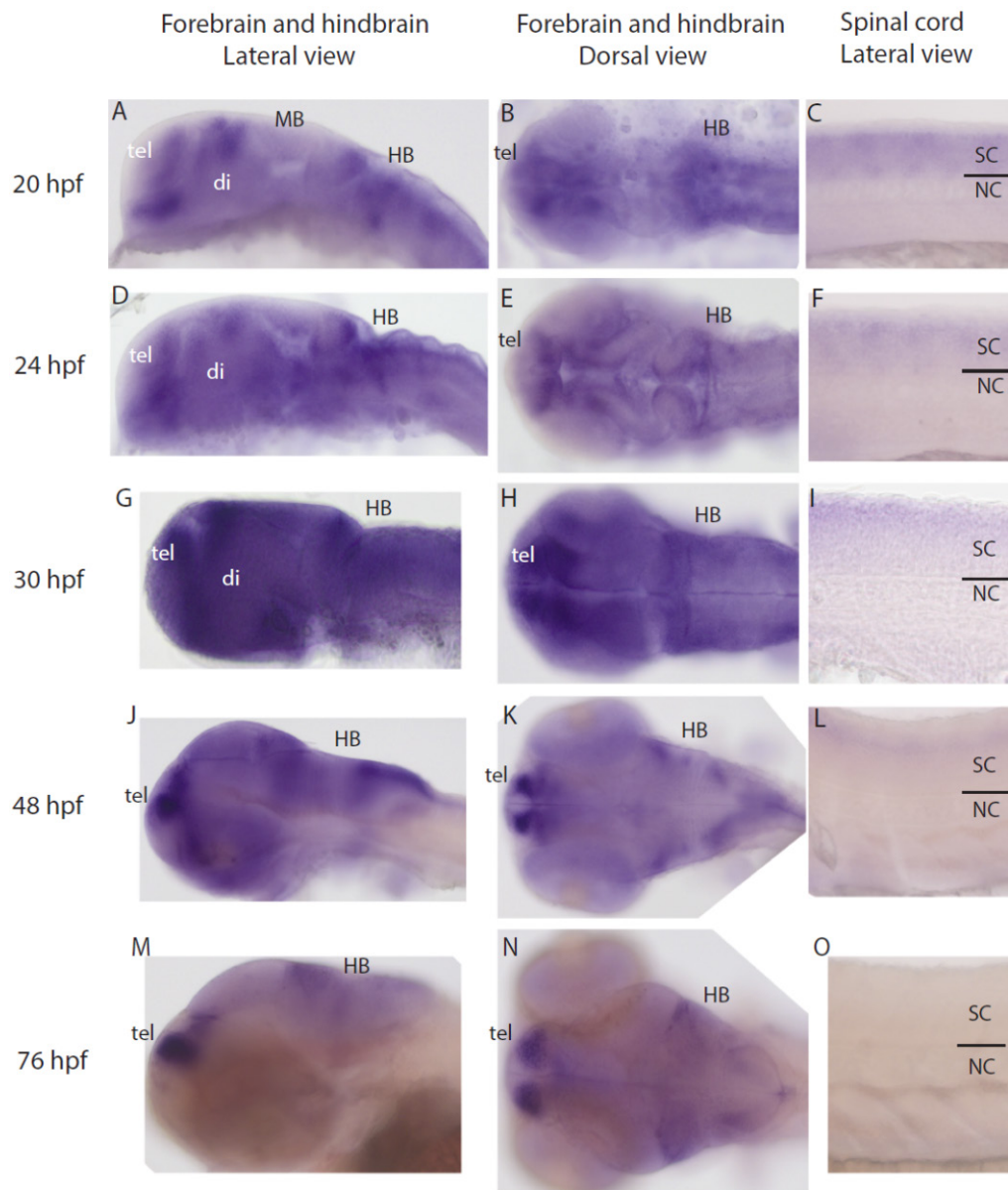
Figure 2.20 *draxin* **mRNA expression in the CNS of zebrafish embryos**

draxin mRNA expression (blue) in the CNS was analyzed by whole mount NBT/BCIP *in situ* hybridization in zebrafish embryos from 20 hpf to 76 hpf. Lateral view of forebrain and hindbrain: A, D, G, J, M with anterior to the left, and dorsal to the top; dorsal view of forebrain and hindbrain of zebrafish heads: B, E, H, K, N with anterior to the left; lateral view of middle region of the spinal cord: C, F, I, L, O with anterior to the left and dorsal to the top. The small bars in the lateral view of the spinal cord panels showing the boundary between SC and NC. tel: telencephalon, di: diencephalon, FB: forebrain, MB: midbrain, HB: hindbrain, SC: spinal cord, NC: notochord.

2.3.2.2 Co-expression of *draxin* and *netrin* in zebrafish embryos

draxin mRNA shows dynamic expression in the forebrain and hindbrain. Interestingly, *netrin* mRNA is known to be expressed in similar brain regions (Lauderdale et al., 1997; Strähle et al., 1997). Thus, I wondered whether these two genes were co-expressed in certain regions of the brain.

In order to detect potential co-expression domains, I performed double *in situ* hybridization experiments for both *netrin* and *draxin* mRNA. Zebrafish *netrin1b* was used in this experiment because it shares a largely overlapping expression pattern with *netrin1a* (Fig. 1.5 C and D, Lauderdale et al., 1997; Strähle et al., 1997). In addition, in order to examine the distribution of the mRNAs in relation to embryonic of axon tracts, I stained the embryos using anti acetylated tubulin antibodies, which labels the major axon tracts. I used 24 hpf embryos for the double *in situ* experiments, because major axon tracts are already founded at this stage (Fig. 1.2 A, Chitnis et al., 1990; Kimmel, 1993; Ross et al., 1992).

Figure 2.21 shows the double *in situ* results from single-plane confocal sections. Co-expression as well as adjacent expression of *draxin* and *netrin1b* mRNA was detected in forebrain regions of 24 hpf zebrafish embryos. Arrowheads indicate co-expression in Figure 2.21 a (dorsal view) and b (lateral view). The co-expression region located posteriorly to the postoptic commissure (POC), arrowheads in Figure 2.21 a'and a''. This region spreads dorsally in the forebrain and overlaps with the supraoptic tract (SOT), shown by arrowheads in Figure 2.21 b' and b''. The two mRNAs were also expressed in ventral regions of the hindbrain along the anterior-posterior axis.

In summary, co-expression of *draxin* and *netrin* mRNA was detected in zebrafish 24 hpf embryos. The co-expression regions partially overlap with the main axonal tracts, the postoptic commissure and the supraoptic tract in the forebrain.
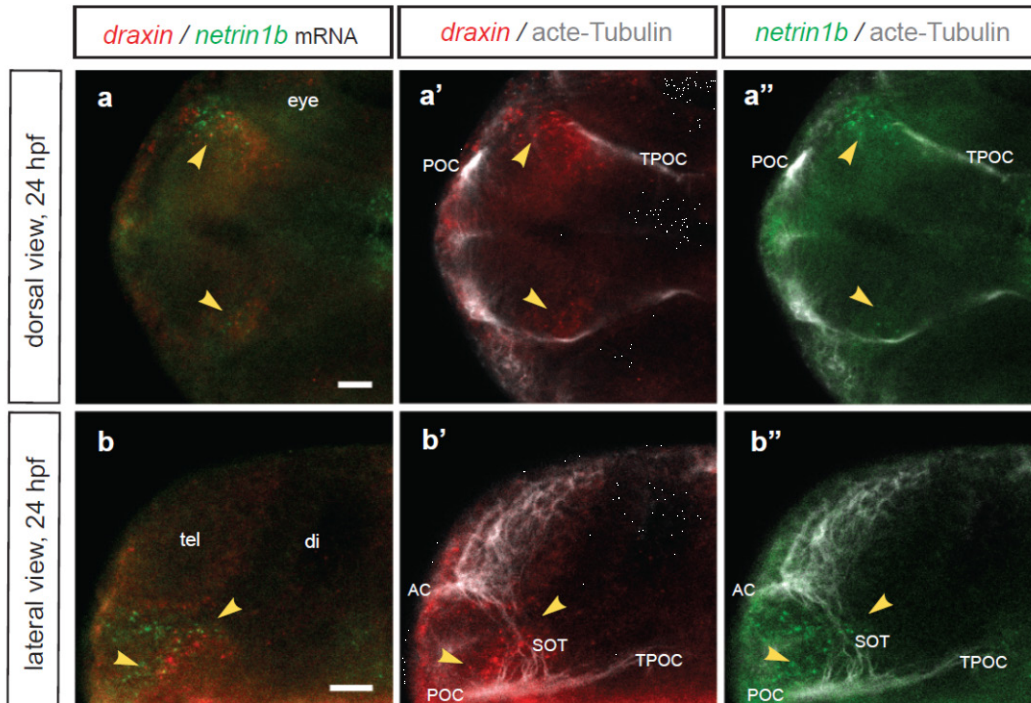
Figure 2.21 Co-expression of *draxin* and *netrin* at axonal tracts in zebrafish 24 hpf embryos

Whole mount double *in situ* hybridization of *draxin* (red) and *netrin1b* (green) mRNA in wild-type 24 hpf zebrafish embryos. The embryos were stained with an anti acetylated tubulin antibody (Acte-Tubulin, white), dorsal view (a-a", anterior to the left) and lateral view (b-b", anterior to the left and dorsal to the top). Arrowheads in (a) show co-expression of *draxin* and *netrin1b* mRNAs in the POC region (dorsal view). In (b), arrowheads show the co-expression in the SOT region (lateral view). tel: telencephalon; di: diencephalon; AC: Anterior Commissure, POC: Postoptic Commissure, TPOC: Tract of the Postoptic Commissure, SOT: Supraoptic Tract. Single plane confocal images were taken using 25X objective lens (Zeiss LSM 780 NLO confocal microscope); scale bar: 20 µm.

2.3.3 Draxin-Netrin binding is detected *in situ* in zebrafish larvae

2.3.3.1 Establishing an *in situ* protein detection assay

In order to determine the distribution of secreted proteins in zebrafish embryos, a novel method for visualizing the expression pattern of Netrin protein was developed. From the previous competition assay (shown in Results, section 2.1.3 in this dissertation), I already obtained indications that Draxin bound to Netrin with high affinity. Thus, I fused a Netrin-binding fragment to a tag to generate an affinity probe for *in vivo* staining. I used the Draxin fragment 209-284 aa as the Netrin-binding probe (blue rectangle in Fig. 2.22 A), and the human IgG Fc (black ellipsoids in Fig. 2.22 A) as tag. Human Fc tag can be detected by anti IgG antibody, thus, enabling the visualization of the distribution of proteins binding to the affinity probe (Fig. 2.22 A).

Several key steps were optimized to conduct this *in situ* protein detection assay. I fixed the target protein *in situ*, while keeping the native binding epitope intact, which was required for binding. To do this, I kept the samples in paraformaldehyde for very short time prior to the staining and washed the sample quickly after the staining. The duration of the fixation and the balance between fixation and permeabilization are dependent on the target protein, while the duration of washing steps are dependent on the binding strength of the target protein and the probe. For these reasons, I experimentally modified the assay according to the stability of the binding partner and the probe used. I gently fixed zebrafish embryos (between 24 and 48 hpf) in a solution of 4 % PFA containing 1 % Triton X-100 for 5-10 minutes at room temperature. Longer fixation decreases the ability to detect bound proteins. I preformed quick washes between the staining and post-staining steps (3 minutes X 3 times). Short-washing can cause increased background staining, whereas excessive-washing can lead to loss of signal.

I performed two sets of experiments to detect *in situ* Netrin distribution using the Draxin$_{209-284aa}$ -human Fc probe:
1) Wild type fish embryos vs. Netrin-1 morphants in which the Netrin-1 protein levels were knocked down
2) *netrin1a* mutant fish vs. siblings
For both experiments, I chose 24 to 48 hpf zebrafish embryos because axonal fine tract mainly develop during this time.

2.3.3.2 *In situ* binding result 1: WT and morphant zebrafish larvae

In wild type 48 hpf zebrafish embryos, I detected signal near floor plate cells using the Draxin$_{209\text{-}284aa}$ - hFc affinity probe (Fig. 2.22 B, arrowheads shown in a''). The floor plate cells in the anterior hindbrain were labeled by the sonic hedgehog-GFP transgenic line (*shh*:GFP, Fig. 2.22 B, a' and b'). Because floor plate cells are a known source for Netrin-1, I hypothesized that the signal detected by the Draxin$_{209\text{-}284aa}$ affinity probe corresponded to extracellular space localized Netrin-1 proteins.

To test the above hypothesis, I injected morpholinos for zebrafish *netrin-1* paralogs *netrin1a* and *netrin1b*, to knockdown both genes at the same time. Comparing the double-knockdown morphants to their WT siblings, the signal derived from the bound probe was barely detectable in the double-knockdown condition (Fig. 2.22 b, b' and b''). This indicates that the Draxin$_{209\text{-}284aa}$ affinity probe indeed detected Netrin-1 proteins.

Figure 2.23 shows the details of Netrin proteins detected by the Draxin$_{209\text{-}284aa}$ probe in 33 hpf WT embryos. An anti-VasnA antibody shows the membrane outline of floor plate cells (Paolo Panza et al., in preparation). The dashed box in Figure 2.23 (a) and (b) indicates the region which is scaled up in (c)-(c'') and (d)-(d'). I used the most anterior region of the notochord as a reference location in the lateral views (the star in (b), (d) and (d'')). The signal was detected in both dorsal and ventral regions of the single layer of floor plate cells (arrowheads in Fig. 2.23 (d), same location in (d'')) as well as membrane associated densities at the dorsal tip of these cells (arrowhead in Fig. 2.23 (c) and (d)). This subcellular localization of Netrin1a protein confirmed the observation from Netrin1a overexpression experiments in Results, section 2.3.1 of this dissertation (Fig. 2.19). Both experiments show that Netrin proteins localized to membrane associated densities. In a middle coronal optical section, the floor plate lateral domains of the mindbrain were also highlighted (right two arrowheads in Fig. 2.23 (c)).

In sum, the results from the binding experiments using a Draxin$_{209\text{-}284aa}$ affinity probe provide strong evidence that Draxin and Netrin-1 are able to interact *in situ* in zebrafish embryos.
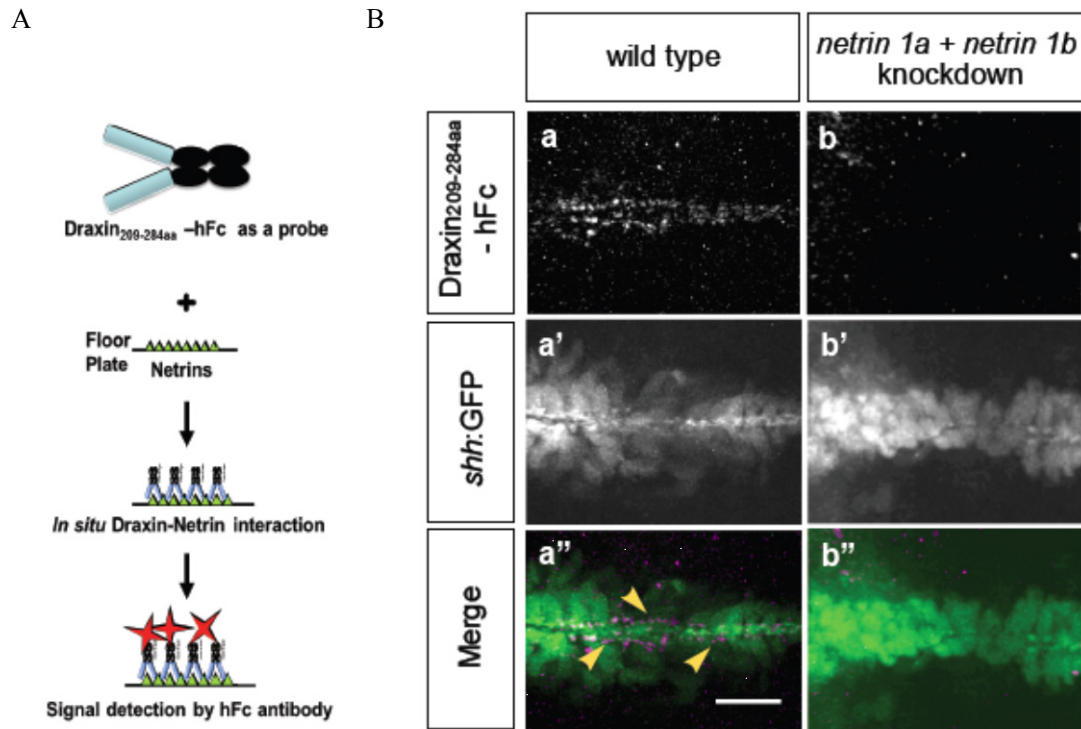
Figure 2.22 *In situ* **detection of the Draxin-Netrin interaction in zebrafish larvae using an affinity probe**

(A) Schematic illustration of the experimental design of *in situ* detection of protein interactions. A Draxin fragment (209-284 aa, indicated by the blue rectangle) was fused to the human IgG protein Fc domain (indicated by the black ellipsoids). The fusion protein was generated in HEK293-6E cells as a probe to detect endogenous Netrins in zebrafish embryos. Mildly fixed embryos were incubated with the affinity probe. (B) Representative microscope images of a single confocal section (at confocal z-stacks of 10 µm in depth) showing the floor plate region of the anterior hindbrain (dorsal view, anterior to the left). The signal from the Draxin 209-284aa-Fc fusion probe is detectable in the floor plate region of 48 hpf WT embryos (B-a", arrowheads), but it it is strongly reduced or absent in *netrin1a* and *netrin1b* double-knockdown embryos (B-b"). A *shh:GFP* transgenic line was used to visualize floor plate cells (B-a', B-b'). Scale bar: 20 µm, n > 10 in two independent experiments.
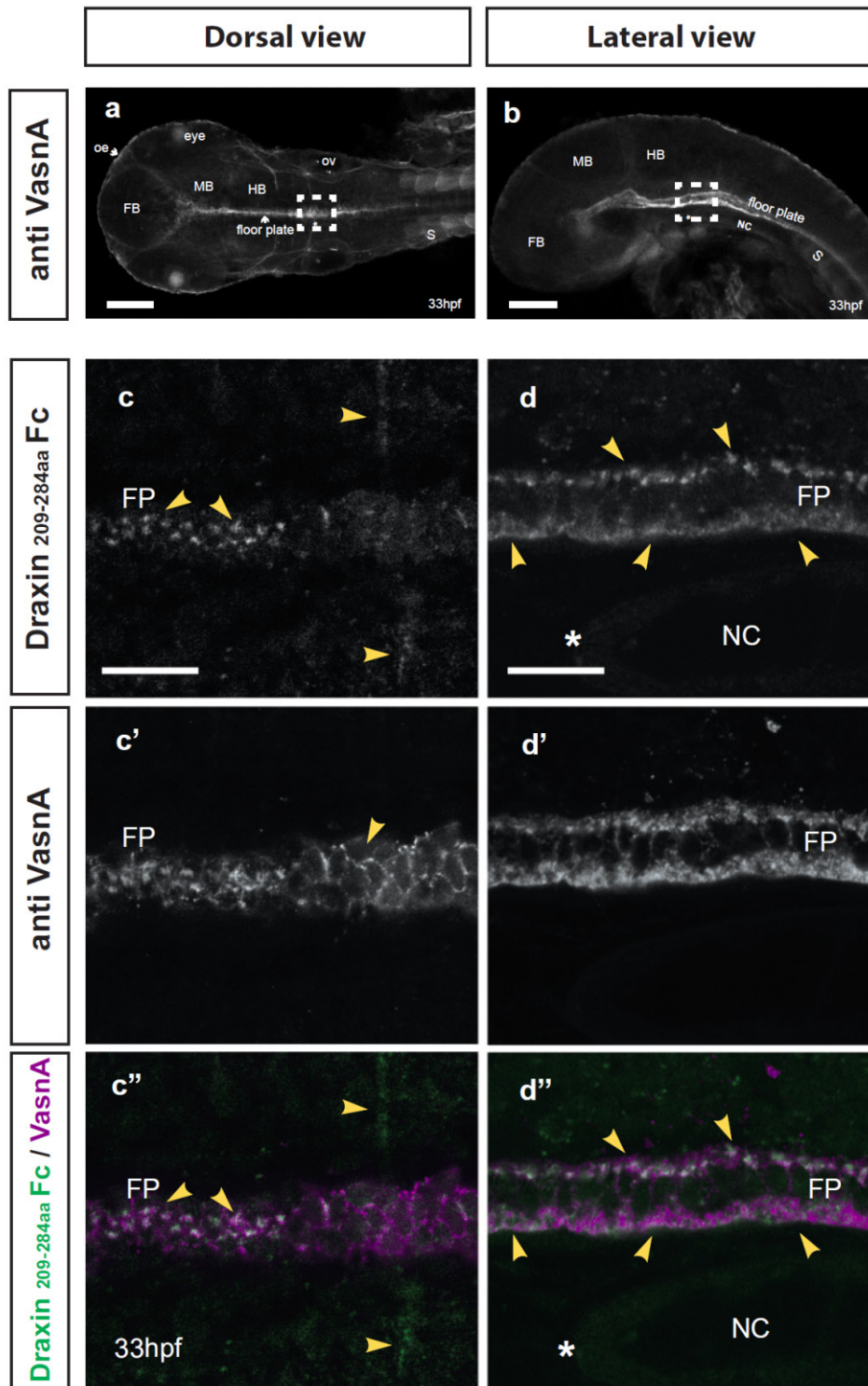
Figure 2.23 Detailed representation of Netrin distributions detected by the Draxin-Fc probe in zebrafish embryos

2.3.3.3 *In situ* binding result 2: *netrin1a* mutant larvae

Since the Draxin-binding-site mapped to the 3rd EGF domain in Netrin (Fig. 2.15), I asked whether the Draxin-Netrin interaction detected *in vivo* indeed requires the 3rd EGF domain in Netrin. A *netrin1a* mutant fish line, *netrin1a* ^{SA12269}, was obtained from the Sanger Institute Zebrafish Mutant Project (Kettleborough et al., 2013) for this purpose. The *netrin1a* ^{SA12269} locus contains a premature nonsense mutation in the first half of the 3rd EGF domain (415Cys to stop) that leads to a protein truncation. The 3rd EGF domain is therefore, non functioned in the heterozegous mutants (Fig. 2.24).

I stained homozygous mutants and WT siblings from the *netrin1a* ^{SA12269} fish line using a Draxin$_{209-284aa}$ - Fc probe to detect endogenous Netrin. In addition, I injected a morpholino for *netrin1b*, to obtain all combinations of *netrin-1* gene expression (e.g. *netrin1a + netrin1b*, *netrin1a* only, and *netrin1b* only). This allowed me to uncover which *netrin-1* gene, *netrin1a* and/or *netrin1b*, was the source of the floor plate located Netrin.

Figure 2.23 (preceding page) Detailed representation of Netrin distributions detected by the Draxin-Fc probe in zebrafish larvae

Representative microscope images showing the floor plate region of whole mount zebrafish larvae stained with the Draxin $_{209-284aa}$ -Fc fusion protein and a VasnA antibody (figure a, c, c' and c": dorsal view, figure b, d, d' and d": lateral view, anterior to the left, 33 hpf). The anti-VasnA antibody outlines the membrane of floor plate cells. Signal was detected at both dorsal and ventral regions of floor plate (arrowheads in d, same location in d") with membrane associated densities at the dorsal tip of the cells (arrowhead in c and d). At the middle coronal optical section, The floor plate cells lateral domains of the hindbrain were also highlighted (right two arrowheads in c). oe: olfactory epithelium, ov: olfactory vesicle, FB: forebrain, MB: midbrain, HB: hindbrain, FP: floor plate, NC: notochord, S: somite. Astrisks label the most anterior region of the notochord which was used as the reference location in b, d and d". The dashed box in a and b indicates the region which is scaled up in c-c" and d-d". Single plane confocal images were taken using 10X (a and b) and 40X ((c and d)) objective lens of a Zeiss LSM 780 NLO confocal microscope; scale bar: 100 μm in a and b, 20 μm in c and d.

It is known from mRNA expression data that *netrin1a* but not *netrin1b* is expressed in the ventral eye region (Lauderdale et al., 1997; Park et al., 2005). Figure 2.25 shows signal from the Draxin$_{209-284aa}$ affinity probe in the ventral retina of WT sibling fish (arrowheads) but not in *netrin1a* [SA12269] fish. The signal was not correlated to *netrin1b* knockdown. This result confirms that the protein detected in the ventral retina is Netrin1a in WT animals. Furthermore, the absence of signal in *netrin1a* [SA12269] fish indicates that the 3rd EGF domain (lacking in the mutant Netrin1a protein) is indeed required for *in situ* detection of Netrin by the Draxin $_{209-284aa}$ affinity probe.

Figure 2.26 shows signal near the hindbrain floor plate. As opposed to the expression pattern in the ventral retina, strong signal in the floor plate was detected in both WT siblings and *netrin1a* [SA12269] mutant fish (arrowheads), but not in the *netrin1b* knockdown condition. This indicates that Netrin1b is probably the major source of Netrin protein in the floor plate region.

In conclusion, these experiments show that the 3rd EGF domain is required for *in situ* binding of endogenous Netrin-1 to the Draxin $_{209-284aa}$ probe in the ventral retina. In addition, Netrin1a is the source of the Netrin proteins detected in the optic region, whereas Netrin1b is most likely the major source of Netrin localized to floor plate cells.
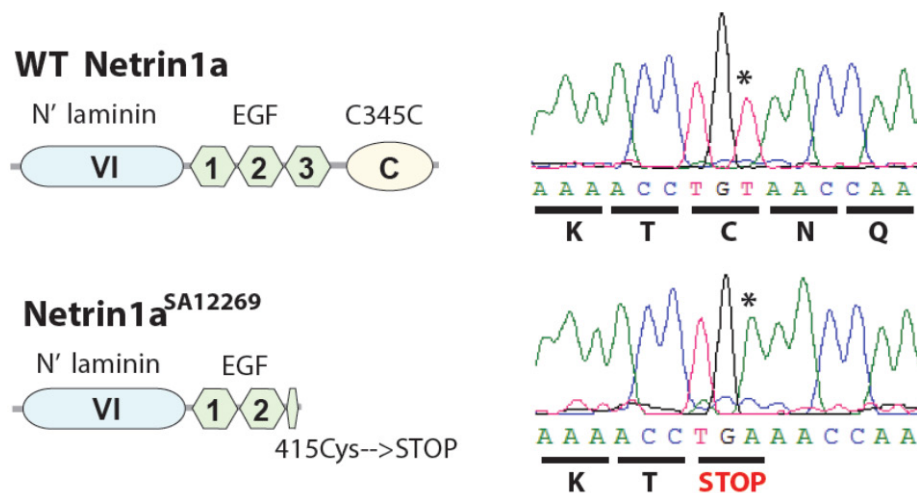
Figure 2.24   Netrin1a mutant allele: *netrin1a^{SA12269}*

Left panel: the *netrin1a* [SA12269] locus contains a premature stop codon in the first half of the 3rd EGF domain (415Cys to stop). Right panel: genotyping results from WT and homozygous mutant fish.
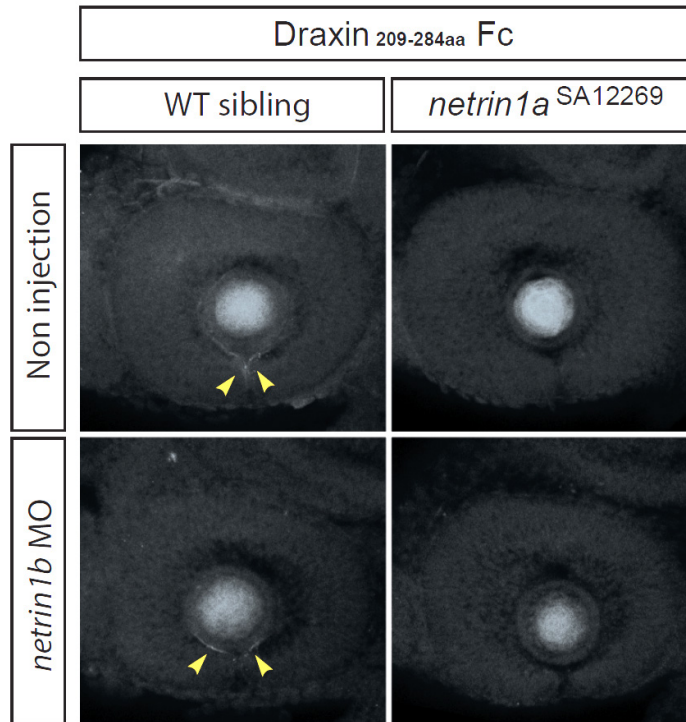
Figure 2.25   The 3rd EGF domain in Netrin1a is required for *in situ* detection *of* Netrin by the Draxin $_{209\text{-}284aa}$ affinity probe

Representative microscope images show that the Draxin $_{209\text{-}284aa}$ affinity probe detected Netrin protein in ventral retina in WT (arrowheads) but not in *netrin1a^{SA12269}* homozygous mutant fish. The signal was not affected in *netrin1b* knockdown fish. Lateral view of eyes from 33 hpf zebrafish. Anterior left, dorsal up. Single plane confocal images were taken using 25X objective lens and a Zeiss LSM 780 NLO confocal microscope.
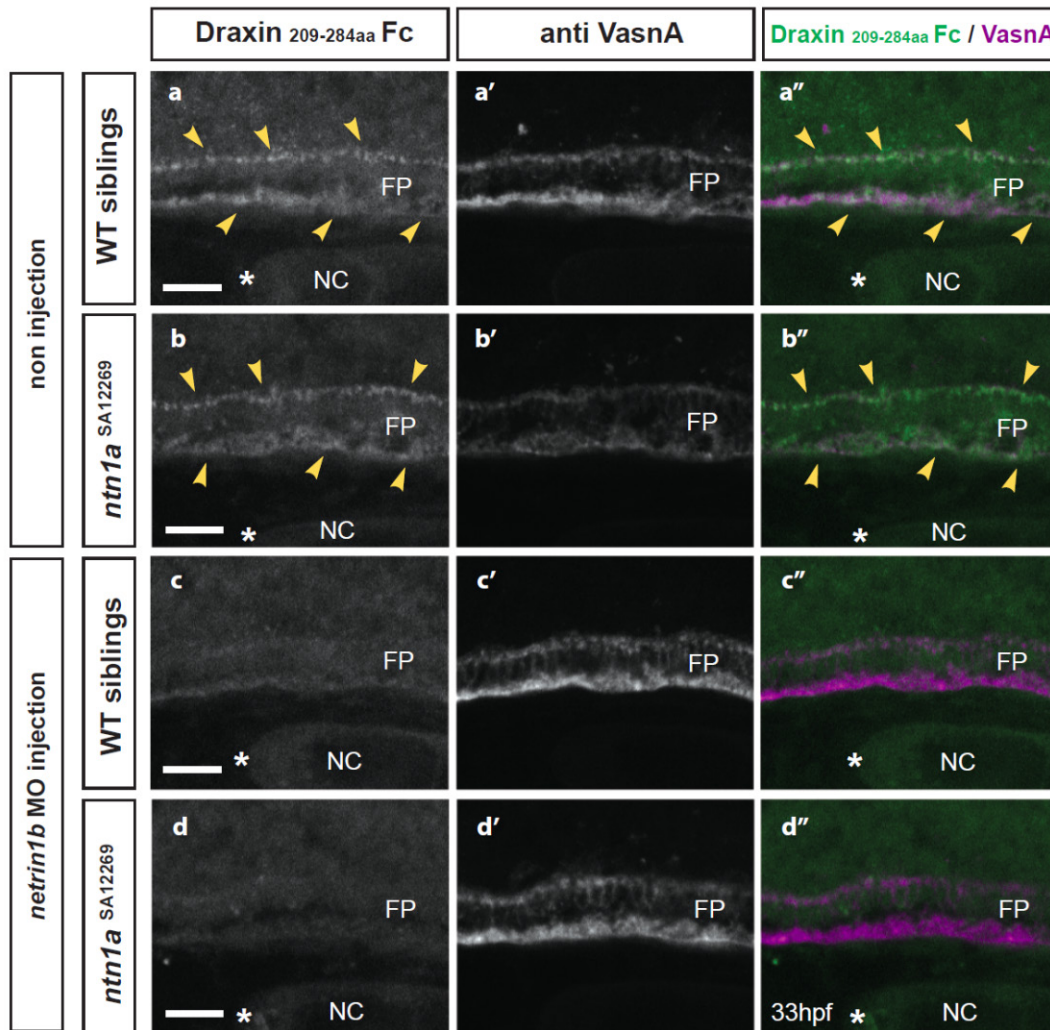
Figure 2.26   Netrin1b but not Netrin1a is highly concentrated in the region of the zebrafish floor plate

Representative microscope images show that the Draxin $_{209-284aa}$-Fc probe detected Netrin in close association with the floor plate. High levels of signal were detected only in uninjected embryos (arrowheads in a, a" for WT siblings, b and b" for *netrin1a*^{SA12269} homozygous mutant fish). An Anti-VasnA antibody outlines the membrane of floor plate cells. Lateral view of the hindbrain floor plate from 33 hpf zebrafish; anterior to the left, dorsal to the top. FP: floor plate, NC: notochord. An asterisk labels the most anterior region of the notochord which was used as the reference location. Single plane confocal images were obtained using 25X objective lens and a Zeiss LSM 780 NLO confocal microscope; scale bar: 20 μm.

Chapter 3

Discussion

3.1 Draxin as a Netrin antagonist

The goal of this study was to discover new players in neural wiring and to explore their working mechanism. Here, I focused on the Netrin signaling system, which is fundamentally involved in the development of the nervous system. Specifically, the aim of this dissertation is to test the function of Draxin, a new binding partner of Netrin, in Netrin signaling during axon pathfinding decisions.

Using biochemical approaches, I detected direct binding between Draxin and Netrin proteins from distinct vertebrate species. I determined how the interaction is able to affect Netrin signaling and showed that Draxin is able to compete with Netrin receptors for binding to Netrin-1. Furthermore, I was able to map the interaction interface to a highly conserved short peptide in Draxin and the 3rd EGF domain of Netrin. The interaction was also detected *in vivo* using two embryonic assays. Thus, I propose the hypothesis in which Draxin can serve as an antagonist in netrin signaling. In this chapter, I mainly discuss the *in vitro* and *in vivo* evidence for this inhibitory hypothesis.

3.1.1 Inhibitory hypothesis

The Netrin family comprises canonical secreted axon guidance cues important for the wiring of nervous systems. Distinct Netrins and Netrin receptors have been identified to carry out the guidance function. However, no direct Netrin modulator has been described yet. Notably, Draxin was found as a "chemorepulsive axon guidance molecule" (Islam et al., 2009). The current understanding is that Draxin functions as a repulsive ligand in axon guidance. Scientists were searching for its endogenous receptors that might carry out the repulsive guidance function (Ahmed et al., 2011).

In my experiments, I observed that Draxin directly binds to several zebrafish Netrin family members. These interactions were also observed using orthologous human proteins (Fig. 2.1 and Fig. 2.2). The interactions between Netrins and Draxins linked the two known signaling systems, thus providing a hint towards a potential inhibitory function of Draxin.

Here, I propose the inhibitory hypothesis: Draxin might modulate Netrin signaling, the physical interaction between Draxin and Netrin might block or modify Netrin's ability to interact with its receptors (Fig. 3.1).
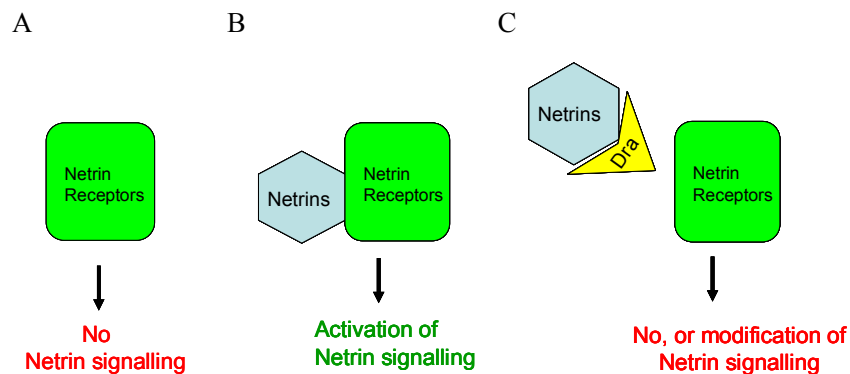
Figure 3.1   Inhibitory hypothesis for Draxin by direct binding to Netrin
(A) and (B), the activation of Netrin signaling is highly dependent on the presence of Netrins. (C), Draxin might function in Netrin signaling by directly binding to the ligand Netrin. The binding blocks or modifies Netrin's ability to interact with its receptors. Dra: Draxin

This hypothesis is strongly supported by results of my *in vitro* binding experiments and the competition assay. Besides the detection of direct binding between Draxin and Netrin, I observed no binding of Draxin to Netrin receptors using our assays (Fig. 2.4 and Fig.2.9). These experiments do not support the model that Draxin functions directly through Netrin receptors. There still was the possibility that Draxin, Netrin and the Netrin receptor form a complex, especially if Netrin shares different binding sites with Draxin and Netrin receptors. However, my results from the competition assay showed that the tagged Draxin is able to outcompete Netrin receptors for Netrin binding (Fig. 2.6 and Fig. 2.7). Also, the binding-sites mapping experiments showed that the Draxin binding site in Netrin is within the 3rd EGF domain (Fig. 2.15), which is the known binding site for Netrin to the Netrin receptors DCC and Neo1 (Finci et al., 2014; Xu et al., 2014). These data show that Netrin shares the same binding site with the Netrin receptors and Draxin, thus a ternary complex containing the three proteins through Netrin is unlikely to form. Hence, the proposed inhibitory hypothesis shown in Figure 3.1 most likely describes how Draxin works in Netrin signaling system inlight of the current results.

3.1.2 Zebrafish and human binding networks of Draxins, Netrins, and Netrin receptors

Based on the obtained binding data by AVEXIS for Draxins, Netrins and the Netrin receptors (Fig. 2.1, Fig. 2.2 and Fig. 2.4 in this dissertation), I summarized the binding networks for both zebrafish and human proteins in Figure 3.2.

In these binding networks, binding is detectable for both zebrafish and human Netrin-1 to the Netrin receptors DCC and UNC5s. This confirmed the previous observations from mammalian Netrin family members (Keino-Masu et al., 1996; Leonardo et al., 1997; Haddick et al., 2014). Both zebrafish and human Draxin proteins bound to laminin γ-chain derived Netrins (zebrafish and human Netrin-1, human Netrin-3), but not to other Netrin family members. No interactions were observed between Draxins and all the tested Netrin receptors.
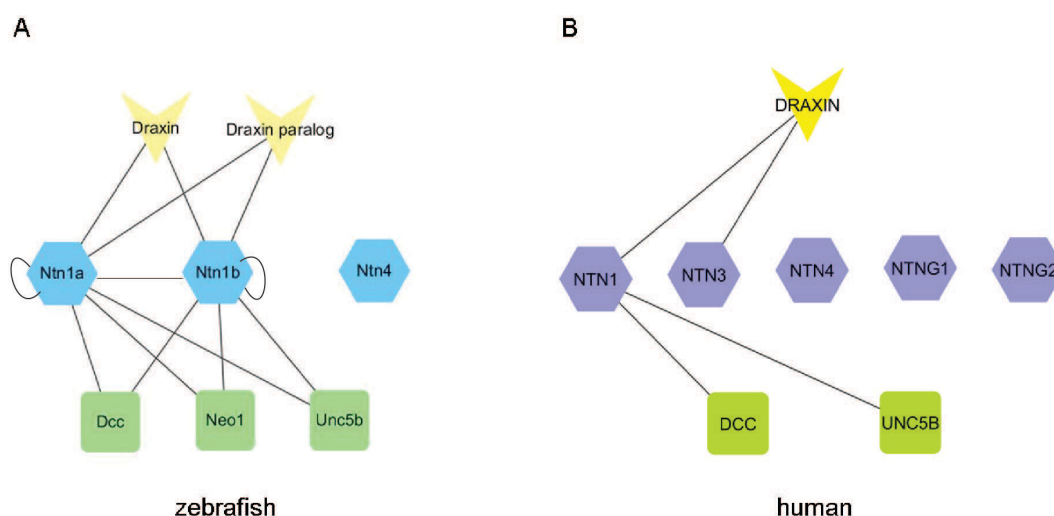
Figure 3.2   Summary of the Draxin-Netrin-Netrin receptor binding networks determined by AVEXIS

Zebrafish (A) and human (B) Draxin-Netrin-Netrin receptor binding networks summarized from Fig. 2.1, Fig. 2.2 and Fig. 2.4. Lines indicate binding. Zebrafish Draxin paralog is si:dkey-1c11.1, Dcc: Netrin receptor deleted in colorectal cancer; Neo1: Netrin receptor neogenin.

How to explain the different connections compared to a previous report?

A previous study claimed that Draxin directly bind to multiple Netrin receptors including DCC, Neogenin, Unc5s and DSCAM (Ahmed et al., 2011). This binding network was based on cell overlay assays as well as pull-down assays. The authors therefore concluded that the Netrin receptors are the missing receptors for Draxin.

How to explain the different connectivity within binding networks? These differences could be due to the different assay systems used in the two studies. AVEXIS detects direct interactions between bait and prey proteins. On the contrary, cell based assay and pull-down assays are prone to detect also indirect binding events. These indirect events might be caused by either a natural complex or a nearest neighbor effect such as interactions mediated by cell surface heparan sulfate proteoglycans. In fact, all individual partners, Draxin, DCC and Netrin-1 are able to bind to heparin (Bennett et al., 1997; Chen et al., 2013; Matsumoto et al., 2007). These facts might support an indirect binding possibility.

Clearly, there are several lines of evidence supporting that Draxin is not able to bind to the Netrin receptors. Direct binding between Draxin and DCC was not detectable by the SPR method (Haddick et al., 2014). Our group obtained similar results using the same assay (Fig. 2.9). SPR is the current golden-standard method to obtain kinetic data from direct binding events. The failure of detecting direct binding between Draxin and Netrin receptors therefore offers a strong argument against Netrin receptors serving also as Draxin receptors. Moreover, in my competition assay, I observed that Draxin is able to outcompete Netrin receptors for Netrin binding. This would not be the case if Draxin was able to directly bind to Netrin receptors. Furthermore, the binding of Draxin to Netrin is also detectable using *in vivo* assays (Fig. 2.19 and Fig. 2.22). All of my data suggest that Draxin is not able to bind to Netrin receptors.

New findings in the Netrin binding networks

Besides the interaction between Draxin and Netrin, there are other interesting findings in the Netrin-Netrin receptor binding networks in this study. The majority of the Netrin family members were identified through homology based searches, and most of the ligand-receptor pairs were assumed from either orthologous fruit fly or rodent interactions, frequently not supported by direct binding evidence. Often, the functional interpretation of a detected phenotype was only based on expression data and binding assumptions. In this study, the ligand-receptor binding networks in Figure

3.2 summarized from results obtained by AVEXIS, provide direct binding evidence.

New findings from the Netrin-Netrin receptor binding networks:

1) DCC and Unc5 family Netrin receptors did not bind to Netrin-4, Netrin-G1 and Netrin-G2 both in zebrafish and human. This confirms that Netrin-4 and Netrin-G family members have their own receptors (Schneiders et al., 2007; Lin et al., 2003) and further illustrates that Netrin-1 does not share known receptors with Netrin4 and Netrin-G family members.

2) Receptors for Netrin1a are also the receptors for Netrin1b in zebrafish. Although the two zebrafish Netrin-1 paralogs—Netrin1a and Netrin1b—share over 88 % protein sequence identity (Lauderdale et al., 1998), this is the first experimental evidence showing that zebrafish Dcc, Unc5b and Neo1 serve as receptors for both Netrin1a and Netrin1b. It raises the possibility that Netrin1a and Netrin1b share a redundant function in regions of co-expression.

3) Homo- and heterotypic- interactions were detected with zebrafish Netrin1a and Netrin1b. In addition, I also observed a very weak homotypic interaction for human Netrin-1 (see Fig. 3.2 for the binding value). This could be explained by a possible dimerization of the Netrin-1 protein (Xu et al., 2014).

4) Surprisingly, using AVEXIS, human DCC and Unc5b did not bind to human Netrin-3. This is not in line with a previous study using the mouse Netrin-3 homolog (Fig. 7-8 in Wang et al.,1999). In that study, mouse Netrin-3 bound to rat DCC, Neo and Unc5s as well as mouse Unc5H3 in a cell based assay. Although cell based assays tend to detect indirect interactions, I cannot exclude the possibility that the protein levels of human Netrin-3 were not high enough for the detection in my AVEXIS experiments. This is because the binding value observed for Draxin, the only positive binding partner, was not high. Thus, these results need further validation.

3.1.3 Kinetic binding data of the Draxin-Netrin interaction indicates biological relevance

The binding strength of an inhibitor to its target ligand needs to be strong in order to outcompete the interactions of the ligand to its endogenous receptors. The kinetic data obtained in SPR experiments show that the binding strength between Draxin and Netrin is in the low nM range. A similar binding strength had been reported for the Netrin-DCC and Netrin-Unc5b interactions (Keino-Masu et al., 1996; Leonardo et al., 1997). In addition, the Draxin vs. Netrin receptor competition experiments showed that the applied Draxin concentrations are of biological relevance. Figure 2.7 shows 50 % inhibition of the Netrin1a-Unc5b interaction by Draxin occurs around 10 nM, and 50 % inhibition of the Netrin1a-Dcc interaction occurs around 50 nM. This is consistent with a biologically relevant role *in vivo*.

The different inhibition efficiencies of Draxin towards DCC, Unc5b and Neo1 probably reflects the distinct binding strengths of Netrin to these receptors. The competition curve is different from a binding curve: the effect of the competition is not only depending on the affinity of the inhibitor to the ligand, it is also highly related to the binding strength of the ligand to the corresponding receptor:

$$\text{A-B} \rightleftharpoons \text{A} + \text{B} + \text{C} \rightleftharpoons \text{A-C}$$
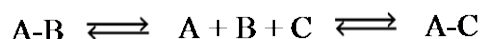
(A: Netrin, B: Netrin receptors, C: Draxin)

It is possible that different ligand-receptor pairs require different inhibitor concentrations to break the interactions. Most likely, the Netrin-Unc5b interaction is more sensitive to the Draxin concentration than the Netrin-DCC or Netrin-Neo1 interactions.

3.1.4 Proposed working model based on *in vitro* experiments

From the competition experiments and the binding site mapping experiments performed in this study, I propose a working model which is presented in Figure 3.3. By directly binding to Netrin-1, Draxin competes with Netrin receptors for Netrin binding. The binding interfaces were narrowed down to a highly conserved 22 aa fragment in Draxin and the 3rd EGF domain in Netrin-1. This suggests that Draxin

functions as an extracellular Netrin signaling modulator in vertebrates.

Interestingly, recent Netrin-1/Netrin receptor structural studies (Finci et al., 2014; Xu et al., 2014) showed that the 3rd EGF domain in Netrin-1, which I identified as the Draxin-binding-domain, is also crucial for Netrin receptor binding. This indicates that Draxin and Netrin receptors are competing for the same binding site in Netrin-1, offering a mechanistic understanding for the proposed working model.
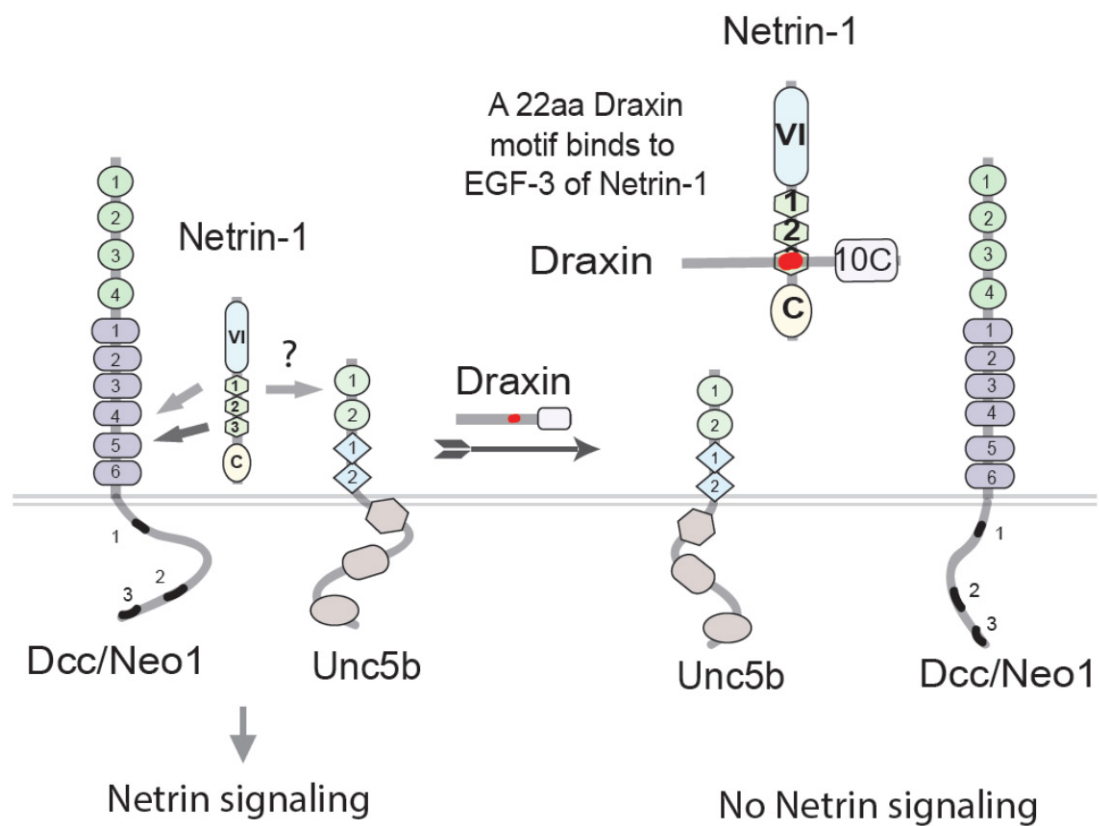
Figure 3.3   Working model of Draxin's function in Netrin signaling

By directly binding to Netrin-1, Draxin competes with Netrin receptors for Netrin binding. The binding interfaces between Draxin and Netirn were narrowed down to a highly conserved 22 aa fragment in Draxin and the 3rd EGF domain in Netrin-1.

3.1.5 Different expression patterns of zebrafish nerin1a and netrin1b

The two zebrafish *netrin-1* genes, *netrin1a* and *netrin1b*, are mainly expressed in ventral regions of the CNS in early zerbafish embryos, but they have slightly different expression patterns in the eyes, spinal cord and floor plate.

In the developing eyes, zebrafish *netrin1a* mRNA is expressed in the ventral optic stalk at 18 hpf, the expression is maintained in the ventral retina at the optic fissure through 32 hpf (Lauderdale et al., 1997). *netrin1b* mRNA, on the other hand, although highly expressed in the forebrain, is not detectable in the eyes (Stähle et al., 1997; Park et al., 2005). Protein expression at 33 hpf, as detected by a Netrin affinity probe shows Netrin protein in the ventral retina of WT fish and *netrin1b* morphants but not in *netrin1a* [SA12269] homozygous mutant fish (Fig. 2.23). These findings support the idea proposed from a mouse study on Netrin-1 (Deiner et al., 1997), suggesting that the zebrafish retinal ganglion neurons use Netrin1a to exit the eyecup but not Netrin1b.

In the trunk, zebrafish *netrin1a* is expressed in the ventral one third to half of the spinal cord from 15 hpf till at least 30 hpf whereas *netrin1b* is only strongly expressed in floor plate cells (Lauderdale et al., 1997; Lauderdale et al., 1998; Stähle et al., 1997). The different expression patterns are supported by *in vivo* binding experiments in this study. Figure 2.26 shows that only Netrin1b but not Netrin1a protein is detectable at floor plate region.

Altogether, the different expression patterns of zebrafish *netrin1a* and *netrin1b* suggest that the two paralogous genes have separate functions although they share the same set of receptors. Furthermore, the expressions of *netrin1a* and *netirn1b* are differently regulated by hedgehog genes (Lauderdale et al., 1998), supporting that the two genes have diverged and gained independent new functions.

Interestingly, the two zebrafish *netrin-1* genes share comparable expression patterns with two chick *netrin* genes in the spinal cord. The zebrafish *netrin1a* is expressed in the ventral half of the spinal cord, which is similar to the chick *netrin-2*. Likewise, the zebrafish *netrin1b* is extensively expressed in the floor plate region just like the chick *netrin-1* (Kennedy et al., 1994; Wang et al., 1999). It is reasonable to hypothesize that zebrafish *netrin1b* shares similar functions with chick *netrin-1,* while zebrafish *netrin1a* is functional comparable to chick *netrin-2.*

3.1.6 Potential co-expression regions of Draxin and Netrin proteins

To interact *in vivo*, Draxin and Netrin proteins need to encounter each other in the embryo. Although there is no direct evidence showing that the two proteins meet *in vivo*, the mRNA expression data shown in this study as well as Netrin mRNA and protein expression data shown in previous studies (Serafini et al., 1996; Kennedy et al., 2006) strongly indicate that both secreted molecules encounter each other mainly in the nervous system. In the following chapter, I discuss about the potential co-localization regions of *draxin* and *netrin* in vertebrates.

mRNA co-expression and adjacent expression regions

I) Nervous system
● Forebrain and forebrain axon tracts
In zebrafish, *draxin* and *netrin* are co-expressed in the ventral anterior diencephalon in 24 hpf embryos. The co-expression regions are overlapping with the major axonal tracts POC and SOT. In addition, adjacent expression regions are found in the forebrain: *draxin* is expressed along the border of the telencephalon, overlapping with the main forebrain commissure—AC whereas *netrin1a* and *netrin1b* are both expressed adjacently to the AC. Also, *draxin* and *netrin1a* are expressed adjacently in the dorsal diencephalon between the axon tracts of the DVDT and the PC (Fig. 2.20 and Fig. 2.21 in this dissertation). In mouse, both *draxin* and *netrin-1* are expressed in the regions of the forebrain commissures AC, CC and HC within E14.5 ± 2 embryos (Islam et al., 2009; Serafini et al., 1996). These adjacent and overlapping expression domains suggest a collaborated function between *draxin* and *netrin* in the formation of forebrain commissures in vertebrates.

● Midbrain
In zebrafish, *draxin* is expressed in the dorsal tectum with a lateral-ventral extension towards one third depth of the midbrain in 24 hpf embryos. On the other hand, *netrin1a* is expressed throughout two thirds of the ventral midbrain with the highest expression region around the ventral midline (compare transverse sections in Fig. 1.5 K and Fig. 1.7 I in the introduction chapters). *draxin* and *netrin1a* show adjacent expression in the zebrafish midbrain.

● Hindbrain
In zebrafish, the two genes show strong expression regions located adjacently within

24 hpf embryos (compare transverse sections in Fig. 1.5 L and Fig. 1.7 J). It is also possible that the two genes are co-expressed in lateral parts of the hindbrain from 24 hpf to 30 hpf. The adjacent strong expression domains in the hindbrain indicate a potential interaction of the two proteins along the expression boundary. In addition, overlapping region of *draxin* with *netrin-2* in dorsal hindbrain are assumed from 36 hpf to at least 72 hpf (compare Fig. 1.5 in this dessertation with Fig. 2M,Q,T,N,R,U in Park et al., 2005).

● Spinal cord

In zebrafish, both *draxin* and *netrin1a* show dynamic expression patterns, and the encoded proteins are likely to meet each other in the spinal cord between 20 hpf and 48 hpf. *draxin* is expressed through out almost the entire spinal cord and *netrin 1a* and *1b* are strongly expressed in the ventral spinal cord in 24 hpf embryos. (compare Fig. 1.5 C, D, M with Fig. 1.7 C, D, K in this study). At 30 hpf, *draxin* is expressed more dorsally and *netrin1a* expressed more ventrally with gradients towards each other. This dorsal-ventral expression in the spinal cord was also described in chick. In 15-19 stage chick embryos, *draxin* is expressed dorsally and the expression of *netrin-2* spands the ventral two thirds of the spinal cord. Similar expression patterns were also observed in mice at E10.5 for *draxin* and *netrin-1* (Islam et al., 2009; Kennedy et al., 1994, Kennedy et al., 2006; Wang et al., 1999).

● Olfactory bulb

In zebrafish, *draxin* is strongly expressed in the ventral telencephalon at 30 hpf, intensive expression is visible in the olfactory bulb between 48 hpf until and 76 hpf. *netrin1a* is expressed at the telencephalic midline and *netrin1b* in the ventral part of the olfactory bulb at 27 to 53 hpf. Thus, *draxin* and *netrins* are probably partially co-expressed in the olfactory bulb and adjacently expressed between the border of the peripheral olfactory organs and the olfactory bulb at the time period when the olfactory axons are navigating to and extending into the central regions of the olfactory bulb (Fig. 1.5 in this study and Fig. 2 in Lakhina et al., 2012). In rat, *netrin-1* is mainly expressed in the peripheral olfactory system on the road where the olfactory axons extend to the olfactory bulb, similar to *netrin-1* expression in zebrafish (Astic et al., 2002).

● Eye

netrin-1 is expressed in the ventral retina, it is suggested to guide the optic nerve grow out of the retina in the mouse system (Deiner et al., 1997). In zebrafish, *netrin1a* expression is surrounding the optic fissure at 24 hpf, similar to the expression in

mouse. Notably, in the same embryonic stages, *draxin* is expressed in the ventral retina dorsal, adjacent to the optic fissure (Miyake et al., 2012).

II) Non neuronal tissues
- Somites

draxin is highly expressed in somites both in zebrafish (11-24 hpf) and chick (stage 15). Strikingly, both zebrafish and chick *netrins* are expressed in large areas in the somites (Hale et al., 2011; Lauderdale et al., 1997; Kennedy et al., 1994 and Wang et al., 1999).

Potential protein co-expression regions

The Draxin and Netrin proteins have the ability to meet each other *in vivo*. Although gradients from secreted proteins are not easy to detect, there is evidence for the protein distribution of Draxin and Netrin in the spinal cord. Draxin protein is highly diffusible in stage 19 chick embryos. It is distributed along the basement membrane from the dorsal top to the ventral half of the spinal cord. Similar distribution was detected for mouse Draxin in E10.5 and 11.5 mouse embryos (Islam et al., 2009). Comparably, in stage 17 chick embryos, Netrin-1 is detectable from its source—floor plate—to the ventral two thirds of the spinal cord. A similar protein gradient has been shown for E9.5 mouse embryos. In the mouse spinal cord, Netrin-1 was detected along the lateral basement membrane till almost the ventral three quarters height (Kennedy et al., 2006). Combined, these findings indicate that Draxin and Netrin proteins are likely to encounter each other in the middle of the spinal cord in chick and mouse embryos.

Secreted proteins form diffusible gradients *in vivo*

The above described protein distribution shows that both Draxin and Netrin proteins are highly diffusible in chick and mouse embryos. Both proteins have the ability to travel far away—half depth of the spinal cord—from their original secreting centers. A quantitative measurement showed that Netrin-1 protein was able to travel 250 μm in the chick spinal cord at stage 17 and 150 μm at stage 23, which is about 20 neural epithelial cells away from the source (Kennedy et al., 2006).

Theoretically, how far a secreted protein is able to travel *in vivo* depends on the mobility of the protein and the surrounding extracellular space. A recent study on the formation of Fgf8 morphogen gradient showed that, two factors—"fast, free diffusion

of single molecules" and "a source-sink mechanism"—contribute to the formation of the Fgf8 gradient (Yu et al., 2009). Where exactly the two secreted proteins—Draxin and Netrin—meet in the native environment needs further studies.

3.1.7 In vivo working model for the Draxin-Netrin interaction

In vivo evidence for Draxin's role in Netrin signaling

Relevant *in vivo* data for Draxin and Netrin-1 already exist in the literature. Analysis of knockout mice and ectopic expression conditions in chick support the idea that Draxin is a Netrin signaling inhibitor. For example, disorganized "thick bundles of TAG-1 positive axons along the basement membrane" were observed in draxin knockout mice (Islam et al., 2009, Fig. 4B). This phenotype could be explained by Draxin mediated perturbation of the Netrin-1 activity gradient. Another example is that chicken Draxin has the ability to "disrupt the routing of commissural axons *in vivo*" when ectopically expressed in the chick spinal cord (Islam et al., 2009, Fig. 3 and Fig. S5). Based on this data, the authors concluded that Draxin acts as "a repulsive guidance protein" (Islam et al., 2009) although this finding is also consistent with the idea that Draxin antagonizes Netrin-1's attraction. Together, these studies provide compelling evidence showing that Draxin plays a role in Netrin signaling.

Advantages of the biochemical approach to determine the working mechanism

The key point of this study is to establish Draxin "as an anti-attractant operating directly on Netrin" rather than "a repulsive guidance ligand". The biochemical approach used in this study focusing on the analysis of direct interactions between Draxin and Netrin is suitable to distinguish the two possibilities. *In vivo* experiments, although informative, are not the best choice to address this question. For example, the above-mentioned literature data show that Draxin loss-of-function and gain-of-function experiments in mouse and chick cause phenotypes of commissural axons, like axon growth, midline crossing and fasciculation defects. These defects are all reminiscent of Netrin-1 perturbations and the phenotypes suggest that Draxin is part of the Netrin signaling pathway. However, they cannot tease apart the different working models. In contrast, the biochemical data obtained in this study help to explain the observed *in vivo* phenotypes and clearly point to the possibility that

Draxin acts "as an anti-attractant operating directly on Netrin".

***In vivo* working model for the Draxin-Netrin interaction in the vertebrate spinal cord**

In the *in vivo* working model, the inhibitory hypothesis coming from the protein interaction data and the results obtained by competition assay were brought in line with gene expression data and the published Draxin and Netrin-1 *in vivo* phenotypes.

Opposing gradients of secreted molecules are frequently observed in early embryonic axis patterning (Lee et al., 2006; Reversade & De Robertis, 2005; De Robertis, 2006). The embryonic dorsal-ventral patterning is mediated by reciprocal gradients which are formed by ventrally expressed BMPs and dorsally expressed chordin/noggin. Much alike, according to the gene expression locations, Draxin and Netrin-1 possibly form reciprocal protein gradients along the dorsal-ventral axis of the developing spinal cord in vertebrates (Fig. 3.4).
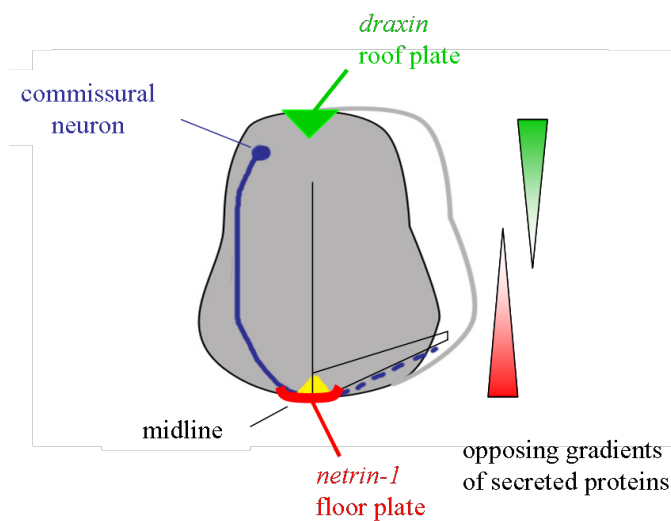
Opposing gradient mechanism in vertebrates spinal cord

Figure 3.4   *In vivo* working model for the Draxin-Netrin interaction in the vertebrate spinal cord

Draxin and Netrin-1 possibly form reciprocal protein gradients along the dorsal-ventral axis of the developing spinal cord in vertebrates.

Results from this study show that by directly binding to Netrin, Draxin prevents the binding of Netrin to its receptors. Draxin acts as a Netrin antagonist thus shaping or sharpening the active Netrin-1 gradient in the spinal cord. The regions where free Netrin is available for efficient activation of Netrin receptors on the growing commissural neurons would shift to a more ventral position due to the Draxin's antagonistic function of Netrin.

A similar mechanism might operate in other brain regions, for example, in the olfactory bulb and midbrain-hindbrain regions where draxin and netrin show reciprocal expressions. In the regions of co-expression (e.g. places surrounding forebrain commissures), Draxin might shape the functional Netrin gradient by directly occupying Netrin proteins. The next step of this research is to test this opposing gradient mechanism in vivo within the mentioned potential regions.

Last, because Draxin only exists in vertebrates, the regulation of Netrin by Draxin might be an invention of vertebrates.

3.2 Potential usage of the Netrin-binding-peptide in Netrin dependent cancer cells

The Netrin-binding partner Draxin, and its 22 aa Netrin-binding-fragment discovered in this study have high potential medical value.

Besides a crucial role in embryonic development, Netrin serves as a survival factor in tumor cells (Arakawa, 2004; Bernet and Fitamant, 2008; Mehlen et al., 2011). Several tumors have been reported to express Netrin-1 and Netrin receptors from the DCC and Unc5 families (Fitamant et al., 2008; Delloye-Bourgeois et al., 2009). These Netrin receptors were described as "dependence receptors" in response to death signals (Mehlen et al., 1998; Forcet et al., 2001; Llambi et al., 2001). Without bound Netrin, the cell surface receptors—DCC and Unc5—are able to activate Caspase signaling, which induces apoptosis, whereas in presence of Netrin, the Netrin receptors are unable to activate cell death thus resulting in survival of the cancer cells. Hence, in order to induce apoptosis in cancer cells (a clean way to "kill" the tumor), a potential therapeutic strategy is to disrupt the interaction between the survival factor (Netrin) and its receptors (DCC and Unc5s).

So far, to disrupt Netrin-Netrin receptor interactions in cancer cells, the strategy is to capture Netrin by decoy receptors (Bernet & Fitamant, 2008). In previous studies, Netrin binding fragments of DCC and Unc5B were used as a "decoy" to interfere with the binding of Netrin to Netrin receptors in cell lines; meanwhile, mouse models were made to facilitate the analysis (Fitamant et al., 2008; Delloye-Bourgeois et al., 2009; Castets et al., 2012; Paradisi et al., 2013). This strategy is successful, although there seems to be a potential problem: a residual binding of Netrin to the full length receptor cannot be prevented, even using high concentrations of the receptor fragments.

In my AVEXIS-based-competition experiment, Draxin or the Draxin protein fragment fused to the Fc protein were able to compete with Netrin receptors for Netrin binding. This offers a potential new strategy to interfere with Netrin-Netrin receptor interactions. The advantage of this strategy is that Draxin is able to completely outcompete Netrin receptors from Netrin binding at biological relevant concentrations according to the competition results.

As a further step, the Draxin competition effect in Netrin-Netrin receptor binding could be tested using cell-based assays. The effect of Draxin on the survival rate of cells using Netrin dependent tumor induction could serve as a clear cut functional read out.

3.3 Novel methods developed in this study

AVEXIS-based-competition assay

A powerful assay developed in this work is the AVEXIS-based-competition assay (Fig. 2.5). This assay is an ELISA-style binding assay suitable for measuring the inhibition effect. Using this assay, it is possible to calculate the inhibition kinetics IC_{50}, which is the inhibitor concentration at half maximal inhibition of the "natural ligand". This value reflects the inhibition effect of an inhibitor—answering the centre question in this study.

The data from AVEXIS-based-competition assays are more quantitative than the data from the original AVEXIS assay. The variability (measured by standard deviation) normally is within 10 % in my experiments. Though the original AVEXIS has the difficulty to accurately quantify the absolute protein amount as a high-through put screen assay, the AVEXIS-based-competition assay, on the other hand, does not calculate the absolute binding value but the relative amount — % binding with and without inhibitor. This improves the original AVEXIS in terms of accuracy.

Compared to other existent *in vitro* competition methods, such as immunoassay (another ELISA-type competition assay), or variations of DELFIA assay and alpha screens, the design concept of the AVEXIS-based-competition assay is simple and similar. The AVEXIS-based competition assay is low-technology oriented, without complicated post-experimental data analysis procedures. Like AVEXIS, it is suitable for studying extracellular proteins, might be a good choice for labs in which the AVEXIS assay is already established or labs specifically interested in extracellular proteins.

In vivo detection of protein-protein interaction in zebrafish embryos

The *in vivo* detection assay (Fig. 2.19 A) was developed along the establishment of the Fluorescence correlation spectroscopy (FCS) method, with the initial aim to detect

protein mobility in living animals. It is suitable to detect binding events *in vivo*, when the extracellular distributions of the tested proteins are distinct from each other. It is a simple qualitative experiment to determine whether a protein-protein interaction is able to occur in living animals.

In contrast to other known methods allowing to detect *in vivo* protein binding, such as co-immunoprecipitation (Co-IP) or affinity-tag purification, the developed *in vivo* detection assay enables to visualize protein localization in the living cell/animal. Compared with yeast-two-hybrid or mammalian two-hybrid assays, the assay is suitable to study extracellular proteins. Since the signal is directly from the tagged protein of interest and not dependent on the amplification of the signal, further quantitative analysis is possible. Furthermore, compared with traditional *in vivo* protein binding assays such as split-GFP, FRET (fluorescence resonance energy transfer) or GRASP (GFP Reconstitution Across Synaptic Partners), the *in vivo* detection assay is relatively simple. It is based on the difference in localization of the proteins of interest visualized by fused fluorophores.

In situ detection of secreted Netrin in zebrafish embryos

The *in situ* Netrin detection assay (Fig. 2.22 A) is one of very few methods that enable the detection of Netrin proteins *in vivo*. This assay allowed for the first time to visualize Netrin protein in zebrafish.

Methodologically, it is not easy to fix and detect secreted proteins *in situ*. That is because the secreted proteins are located outside the cells and can easily diffuse away from their original source during the antibody staining procedures. Although numerous evidence showed a gradient expression of *netri*n mRNA in chick and mouse, only one group managed to visualize the Netrin protein gradient using one set of antibodies with very careful adjustment of the fixation conditions and antigen epitope enhancement procedures (Kennedy et al., 2006).

The $Draxin_{209-284aa}$ affinity probe is a good *in vivo* Netrin-binding probe in zebrafish. Full-length Draxin and the $Draxin_{231-252aa}$ probe, both bind to Netrin, but have more binding background under identical staining conditions. Using the developed protocol, the $Draxin_{209-284aa}$ probe most likely only allows detecting high Netrin concentrations, eg. membrane associated Netrin *in vivo*. Further optimize of the staining protocol is required in order to detect the full-range Netrin gradient.

Chapter 4

Materials & Methods

4.1 Zebrafish embryological methods

4.1.1 Zebrafish maintenance

All zebrafish experiments were carried out in accordance to the regulations enacted by the state of Baden-Württemberg, Germany. Zebrafish were bred and maintained as previously described (Nüsslein-Volhard and Dahm, 2002). Adult fish were maintained with 14 hour-light, 10 hour-dark cycle at 28.5 degree. Eggs were collected in E3 medium (5 mM NaCl, 17 mM KCl, 0.33 mM $CaCl_2$, 0.33 mM MgSO4, 10^{-5} % methylene blue) and raised until larval stage day 7.

Fish lines for raising were disinfected between 10 hpf and 28 hpf. Embryos were treated in bleaching solution (380 µl/L 12% NaClO, Carl Roth 9062.3) for 5 minutes followed by 5 minutes wash in water and repeated twice. 10 µl pronase (30 mg/ml, Roche 11459643001) were added per Petri dish (30 ml volume) to easy the hatching.

The following zebrafish (Danio rerio) strains were used in this study: Tübingen wild type, *alb* (*albino*), *shh*:GFP, *netrin1a* mutant allele sa12269 (Sanger Institute Zebrafish Mutation Resource).

4.1.2 PTU treatment and Anasthesia

To keep the transparency of embryos, 0.003 % 1-phenyl 2-thiourea (PTU, Sigma-Aldrich P7629) in E3 was applied to prevent melanisation of embryos before stage 24 hpf. Staging were according to previous description (Nüsslein-Volhard and Dahm, 2002). Embryos and adult fishes were anesthetized using 1: 10 to 1:100 dilutions of 0.4% ethyl -m-aminobenzoate methanesulfonate (MESAB, Sigma-Aldrich A5040). Higher doses of MESAB were used to euthanize fish.

4.1.3 Genotyping

Preparation of fin-clip and single larval genomic DNA was preformed according to Nüsslein-Volhard and Dahm, 2002. Tissue was digested using either Proteinas K (1.7 mg/ml) incubated at 55 °C for 240 minutes or NaOH (50 mM) incubated at 95 °C for 20 minutes (Meeker et al., 2007).

Primer OligST#1877 and #1880 (Table 4.1) and JumpStart[tm] REDTaq[®] DNA polymerase (Sigma-Aldrich P1107) were used for amplify the genomic DNA from

netrin1a sa12269 fish, following by the sequencing.

4.1.4 Morpholino injection

Knockdown of *netrin1a* and *netrin1b* were used to generate zebrafish embryos with reduced Netrin protein expression levels using morpholino antisense oligonucleotides (Gene-Tools). Morpholino oligonucleotides were injected into the yolk of one-cell stage embryos under a dissection microscope (Zeiss, Stemi 2000).

Morpholino sequences and concentrations were used as described in Kastenhuber et al., 2009; Suli et al., 2006:

netrin1a: 5′-ATGATGGACTTACCGACACATTCGT-3′
netrin1b: 5′-CGCACGTTACCAAAATCCTTATCAT-3′

4.1.5 Whole-mount *in situ* hybridization

Embryos were fixed overnight at 4 °C using 4 % formaldehyde (Thermo Scientific 28908)/PBS followed by dehydrated with MeOH series. In the cases of using perodiase to visualize signals, the embryos were incubated within 3 % H_2O_2 for 20 minutes to inhibit endogenous peroxidase activity prior to the hybridization. Embryos were then rehydrated and digested with Proteinase K (10 μg/ml, Merck 1245680100). Different duration of proteinase K treatment was performanced according to the stages of the embryos.

RNA probes encoding full length *draxin* and *netrin1b* were labeled with either Digoxigenin (DIG) or Fluorescein (Roche labeling kits). DIG-labeled probe was used for single mRNA detection. The DIG probe was detected with antibodies conjugated to alkaline phosphatase, and visualized with 4-nitro blue tetrazolium (NBT) and 5-bromo-4-chloro-3-indoyl-phosphate (BCIP). The *in situ* hybridization was carried out within 50 % formamide (Sigma, F9037) following the description in Nüsslein-Volhard and Dahm, 2002. The double *in situ* hybridization was preformed as previously described (Clay and Ramakrishnan, 2005). DIG and Fluorescein labeled probes were amplified with antibodies conjugated to horseradish peroxidase (HRP), and visualized using Tyramide Signal Amplification (TSA) (Invitrogen T30953, T20912). Embryos were kept in 88 % Glycerol protected from light until they were mounted and photographed

4.1.6 Immunohistochemistry

For the acetylated Tubulin antibody staining, embryos were fixed in 4 % PFA at 4 °C overnight. The samples were washed in PBS, dehydrated with MeOH series and stored at -20 °C in 100 % MeOH until used. Embryos were premeabilized in pre-chilled acetone for 5 min at -20 °C and washed with 100 % MeOH. Afterwards, embryos were rehydrated and washed 3 times with PBST (PBS containing 0.5 % Triton X-100, Sigma-Aldrich T8787). For embryos that were already performed *in situ* hybridization, previous steps were omitted. Embryos were then blocked in 10 % normal goat serum (NGS, Gibco PCN5000) in PBST for 3-6 hours at room temperature. Subsequently, primary antibody (mouse monoclonal anti-acetylated Tubulin, 1: 1000, Sigma-Aldrich T6793) was added within 1 % NGS/PBST. After an overnight incubation at 4 °C, the samples were then washed several times with PBST, and again blocked with 10 % NGS. The secondary antibodies were added at a 1: 250 dilution, incubated at 4 °C overnight and protected from light. After several washes with PBST, the embryos were post-fixed with 4 % PFA for 20 min, washed again and kept in 88 % glycerol for imaging.

4.1.7 *In situ* protein detection

A Netrin binding fragment of Draxin (209-284 aa) fused to the Fc region of human IgG (Draxin 209-284 aa-hFc) was expressed in HEK293-6E cells and used as an affinity probe to detect binding partners in zebrafish embryos. Draxin 209-284 aa-hFc *in situ* staining was performed in embryos of WT, *netrin1b* morphant and *netrin1a/netrin1b* morphant.

WT embryos (24 hpf and 48 hpf) were dechorionated by incubation in 0.1 mg/ml Pronase at RT for 1-2 h. Embryos were then prefixed for 10 min at RT in 4 % PFA containing 1 % Triton X-100. After one and half hours permeabilization with PBST (1 % Triton X-100), the embryos were blocked with 10 % NGS/PBST (0.1 % Triton) at RT for 1-3 hours. Afterwards, the embryos were stained with fresh made supernatant containing the Draxin-hFc fusion probe (with dilutions up to 1:3) overnight at 4 °C. Followed by 3 short washes (10 min in total (key step)), the embryos were post-fixed in 4 % PFA overnight at 4°C. After several washes in PBST (0.1 % Triton), the embryos were blocked with 10 % NGS for 3-6 hours at RT and subsequently incubated with a secondary antibody (goat anti human IgG Alexa Fluor 488 or 568, Invitrogen, 1:250 dilution) overnight at 4 °C. After 3 washes in PBST (0.1 % Triton), the embryos were post-fixed for 20 min at RT, and mounted for

imaging.

4.1.8 *In vivo* binding detection

Constructs to express Draxin and Netrin1a fluorescent fusion proteins were generated using the Gateway cloning system (Kwan et al., 2007). To identify functional fusion constructs, the constructs were expressed and tested using AVEXIS (see table 4.1 for used primers and Method section 4.3 for AVEXIS pair wise binding assay). The following functional constructs were selected: Draxin-sfGFP, Ntn1a-sfGFP and Ntn1a-mCherry.

Capped mRNAs for injection were *in vitro* synthesized using the mMessage mMachine Kit with T7 or SP6 RNA polymerase according to the manufacturer's instructions.

The injection was preformed in dechorionated embryos. Embryos were dechorionated with pronase (1 mg/ml pronase, ca. 5 min). 1 nl mRNA were injected into the central of the zygote at 1-2 cell stage. Draxin-sfGFP or Ntn1a-sfGFP mRNAs (100 pg/embryo) were injected in combination with membrane-tagged RFP (memRFP, 10-15 pg/embryo). Echo amount of Draxin-sfGFP and Ntn1a-mCherry (100-200 pg/embryo) were injected for the combinations. After injection, embryos were cultured in agar coated dish at 28.5 °C.   A glass pipet was used to carefully move the embryos when necessary. At sphere stages (4 hpf), living embryos were immobilized in 1 % low-melting point agarose/E2 (NuSieve GTG Agarose, Lonza 50080) containing MESAB in glass-bottom Petri dishes (MatTek, P35G-1.5-14-C). Embryos were arragned with the animal pole facing the coverslip. A signle confocal section were taken, which a region corresponding to approximately 15 μm beneath the enveloping layer of the embryos.

4.1.9 Image acquisition

A digital AxioCam camera attached to a Zeiss Axioplan 2 microscope was used to take images of NBT-BCIP *in situ* hybridization. Zeiss LSM 510 Meta concocal microscope and Zeiss LSM 780 NLO confocal microscope were used to image samples from double *in situ* assay and *in vivo* binding assays.

4.2 Molecular Methods

4.2.1 Generation of AVEXIS constructs

Total RNA were isolated from different stages of WT zebrafish embryos, and used to generate cDNA. These mixed-staged cDNA were used as templates to amplify DNA sequences encoding the ectodomain of proteins of interest by PCR using KOD polymerase. Human genes (*DRAXIN*, *NTN-1*, *NTN-2*, *NTN-4*, *NTN-G1*, *NTN-G2*, *DCC* and *UNC5B*) were amplified from human fetal brain cDNA (Agilent Technologies, 780606). DNA constructs were transferred to Zero Blunt II-TOPO vector for sequence verification and amplification. The right clones were used to generate AVEXIS expression vectors for both bait (CD4d3+4-bio (http://www.addgene.org/32402/) and prey form CD4d3+4-blac (http://www.addgene.org/32403/). To enhance the expression yield, Kozak sequence were included at N-terminus. Recognition sites for restrictive enzyme NotI (N-terminus) and AscI (C-terminus) were added to easy the the DNA transferring between different vectors. (Primers are listed in Table 4.1 and Kits are listed in Table 4.3.)

4.2.2 Generation of truncated and deleted proteins

To generate truncated and deleted proteins, overlap extension PCR was used (http://en.wikipedia.org/wiki/Overlap_extension_polymerase_chain_reaction).
Primers containing at least 24 bp overlapping were designed to connect the two parts of the sequences. Signal peptide sequences were always kept at N-terminus to ensure the expression of the protein. A 3-aa linker (G-A-P) was used to link between the signal peptide and subsequent peptide sequence unless otherwise specified.

4.2.3 Generation of variations of AVEXIS vectors

To express C-terminal his-tagged proteins, a new vector was generated from the AVEXIS bait vector. Biotinylation site in bait vector (Fig. 1.9) was replaced with the DNA sequence encoding 6 X hisidine. The monomoeric prey vector used for binding site mapping was generated from AVEXIS prey vector. To this end, COMP domain (Fig. 1.9) was removed by overlap extension PCR. The vector for expressing Fc fusion proteins was also generated from the AVEXIS vector. A sequence encoding human IgG Fc fragment was replaced with a sequence encoding CD4+biotinylation site.

4.3 Biochemical Methods

4.3.1 Bioinformatics analysis of proteins

Protein features were analyzed by online bioinformatics' tools:

SMART: http://smart.embl-heidelberg.de/, for protein domain annotation

SignalP 4.0 server: http://www.cbs.dtu.dk/services/SignalP-4.0, for signal-peptid prediction

HHpred server from the Tuebingen Bioinformatics Toolkit: http://toolkit.tuebingen.mpg.de/, for homologous protein detection and protein structure prediction

TMHMM v 2.0 server: http://www.cbs.dtu.dk/services/TMHMM/, for transmembrane domain analysis and GPI identification.

NetNGlyc 1.0 server: http://www.cbs.dtu.dk/services/NetNGlyc/, for the prediction of protein-sugar binding regions

4.3.2 His-tagged Protein purification

His_6-tagged-Draxin were purified using HisTrap HP kit (GE Healthcare, 71-5027-68 AH) and followed the manufactory instructions. Purified proteins were kept at -80 °C until used.

4.3.3 Recombinant protein production

All recombinant proteins used for AVEXIS assays and *in situ* experiments were expressed in HEK293-6E cells via polyethylenimine (PEI) mediated transient transfections (Durocher et al., 2002). HEK293-6E cells were grown in FreeStyle medium (Gibco, 12338-018) supplemented with 1 % fetal bovine serum (FBS). The culture supernatants (20 ml-200 ml) containing the secreted recombinant proteins were collected 5-6 days post transfection. Bait protein supernatants were dialyzed in HEPES-buffered saline (HBS) pH 7.4 (140 mM NaCl, 5 mM KCl, 2 mM $CaCl_2$, 1 mM $MgCl_2$, 10 mM HEPES) to remove excessive free biotin. Both bait and prey containing supernatants were stored at 4 °C until they were used.

4.3.4 AVEXIS (library screen)

AVEXIS (library screen), AVEXIS pair wise binding assay and the AVEXIS-based competition assay were preformed as described (Bushell et al., 2008). Modifications are indicated in the following paragraphs. Table 4.4 lists the identity of proteins used

in the library screens.

For all of the AVEXIS assays, streptavidin coated 96-well microtiter plates (Nunc, 10143632) were incubated with 2 % BSA/HBS for 1 hour at RT to block unspecific bindings prior to the addition of samples. Concentrations of tested proteins were normalized, either by diluting or concentrating. To reduce background binding that were potentially mediated by glycosaminoglycan (GAG) conditioned cell culture medium was used for diluting. And Vivaspin$^®$20 concentrators (10, 000 MWCO for bait proteins, 30, 000 MWCO for prey protein) were used for concentrating. Nitrocefin (Calbiochem, 484400; 50 µl, 100 µg/ml)—the colorimetric substrate—was added for visualizing the binding events. 486 nm absorbance reads were taken after 30 min, 1, 2 and 3 hours incubation (RT) as well as overnight incubation at 4 °C using a µQuant spectrophotometer (Bio-Tek Instruments). Moreover, all plates were visually inspected to identify rare cases of false positive wells. Wells with no visual detectable substrate turnover (still yellow) but substantially increased absorbance values at 486nm, usually caused by presence of small particles, were taken out.

4.3.5 AVEXIS pair wise binding assay

In the AVEXIS pair wise binding assay, Matn4 (Mann et al., 2004) was used as an internal control for normalizing captured prey proteins. So that, for each prey protein tested, an additional well containing Matn4 bait protein was added. 486 nm absorbance values that were 1.5 fold above background level were defined as positive interactions.

4.3.6 AVEXIS-based competition assay

In the AVEXIS-based competition assay, after bait protein immobilization, prey proteins were added together with indicated concentrations of potential inhibitors. The concentration of prey proteins was adjusted to values ensuring 2 to 5 fold signal over background values reached within 1-2 hours incubation at RT for the tested unchallenged interactions. Purified full-length His$_6$-tagged Draxin fused to rat CD4 (domain3+4), and Draxin-hFc (full-length Draxin-hFc, Draxin aa231-252-hFc, Draxin aa231-252-hFc) versions were used as the tested inhibitors.

Concentrations of hFc proteins were normalized as following: MaxiSorp^{TM} 96-well plates (Thermo, 442404) were incubated with hFc proteins overnight at 4 ℃, including commercial human IgG (Calbiochem, 401104) as a reference. All of the hFc

proteins and the human IgG reference were diluted with suitable series. Fc protein sample coated plate was washed once with PBS and blocked with 0.5 % BSA/PBS for 1 hour at RT. After blocking, the plate was washed twice with PBS and incubated with human IgG antibody conjugated with alkaline phosphatase (Sigma-Aldrich A9544) diluted 1:2000 with 0.2 % BSA/PBS with 50 μl per well for 1 hour at RT. After three washes with PBS, para-Nitrophenylphosphate (pNPP, Sigma-Aldrich P7998) were added with 50 μl per well to visualize alkaline phosphatase activity. After incubating for 30 min to 1 hour at RT, 420 nm absorbance reads were taken using μQuant spectrophotometer. Samples with concentrations around 1000 μg/ml were used for the competition assay.

4.3.7 Variation of AVEXIS-based competition assay

Similar with AVEXIS-based competition assay, in the variation assay (Fig. 2.8), the concentration of prey proteins was adjusted to values ensuring 2 to 5 fold signal over background values. After bait proteins were immobilized on the microtiter plates and the unbound proteins were removed, His$_6$-tagged full length Draxin was added 30 min before, together with or 30 min after addition of prey proteins. To keep the three groups in parallel, solutions of previous step were pull out and new solutions were added without washing the plate. To reduce the manipulating time, dilution series of Draxin within and without prey proteins were arranged in a plate prior to the competition step, and solutions were added using a multiple channel pipette.

4.3.8 SPR

Kinetic analysis of Draxin and Netrin interactions were preformed on a Biacore 3000 (GE healthcare) at 25 °C using a SA sensor chip. 0.01 M HEPES, PH 7.4, 0.15 M NaCl, 0.005% Surfactant P20 (HBS-P) running buffer was at a flow rate of 30 μl/min. Serial dilutions of purified human Draxin (R&D systems, 6148-DR-025/CF, 0 nM, 1.2 nM. 2.3 nM, 4.7 nM, 9.4 nM, 18.8 nM) were injected over immobilized C-terminal biotinylated human Netrin-1, ectodomains of DCC and UNC5B on a streptavidin-coated sensor chip. C-terminal biotinylated human Netrin-G1 immobilized on the chip was used as a reference. Dissociation curves of interaction between Draxin and Netrin were fitted using the BIAevaluation software 4.1. The implemented heterogeneous ligand model was employed to estimate the binding constant.

Table 4.1   List of primers

<u>code</u>	<u>name</u>	<u>Sequence</u>

Genotyping of Netrin1a mutant sa12269:

OligST1877	Netrin1a mutant_intron_Fw	GCATTCTCAGGACACTACTTGTG
OligST1880	Netrin1a mutant_intron_Rev	CAAGACATTGTGCCAGATTCCAC

Generating flurophore fusion proteins for binding activity test by AVEXIS

OligST215	Draxin_fw_NotI	gcggccgccaccATGGTGGCTCCTGGCTTGTGTCAACTCTT
OligST43	Netrin1a_fw_NotI	gcggccgccaccATGGTGAGAGTCTCTGATGCTTTGGTCAC
OligST1776	sfGFP_rev_AscI	ggcgcgccTTTGTACAGCTCATCCATGC
OligST1635	eGFP_rev_AscI	ggcgcgccTAGGGCTGCAGAATCTAGAGGCTCG
OligST1636	mCherry_rev_AscI	ggcgcgccCTTGTACAGCTCGTCCATGCCGCCG

Human genes

OligST1350	DRAXIN_fw_NotI	gcggccgccaccATGGCTGGGCCTGCCATCCACACCGCTC
OligST1351	DRAXIN_rev_AscI	ggcgcgccGACGTTGATGAAGGATCCCTGGTC
OligST1352	NTN1_fw_NotI	gcggccgccaccatggTGCGCGCAGTGTGGGAGGCGCTGG
OligST1353	NTN1_rev_AscI	ggcgcgccGGCCTTCTTGCACTTGCCCTTCTT
OligST1814	NTN3_fw_NotI	gcggccgccaccATGCCTGGCTGGCCCTGGGGGCTGCTGC
OligST1815	NTN3_rev_AscI_v1	ggcgcgccGGCGGCGCTGCAGCGCCCCCGCCGTT
OligST1816	NTN3_rev_AscI_v3	ggcgcgccGCTGATGCGGTAGCTGCCACGGGCAG
OligST1809	NTN4_fw_NotI	gcggccgccaccATGGGGAGCTGCGCGCGGCTGCTGCTGC
OligST1810	NTN4_rev_AscI_v1	ggcgcgccCTTGCACTCTCTTTTTAAAATATCCA
OligST1811	NTN4_rev_AscI_v2	ggcgcgccATTTCCTAATGTCTGTTCCTTACATT
OligST1805	NTNG1_fw_NotI	gcggccgccaccATGTATTTGTCAAGATTCCTGTCGATTC
OligST1806	NTNG1_rev_AscI	ggcgcgccGCAGCTGCCAGCCTCCTCGCACCGCA
OligST1795	NTNG2_fw_NotI	gcggccgccaccATGCTGCATCTGCTGGCGCTCTTCCTGC
OligST1796	NTNG2_rev_AscI_v2	ggcgcgccGGGCGCGCGGTCGCAGTCCAGACCGC
OligST1797	NTNG2_rev_AscI_v1	ggcgcgccCAGACCGCCGTCATCGTCGGCGGGGT
OligST1339	hDCC_fw	GTGCATGTGTGTGAGTGCTG
OligST1340	hDCC_rev	AGTTCCCGGAAAATTCACCT
OligST1348	UNC5B_fw_NotI	gcggccgccaccATGGGGGCCCGGAGCGGAGCTCGGGGGCG
OligST1349	UNC5B_rev_AscI	ggcgcgccCGCCGCATCCCCTGAGGCCTCCAG

Zebrafish genes

OligST215	Draxin_fw_NotI	gcggccgccaccATGGTGGCTCCTGGCTTGTGTCAACTCTT
OligST216	Draxin_rev_AscI	ggcgcgccGACGGTAATAAAAGCTCCTTGGTTG
OligST1215	Draxin_paralogue_fw_NotI	gcggccgccaccATGGCAGTTTCCTGTTGGTATT
OligST1216	Draxin_paralogue_rev_AscI	ggcgcgccGATGGACATCTCCCTTGTGTACTTC
OligST43	Netrin1a_fw_NotI	gcggccgccaccATGGTGAGAGTCTCTGATGCTTTGGTCAC
OligST44	Netrin1a_rev_AscI	ggcgcgccTGCTTTCTTGCATTTTCCTTTCTTC
OligST1148	Ntn1b_fw_NotI	gcggccgccaccATGGTAAGGATTTTGGTAACGTGC
OligST1486	Ntn1b_rev_AscI	ggcgcgccGGGAGCAGCAACTGGAATTT
OligST1124	Ntn2_fw_NotI	gcggccgccaccATGGGGAGATTTCAGACTTTGCTTTCTAT
OligST1487	Ntn2_rev_AscI	ggcgcgccTGCAGGCTCCTCTGTAGTGC
OligST1482	Ntn4_fw_NotI	gcggccgccaccATGGAGCTGACGGGGAGATG
OligST1488	Ntn4_rev_AscI	ggcgcgccGTCTCCGGTGTAAGGGTCAC
OligST965	Dcc_fw_NotI	gcggccgccaccATGGGCTGCGTCACTGG
OligST930	Dcc_rev_AscI	ggcgcgccCGGGGTCACGCTGCCG
OligST966	Dscam_fw_NotI	gcggccgccaccATGTGGATATTGGCCATCATC
OligST933	Dscam_rev_AscI	ggcgcgccGGGGTCCTTCACCAGAGTCTTC

Table 4.2   List of antibodies

Primary antibodies	Source	Working dilution
mouse monoclonal anti-acetylated Tubulin	Sigma-Aldrich T6793	1:1000
sheep anti Digoxigenin	Roche 1333089	1:5000
sheep anti Fluorscein, conjugated with HRP	Roche 11426346910	1:500
rabbit anti VasnA	Paolo Panza	1:1000

Secondary antibodies	Source	Working dilution
goat polyclonal anti-mouse IgG Alexa 488	Molecular Probes A-11029	1:250
goat polyclonal anti-mouse IgG Alexa 546	Molecular Probes A-11030	1:250
goat polyclonal anti-mouse IgG Alexa 647	Molecular Probes A-21236	1:250
goat anti human IgG Alexa 488	Invitrogen A-11013	1:250
goat anti human IgG Alexa 568	Invitrogen A-21090	1:250
goat anti human IgG Alexa 633	Invitrogen A-21091	1:250
Rabbit anti sheep, conjugated with HRP	Invitrogen 618620	1:2000
sheep anti Digoxigenin conjugated with alkaline phosphatase	Roche 11093274910	1:2000
Goat anti-Human IgG (Fc specific) conjugated with Alkaline Phosphatase	Sigma-Aldrich A9544	1:2000

Table 4.3   List of molecular kits

Name of the Kit	company	Purpose
TRIzol® Reagent	Invitrogen 15596-018	isolate total RNA from embryos
Cloned AMV Reverse Transcriptase	Invitrogen 12328-019	synthesize cDNA from RNA
KOD Hot Start DNA Polymerase	Merck Millipore 71086	amplify PCR products from cDNA
Zero Blunt® TOPO® PCR Cloning Kit	Invitrogen 45-0245	blunt PCR cloning
NEB Quick LigationTM Kit	NEB M2200	ligation
QIAquick® PCR Purification Kit	QIAGEN 28106	gel purificaiton
One Shot® TOP10 Chemially Competent *E.coli*	Invitrogen C4040	transformation of plasmid DNA into E.coli
Subcloining Efficiency™ DH5aTM Competent Cells	Invitrogen 18265	transformation
QIAprep® Spin Miniprep Kit	QIAGEN 27106	plasmid mini prep
Antarctic Phosphatase Kit	NEB M0289	removes 5' phosphates from DNA
QIAGEN® Plasmid Maxi Kit	QIAGEN 12165	plasmid maxi prep
JumpStartTM REDTaq® DNA polymerase	Sigma-Aldrich P1107	genotyping
mMESSAGE mMACHINE® Kit	Ambion AM1340 or AM1344	*in vitro* synthesize mRNA for injections
MEGAscript® Kit	Ambion AM1330 or AM1334	transcribe RNA for in situ hybridization probes
MEGAclear™ Kit	Ambion 1908	pruify RNA molecules

Table 4.4   Protein identities used for library screen

	Draxin prey	Draxin bait	Netrin-1a EGF3 prey	Netrin-1a EGF3 bait
1	Ntn1a	Ntn1a	Draxin	Draxin
2	Vwde	Ngf	Efna2	Neo1
3	Lum	Flrt1a	Nrp1a	Ek1 V2
4	Draxin	Cxadr	Ephb4b	Vcam1
5	Calr3b	Draxin_V2	Hapln1	Cxcl12a
6	Cdh2	Elfn2a	Dlb	Mpzl2
7	Efna3b	Efna2	Ror2	Calrl2
8	Epha4a	Fgfrl1a	Tac3a	Ednra
9	Efna3a	Igfbp7	Wnt11	Ngf
10	Pcdh17	Igsf11	Alcama	Robo3
11	Frzb	Bsg	Neo1	Lrrtm1
12	Metrnl	Ildr2	Ednra	Glra1
13	Tnw	Lrrc38	Vwde	Galn V2
14	Alcama	sc:d0413	Lrrc4c	Metrnl
15	Neo1	Calr3b	Csf1b	Cspg4
16	Cd59	Cdon	Kal1a	Optc
17	Cntn2	Ednrab	Cdh2	Cntfr
18	Creld2	Mxra8b	Fgfr4	Bcan
19	Nenf	Nradd	Cadm4	Tsku
20	Mdka	Opcml	Cntn1a	Lrtm2
21	Csf1ra	Robo1	Erbb2F	Ncam1b
22	Si:ch211-286c4.6	sc:d0316	Epha4a	Sc:d411
23	Fgf3	Spon2a	m1036	Jam2b
24	Igfbp1a	Tmem59l	Si:ch211-251b21.1	Cadm4
25	Nrp2b	Tpbgb	Pcdh17	Wfdc1
26	Lrrn1	Cadm1b	Nradd	Calua
27	Mpz	Cadm2a	Sparc	Rgma
28	Sparc	Cdh2	Chodl	Met
29	Cxcl12b	Zgc:165604	Mpzl2	Creld2
30	Oc90	Fgfr2	Clu	Mpzl3
31	Fsta	Jam3b	Mpz	Igfbp7
32	Mpzl2	Lrit1a	Igfbp1a	Efna5b
33	Kal1a	Lrit2	Fgf3	Flrt1a
34	m1036	Slc22a7a (M964)	Oc90	Flrt1a
35	Fstl1a	Alcamb	Fsta	Sc:d0348
36	Rnaset2	Nptna	Epha7	Nptnb
37	Sfrp1a	Nrp2b	Galn V2	sc:d0413
38	Fgfr2	Ret	Unc5b	Cart4
39	Dkk1b	si:zfos-1011f11.1	Calr3b	Kal1a
40	Igsf21b	Slitrk2	Cspg4	Vstm4a
41	Dla	Unc5b	Cxcl12b	Pcdh10a

42	Wnt1	Wfdc1	Nrp2b	Nrp1a
43	Calr3a	Calua	Efna5b	Nrp1b
44	Clu	Chodl	Fgfr2	Tmem59l
45	Ednrab	Creld2	Csf1ra	Calr3a
46	Igsf11	Cxcl12b	Lum	Ptpra
47	si:zfos-1011f11.1	Edn3b	Elfn2a	Cadm2a
48	Si:ch211-251b21.1	Efna5b	Tnw	Fgfrl1a
49	Efna2	Efnb2a	Fibina	Ephb4a
50	Epha7	Ek1 V2	Wu:fc46h12	Hfe2
51	Lrrc4c	Ek1	Calua	Epha7
52	Erbb2F	Epha7	Pcdh18a	Ntm
53	Wu:fc46h12	Ephb4a	Cntn2	Flrt2
54	Ephb4b	Fstl1a	Tnfrsf21	Elfn2a
55	Tac3a	Glra1	Efnb3b	Tnw
56	Nradd	Jam2b	Calr3a	Urp2
57	Cadm4	Lingo1b	Jam2a	Slc22a7a
58	Cntn1a	Sc:d0348	Igsf11	Cd59
59	Mdkb	Lrrc4c	Ror1	Igfbp1a
60	Urp2	Lum	si:zfos-1011f11.1	Vasna
61	Sema3d	m1036	Fstl1a	Nradd
62	Efna5b	m1038	Pttg1ipb	Lft2
63	m1038	Manf	zgc:161979	Sparc
64	zgc:110239	Met	Nenf	Lrit1a
65	zgc:161979	Mpzl3	Defbl1	Prnpb
66	Wnt11r	Ncam1a	Mdka	Nrp2b
67	Ror1	Lrrc4.1	Prnpb	Sema6dl
68	Chga	Pik3ipl	Frzb	Jam2a
69	Ephb3a	Ptpra	Creld2	Efnb2a
70	Dlb	Hfe2	Wnt1	Chodl
71	Lrrc4.1	Rtn4rl2a	Dkk1b	Chodl
72	Fibina	si:ch1073-70f20.1	Lrrn1	Fstl1a
73	Prnpb	Ntrk2b	Lrrc4.1	Tpbga
74	Galn V2	Tpbga	Rnaset2	Zgc:165604
75	Fgfr4	Tac3a	Igsf21b	Cadm1b
76	Hapln1	Cd276	Chga	Lrrc4.1
77	Chodl	Bcan	Ednrab	Robo1
78	Nrp1a	Cadm3	Prtgb	Lrrc3
79	Ednra	Calr3a	m1038	Opcml
80	Calua	Cspg4	zgc:110239	Lingo1b
81	Unc5b	Dla	Rgma	sc:d0316
82	Rgma	Efnb3	Dla	Cdon
83	Pcdh18a	Fgfbp1	Sema3d	Mxra5
84	Tnfrsf21	Fgfr4	Sfrp1a	Ramp2
85	Ror2	Flrt2	Ptpra	Fibina

86	Ptpra	Fsta	Ephb3a	Spon2a
87	Csf1b	Gas1b	Wnt11r	Egfra
88	22aa-Draxin	Igsf21a	Efna3b	Ednrab
89	Bcan	Lrrc24		wu:fc46h12
90	Efnb3b	Islr2		Rbp4l
91	Pttg1ipb	Jam2a		Rnaset2
92	Cspg4	Kal1a		C6
93	Jam2a	Lingo1a		Cdh2
94	Prtgb	Cd59		Oc90
95	Islr2	Mxra5		Dla
96	Wfdc1	Lrrtm1		Lrit2
97	Cart4	Lrtm2		Calr3b
98	Ltk	Ltk		Ncam1a
99	Igfbp7	Matn4		Ret
100	Edn3	Mpzl2		Fsta
101	Epha3like	Negr1		Lrrc4c
102	Ptn	Nrp1b		Igsf21a
103	Wnt11	Nrp1a		Ildr2
104	Elfn2a	Optc		Nptna
105	Defbl1	Pcdh10a		Cxadr
106	Vasna	Pcdh17		Rtn4rl1b
107	Notchl	Igdcc3		Ek1 V2
108	Dner	Sc:d189		Efna2
109	Manf	Rbp4l		Efnb3
110	Galn	Rgmb		Tnfrsf21
111	Notch3	Sema6dl		Matn4
112	Ntm	Tnfrsf21		Sc:d189
113	Edn3b	Tnw		Slitrk2
114	Ryk	Vstm4a		Lrrc24
115	Vasnb	A2BID0		Fgfr2
116	Si:dkey-1c11.1	Bmper		Fgfr2
117	Dlc	C6		Mxra8b
118	Jag2	Cntfr		Tpbgb
119	Jag2_2	Csf1a		Ntrk2b
120	Dlk1	Dkk1b		Fgfr4
121	Ephb4a	Draxin		Mxra5
122	Lrrtm1	Edn3		Ltk
123	Mxra8a	Ednra		A2BID0
124	Dcc	Efna3b		m1028
125	Jag1a	Epha4a		Csf1a
126	Jag1b	Rtn4rl1b		Csf1b
127	Ctgfa	Fibina		Igsf21b
128	Spon1b	Galn		Tac3a
129	Spon2a	Zmp:0000000665		m1036

130	Lrit2	Igfbp1a	C8a
131	Dld	Igsf21b	Tac3a
132	Notch2-like	Lrrc3	Cd276
133		m922	m1038
134		Rnaset2	Bmper
135		Ntm	Pik3ipl
136		Rgma	Ctsba
137		Loc100004582	Lrrn1
138		Sc:d411	m1098
139		Tsku	Epha4a
140		Vcam1	Cxcl12b
141		Kitb	Rtn4rl2a
142		C8a	Lrrc38
143		Cadm4	Unc5b
144		Calrl2	Cadm3
145		Cntn2	Gas1b
146		Egfra	Csf1ra
147		Lft2	Tnw
148		m1028	Fgfbp1
149		Neo1	Pcdh17
150		Nptnb	Manf
151		Oc90	Alcamb
152		Prnpb	Jam3b
153		Ramp2	Bsg
154		Sparc	Lrrtm4l1
155		Vasnb	Ryk
156		Cart4	Dkk1b
157		Ctsba	Kitb
158		Lrrtm4l1	Pttg1ipb
159		Lrrn1	Zmp:0000000665
160		Pttg1ipb	C8b
161		Q567y1	Galn
162		Ryk	Igdcc3
163		Vasna	
164		wu:fc46h12	
165		Csf1b	
166		m1098	
167		Npb	
168		Csf1ra	
169		Galn v2	
170		Ncam1b	
171		Metrnl	
172		Urp2	

Proteins are listed according to desending

values of detected binding strength

Table 4.4   Protein identities used for library screen (continue*)

#	Protein Name	ECD (aa 1 to indicated Nr.)	Type	Genbank Accession #	Source
1	Calr3a	418	SEC	KM655574	Cloned from cDNA
2	Calr3b	417	SEC	KM655575	Cloned from cDNA
3	Calua	317	SEC	KM655576	Cloned from cDNA
4	Cxcl12b	97	SEC	KM655577	Cloned from cDNA
5	Ephb4a	543	TM	KM655578	Cloned from cDNA
6	Fgf8a	210	SEC	KM655579	Cloned from cDNA
7	Fstl1a	314	SEC	KM655580	Cloned from cDNA
8	Lft2	362	SEC	KM655581	Cloned from cDNA
9	Matn4	616	SEC	KM655582	Cloned from cDNA
10	Metrnl	286	SEC	KM655583	Cloned from cDNA
11	Ntn1a	603	SEC	KM655584	Cloned from cDNA
12	Oc90	939	SEC	KM655585	Cloned from cDNA
13	Ptn	158	SEC	KM655586	Cloned from cDNA
14	Shha	418	SEC	KM655587	Cloned from cDNA
15	Shhb	416	SEC	KM655588	Cloned from cDNA
16	Sparc	291	SEC	KM655589	Cloned from cDNA
17	Tnfrsf21	352	TM	KM655590	Cloned from cDNA
18	Spon2a	334	SEC	KM655591	Cloned from cDNA
19	Manf	180	SEC	KM655592	Cloned from cDNA
20	Si:ch1073-70f20.1	131	SEC	KM655593	Cloned from cDNA
21	Clu	449	SEC	KM655594	Cloned from cDNA
22	Urp2	243	SEC	KM655595	Cloned from cDNA
23	CD59	92	GPI	KM655596	Cloned from cDNA
24	Bcan	361	SEC	CU458953	Gift from G.J. Wright
25	Ntm	311	GPI	CU458872	Gift from G.J. Wright
26	Igfbp7	248	SEC	CU458927	Gift from G.J. Wright
27	Optc	321	SEC	CU468787	Gift from G.J. Wright
28	Bgnb	375	SEC	CU468793	Gift from G.J. Wright
29	Cadm4	328	TM	CU638749	Gift from G.J. Wright
30	Islr2	567	TM	CU468789	Gift from G.J. Wright
31	Rgmb	410	GPI	KM655597	Cloned from cDNA
32	Mdkb	147	SEC	KM655598	Cloned from cDNA
33	Mdka	148	SEC	KM655599	Cloned from cDNA
34	Dlc	508	TM	CU458991	Gift from G.J. Wright
35	Ngf	194	SEC	KM655600	Cloned from cDNA
36	Nradd	237	TM	KM655601	Cloned from cDNA
37	Pcdh17	679	TM	KM655602	Cloned from cDNA

38	Cdh2	710	TM	KM655603	Cloned from cDNA
39	Cspg4	1012	TM	KM655604	Gift from H. Knaut
40	Cspg4 V2	1081	TM	KM655605	Gift from H. Knaut
41	Pcdh10b	679	TM	KM655606	Cloned from cDNA
42	Npb	136	SEC	KM655607	Cloned from cDNA
43	Nrp1b	894	TM	KM655608	Cloned from cDNA
44	Ephb4b	539	TM	KM655609	Cloned from cDNA
45	Tmem59l	253	TM	KM655610	Cloned from cDNA
46	Neo1	1060	TM	CU458829	Gift from G.J. Wright
47	Cntfr	325	TM	CU458971	Gift from G.J. Wright
48	Bsg	214	TM	CU458968	Gift from G.J. Wright
49	Mpzl2	146	TM	CU458956	Gift from G.J. Wright
50	Dla	534	TM	CU458989	Gift from G.J. Wright
51	Epha4a	546	TM	KM655611	Cloned from cDNA
52	Ptpra	179	TM	KM655612	Cloned from cDNA
53	Rgma	418	GPI	KM655613	Cloned from cDNA
54	Lrit2	459	TM	CU468740	Gift from G.J. Wright
55	Met	933	TM	KM655614	Cloned from cDNA
56	Creld2	341	SEC	KM655615	Cloned from cDNA
57	Vstm4a	156	TM	CU638745	Gift from G.J. Wright
58	Cadm2a	328	TM	CU458965	Gift from G.J. Wright
59	Lrit1a	546	TM	CU468741	Gift from G.J. Wright
60	Fgfrl1a	356	TM	CU458922	Gift from G.J. Wright
61	Kirrela	501	TM	CU458877	Gift from G.J. Wright
62	Ncam1a	700	TM	CU458885	Gift from G.J. Wright
63	Ret	633	TM	KM655616	Cloned from cDNA
64	Fsta	322	SEC	KM655617	Cloned from cDNA
65	Sfrp1a	296	SEC	KM655618	Cloned from cDNA
66	Hfe2	384	GPI	KM655619	Cloned from cDNA
67	Lrrc4c	534	TM	CU468806	Gift from G.J. Wright
68	Ildr2	176	TM	CU638797	Gift from G.J. Wright
69	Nptna	218	TM	CU458932	Gift from G.J. Wright
70	Cxadr	241	TM	CU458753	Gift from G.J. Wright
71	Rtn4rl1b	447	TM	CU468752	Gift from G.J. Wright
72	Nrp2b	853	TM	KM655620	Cloned from cDNA
73	Sema6dl	659	TM	CU458860	Gift from G.J. Wright
74	Mpzl3	148	TM	CU458906	Gift from G.J. Wright
75	Jam2a	226	TM	CU458944	Gift from G.J. Wright
76	Efna5b	201	GPI	KM655621	Cloned from cDNA
77	Efnb2a	223	TM	KM655622	Cloned from cDNA
78	Chodl	235	TM	KM655623	Cloned from cDNA
79	Epha7	550	TM	KM655624	Cloned from cDNA

80	Ek1 v2	551	TM	KM655625	Cloned from cDNA
81	Ek1	544	TM	KM655626	Cloned from cDNA
82	Efna3b	194	GPI	KM655627	Cloned from cDNA
83	Efna2	173	GPI	KM655628	Cloned from cDNA
84	Efnb3b	218	TM	KM655629	Cloned from cDNA
85	Vcam1	766	TM	CU458903	Gift from G.J. Wright
86	Lrrtm4l1	456	TM	CU468766	Gift from G.J. Wright
87	Rtn4rl2a	458	TM	CU468805	Gift from G.J. Wright
88	Kal1a	652	SEC	KM655630	Cloned from cDNA
89	Tpbga	307	TM	CU468751	Gift from G.J. Wright
90	Tsku	366	SEC	CU468770	Gift from G.J. Wright
91	Sc:d189	342	TM	CU458946	Gift from G.J. Wright
92	Lrrc38	245	TM	CU468759	Gift from G.J. Wright
93	Zgc:165604	234	TM	CU458996	Gift from G.J. Wright
94	Unc5b	376	TM	CU458889	Gift from G.J. Wright
95	Alcamb	504	TM	CU458904	Gift from G.J. Wright
96	Jam3b	236	TM	CU458938	Gift from G.J. Wright
97	Wfikkn1	431	SEC	CU638805	Gift from G.J. Wright
98	Slitrk2	622	TM	CU468746	Gift from G.J. Wright
99	Lrrc24	444	TM	CU468764	Gift from G.J. Wright
100	Cadm3	349	TM	CU638752	Gift from G.J. Wright
101	Igdcc3	589	TM	CU638789	Gift from G.J. Wright
102	Cadm1b	310	TM	CU638788	Gift from G.J. Wright
103	Fgfr2	24-295	TM	CU458909	Gift from G.J. Wright
104	Cd276	238	TM	CU638774	Gift from G.J. Wright
105	Mxra8b	285	TM	CU638746	Gift from G.J. Wright
106	Tpbgb	316	TM	CU468771	Gift from G.J. Wright
107	Lrrc4.1	543	TM	CU468781	Gift from G.J. Wright
108	Robo1	866	TM	CU458748	Gift from G.J. Wright
109	Prtgb	935	TM	KM655631	Cloned from cDNA
110	Lrfn5a	528	TM	CU468768	Gift from G.J. Wright
111	Lrrtm4l2	445	TM	CU468765	Gift from G.J. Wright
112	Sema3d	764	SEC	KM655632	Cloned from cDNA
113	Bsg	319	TM	CU638778	Gift from G.J. Wright
114	Mxra8a	296	TM	CU638765	Gift from G.J. Wright
115	Galn	142	SEC	KM655633	Cloned from cDNA
116	Csf1b	212	TM	KM655634	Cloned from cDNA
117	Gas1b	263	SEC	KM655635	Cloned from cDNA
118	Zmp:0000000665	335	SEC	KM655636	Cloned from cDNA
119	Ryk	224	TM	KM655637	Gift from G. Weidinger
120	Kitb	204	TM	CU458998	Gift from G.J. Wright
121	Fgfr1b	283	TM	CU458868	Gift from G.J. Wright

122	Lrrtm1	429	TM	CU468794	Gift from G.J. Wright
123	Flrt2	541	TM	CU468790	Gift from G.J. Wright
124	Elfn2a	403	TM	CU468797	Gift from G.J. Wright
125	Lrtm2	306	TM	CU468758	Gift from G.J. Wright
126	Lrrtm2	447	TM	CU468747	Gift from G.J. Wright
127	Flrt1a	558	TM	CU468788	Gift from G.J. Wright
128	Ntrk2b	401	TM	CU468742	Gift from G.J. Wright
129	Sc:d0348	542	TM	CU468772	Gift from G.J. Wright
130	Ncam1b	710	TM	CU458747	Gift from G.J. Wright
131	Sema4c	666	TM	CU458995	Gift from G.J. Wright
132	Jam2b	240	TM	CU458870	Gift from G.J. Wright
133	Lrrc3	209	TM	CU468760	Gift from G.J. Wright
134	Opcml	311	GPI	CU638768	Gift from G.J. Wright
135	Cntn1a	1013	GPI	CU458969	Gift from G.J. Wright
136	Lingo1b	553	TM	CU468744	Gift from G.J. Wright
137	Sc:d0316	508	TM	CU468743	Gift from G.J. Wright
138	Sc:d0413	656	TM	CU468799	Gift from G.J. Wright
139	Negr1	317	GPI	CU458871	Gift from G.J. Wright
140	Cntn2	576	GPI	CU458883	Gift from G.J. Wright
141	Lingo1a	549	TM	CU468767	Gift from G.J. Wright
142	Dlb	518	TM	CU458990	Gift from G.J. Wright
143	Pcdh10a	679	TM	KM655638	Cloned from cDNA
144	Si:zfos-1011f11.1	236	TM	CU458914	Gift from G.J. Wright
145	Lum	344	SEC	CU468778	Gift from G.J. Wright
146	Igsf11	247	TM	CU458869	Gift from G.J. Wright
147	Glra1	245	TM	KM655639	Gift from R.J. Harvey
148	Wnt11	353	SEC	KM655640	Gift from G. Weidinger
149	Fgfr4	476	TM	CU458754	Gift from G.J. Wright
150	Csf1ra	513	TM	CU458899	Gift from G.J. Wright
151	Mxra5	861	SEC	KM655641	Cloned from cDNA
152	Tnw	932	SEC	KM655642	Cloned from cDNA
153	Cdon	825	TM	KM655643	Cloned from cDNA
154	Galn V2	118	SEC	KM655644	Cloned from cDNA
155	Zgc:110239	326	SEC	KM655645	Cloned from cDNA
156	Nenf	158	SEC	KM655646	Cloned from cDNA
157	Pttg1ipb	89	TM	KM655647	Cloned from cDNA
158	Grem2	166	SEC	KM655648	Cloned from cDNA
159	Wfdc1	220	SEC	KM655649	Cloned from cDNA
160	Si:dkey-251i10.2	170	SEC	KM655650	Cloned from cDNA
161	Cart4	105	SEC	KM655651	Cloned from cDNA
162	Olfml2bb	466	SEC	KM655652	Cloned from cDNA
163	Igfbp1a	262	SEC	KM655653	Cloned from cDNA

164	Rbp4l	196	GPI	KM655654	Cloned from cDNA
165	Pik3ip1	169	TM	KM655655	Cloned from cDNA
166	C7b	229	SEC	KM655656	Cloned from cDNA
167	C6	280	SEC	KM655657	Cloned from cDNA
168	Zgc:174888	226	GPI	KM655658	Cloned from cDNA
169	Csf1a	482	TM	KM655659	Cloned from cDNA
170	C8a	297	SEC	KM655660	Cloned from cDNA
171	Fibina	226	SEC	KM655661	Cloned from cDNA
172	Si:ch211-286c4.6	96	GPI	KM655662	Cloned from cDNA
173	Fgfbp1	196	SEC	KM655663	Cloned from cDNA
174	Loc100004582	205	TM	KM655664	Cloned from cDNA
175	Tac3a	125	SEC	KM655665	Cloned from cDNA
176	Ltk	453	TM	KM655666	Gift from R.N. Kelsh
177	Ednraa	93	TM	KM655667	Cloned from cDNA
178	Ppp3r1a	170	TM	XP_692770.2	Cloned from cDNA
179	Calr	417	SEC	KM655668	Cloned from cDNA
180	Rnaset2	240	SEC	KM655669	Cloned from cDNA
181	Ctsba	330	SEC	KM655670	Cloned from cDNA
182	Slc22a7a	106	Multiple TM	KM655671	Cloned from cDNA
183	Si:ch211-243a20.3	186	SEC	KM655672	Cloned from cDNA
184	Nrp1a	584	TM	KM655673	Cloned from cDNA
185	Igsf21b	473	SEC	KM655674	Cloned from cDNA
186	Ednrab	68	Multiple TM	KM655675	Cloned from cDNA
187	Odc1	105	SEC	XP_005169396.1	Cloned from cDNA
188	Wu:fc46h12	164	SEC	KM655676	Cloned from cDNA
189	Ramp2	93	TM	KM655677	Cloned from cDNA
190	Egfra	389	TM	AAS45493.1* identity: 98%	Cloned from cDNA
191	Bmper	609	SEC	KM655678	Cloned from cDNA
192	Edn3a	143	SEC	XP_009293151.1	Cloned from cDNA
193	Edn3b	153	SEC	XP_001919586.1	Cloned from cDNA
194	Ptprz1b	411	TM	KM655679	Gift from C. Winkler
195	Ptprz1b	624	TM	KM655680	Gift from C. Winkler
196	Musk	565	TM	CU458887	Gift from G.J. Wright
197	Efna3a	196	GPI	KM655681	Cloned from cDNA
198	Ptprz1a	416	TM	KM655682	Cloned from cDNA
199	Ntn1b	458	SEC	KM655683	Cloned from cDNA
200	Ntn2	473	SEC	KM655684	Cloned from cDNA
201	Ntn4	434	SEC	KM655685	Cloned from cDNA
202	Vasna	583	TM	CU468763	Gift from G.J. Wright
203	Draxin	360	SEC	KM655686	Cloned from cDNA
204	Si:dkey-1c11.1	351	SEC	KM655687	Cloned from cDNA
205	Ctgfa	345	SEC	KM655688	Cloned from cDNA

206	Frzb	315	SEC	KM655689	Cloned from cDNA
207	Prnpb	578	GPI	KM655690	Cloned from cDNA
208	Spon1b	803	SEC	KM655691	Cloned from cDNA
209	Hapln1	328	SEC	KM655692	Cloned from cDNA
210	Hhip	693	SEC	KM655693	Cloned from cDNA
211	Wnt4b	358	SEC	KM655694	Cloned from cDNA
212	Fzd8a	238	7TM	KM655695	Cloned from cDNA
213	Fgf3	249	SEC	KM655696	Cloned from cDNA
214	Pcdh18a	701	TM	KM655697	Cloned from cDNA
215	Ndr2	501	SEC	KM655698	Cloned from cDNA
216	Shisa9a	134	TM	KM655699	Cloned from cDNA
217	Ephb3a	535	TM	KM655700	Cloned from cDNA
218	Wnt1	370	SEC	KM655701	Cloned from cDNA
219	Alcama	497	TM	CU458879	Cloned from cDNA
220	Ror1	412	TM	KM655702	Gift from G. Weidinger
221	Vwde	212	SEC	KM655703	Cloned from cDNA
222	Mpz	143	TM	CU458863	Gift from G.J. Wright
223	Igfbp1 version 2	262		AJG05999.1	Cloned from cDNA
224	Erbb2	645	TM	KM655704	Cloned from cDNA
225	Wnt11r	352	SEC	KM655705	Cloned from cDNA
226	Si:ch211-170d8.2	297	SEC	KM655706	Cloned from cDNA
227	Plxna3	1240	TM	KM655707	Cloned from cDNA
228	Dkk1b	241	SEC	KM655708	Gift from G. Weidinger
229	Defbl1	67	SEC	KM655709	Cloned from cDNA
230	Zgc:161979	130	SEC	KM655710	Cloned from cDNA
231	Chga	371	SEC	KM655711	Cloned from cDNA
232	Ror2	404	TM	KM655712	Cloned from cDNA
233	Musk sv1	300	TM	CU458888	Gift from G.J. Wright
234	Musk sv2	217	TM	CU458887	Gift from G.J. Wright
235	Dcc	1069	TM	KM655713	Cloned from cDNA
236	Wif1	378	SEC	KM655714	Cloned from cDNA
237	Gdf11	389	SEC	KM655715	Cloned from cDNA
238	zgc:110372	306	SEC	CU458930	Gift from G.J. Wright
239	Cntn2	1022	GPI	KM655716	Cloned from cDNA
240	Wnt4a	352	SEC	KM655717	Cloned from cDNA
241	Gpc1b	559	SEC	KM655718	Cloned from cDNA
242	Phb	271	SEC	KM655719	Cloned from cDNA
243	Robo4	591	TM	CU458880	Gift from G.J. Wright
244	Hepacam2	336	TM	CU458977	Gift from G.J. Wright
245	Zgc:66118	220	SEC	CU458950	Gift from G.J. Wright
246	Tapbp	401	SEC	CU458751	Gift from G.J. Wright
247	Igdcc4	421	TM	CU638782	Gift from G.J. Wright

248	Amigo1	368	TM	CU468749	Gift from G.J. Wright
249	Lrfn1	523	TM	CU468795	Gift from G.J. Wright
250	Lngo3a	539	TM	CU468775	Gift from G.J. Wright
251	Nptnb	331	TM	CU458926	Gift from G.J. Wright
252	Elfn1b	420	TM	CU468785	Gift from G.J. Wright
253	Pdgfra	786	TM	CU458757	Gift from G.J. Wright
254	Spon1a	808	SEC	KM655720	Cloned from cDNA
255	Scube2	854	SEC	KM655721	Cloned from cDNA
256	Grin1a	226	TM	KM655722	Cloned from cDNA
257	Wnt8a	359	SEC	KM655723	Gift from G. Weidinger
258	Nfasca	727	TM	CU458816	Gift from G.J. Wright
259	Lrrn3	624	TM	CU468756	Gift from G.J. Wright
260	Fzd7b	238	7TM	KM655724	Cloned from cDNA
261	Glrbb	266	4TM	KM655725	Gift from R.J. Harvey
262	Pmelb	547	TM	KM655726	Cloned from cDNA
263	Si:ch211-251b21.1	394	TM	KM655727	Cloned from cDNA
264	Wnt8b	358	SEC	KM655728	Cloned from cDNA
265	C1qc	244	SEC	KM655729	Cloned from cDNA
266	C8b	262	SEC	KM655730	Cloned from cDNA
267	Wnt10b	427	SEC	KM655731	Cloned from cDNA
268	Megf10	850	TM	KM655732	Cloned from cDNA
269	Cart3	117	SEC	KM655733	Cloned from cDNA
270	Si:dkey-226k3.4	102	SEC	KM655734	Cloned from cDNA
271	Tgfbi	677	SEC	KM655735	Cloned from cDNA
272	Nrg2b	705	TM	XP_005157176.1	Cloned from cDNA

*Table S3, Gao et al., 2015

Bibliography

Ahmed, G., Shinmyo, Y., Ohta, K., Islam, S.M., Hossain, M., Naser, I. Bin, Riyadh, M.A., Su, Y., Zhang, S., Tessier-Lavigne, M., et al. (2011). Draxin inhibits axonal outgrowth through the netrin receptor DCC. J. Neurosci. *31*, 14018–14023.

Arakawa, H. (2004). Netrin-1 and its receptors in tumorigenesis. Nat. Rev. Cancer *4*, 978–987.

Astic, L., Pellier-Monnin, V., Saucier, D., Charrier, C., and Mehlen, P. (2002). Expression of netrin-1 and netrin-1 receptor, DCC, in the rat olfactory nerve pathway during development and axonal regeneration. Neuroscience *109*, 643–656.

Bennett, K.L., Bradshaw, J., Youngman, T., Rodgers, J., Greenfield, B., Aruffo, a., and Linsley, P.S. (1997). Deleted in Colorectal Carcinoma (DCC) Binds Heparin via Its Fifth Fibronectin Type III Domain. J. Biol. Chem. *272*, 26940–26946.

Berner, A., and Fitamant, J. (2008). Netrin-1 and its receptors in tumour growth promotion. Expert Opin Ther Targets *8*, 995–1007.

Bloch-Gallego, E., Ezan, F., Tessier-Lavigne, M., and Sotelo, C. (1999). Floor plate and netrin-1 are involved in the migration and survival of inferior olivary neurons. J. Neurosci. *19*, 4407–4420.

Bonhoeffer, F., and Huf, J. (1980). recognition of cell types by axonal growth cones in vitro. 162–164.

Bonhoeffer, F., and Huf, J. (1982). In vitro experiments on axon guidance demonstrating an anterior-posterior gradient on the tectum. EMBO J. *1*, 427–431.

Bouchard, J.-F., Moore, S.W., Tritsch, N.X., Roux, P.P., Shekarabi, M., Barker, P. a, and Kennedy, T.E. (2004). Protein kinase A activation promotes plasma membrane

insertion of DCC from an intracellular pool: A novel mechanism regulating commissural axon extension. J. Neurosci. *24*, 3040–3050.

Brose, K., Bland, K.S., Wang, K.H., Arnott, D., Henzel, W., Goodman, C.S., Tessier-lavigne, M., Kidd, T., Way, D.N.A., and Francisco, S.S. (1999). Slit Proteins Bind Robo Receptors and Have an Evolutionarily Conserved Role in Repulsive Axon Guidance. Cell *96*, 795–806.

Brown, B.M.H., Boles, K., Merwe, P.A. Van Der, Kumar, V., Mathew, P.A., and Barclay, A.N. (1998). 2B4, the Natural Killer and T cell immunoglobulin Superfamily Surface Protein , Is a Ligand for CD48. J.exp.Med *188*, 2083–2090.

Bushell, K.M., Söllner, C., Schuster-boeckler, B., Bateman, A., and Wright, G.J. (2008). Large-scale screening for novel low-affinity extracellular protein interactions. Genome Res. *18*, 622–630.

Castets, M., Broutier, L., Molin, Y., Brevet, M., Chazot, G., Gadot, N., Paquet, A., Mazelin, L., Jarrosson-Wuilleme, L., Scoazec, J.-Y., et al. (2012). DCC constrains tumour progression via its dependence receptor activity. Nature *482*, 534–537.

Chen, Q., Sun, X., Zhou, X., Liu, J., Wu, J., Zhang, Y., and Wang, J. (2013). N-terminal horseshoe conformation of DCC is functionally required for axon guidance and might be shared by other neural receptors. J. Cell Sci. *126*, 186–195.

Cheng, H., and Flanagan, J.G. (1994). Identification and Cloning of ELF-I , a Developmentally Expressed Ligand for the Mek4 and Sek Receptor Tyrosine Kinases. Cell *79*, 157–168.

Chitnis, A.B., Arbor, A., and Kuwadai, J.Y. (1990). Axonogenesis in the Brain of Zebrafish Embryos. J. Neurosci. *10*, 1892–1905.

Cirulli, V., and Yebra, M. (2007). Netrins: beyond the brain. Nat. Rev. Mol. Cell Biol. *8*, 296–306.

Clay, H., and Ramakrishnan, L. (2005). Multiplex Fluorescent In Situ Hybridization in Zebrafish Embryos Using Tyramide Signal Amplification. Zebrafish.

De Robertis, E.M. (2006). Spemann's organizer and self-regulation in amphibian embryos. Nat Rev Mol Cell Biol. *7*, 296–302.

Deiner, M.S., Kennedy, T.E., Fazeli, A., Serafini, T., Tessier-Lavigne, M., and Sretavan, D.W. (1997). Netrin-1 and DCC mediate axon guidance locally at the optic disc: loss of function leads to optic nerve hypoplasia. Neuron *19*, 575–589.

Delloye-Bourgeois, C., Brambilla, E., Coissieux, M.-M., Guenebeaud, C., Pedeux, R., Firlej, V., Cabon, F., Brambilla, C., Mehlen, P., and Bernet, A. (2009). Interference with netrin-1 and tumor cell death in non-small cell lung cancer. J. Natl. Cancer Inst. *101*, 237–247.

Dickson, B.J., and Zou, Y. (2010). Navigating intermediate targets: the nervous system midline. Cold Spring Harb. Perspect. Biol. *2*, a002055.

Diehn, M., Bhattacharya, R., Botstein, D., and Brown, P.O. (2006). Genome-scale identification of membrane-associated human mRNAs. PLoS Genet. *2*, e11.

Durocher, Y., Perret, S., and Kamen, A. (2002). High-level and high-throughput recombinant protein production by transient transfection of suspension-growing human 293-EBNA1 cells. Nucleic Acids Res. *30*, E9.

Filosa, S., Rivera-pérez, J.A., Gómez, A.P., Gansmuller, A., Sasaki, H., Behringer, R.R., and Ang, S. (1997). goosecoid and HNF-3β genetically interact to regulate neural tube patterning during mouse embryogenesis. Development *124*, 2843–2854.

Finci, L.I., Krüger, N., Sun, X., Zhang, J., Chegkazi, M., Wu, Y., Schenk, G., Mertens, H.D.T., Svergun, D.I., Zhang, Y., et al. (2014). The crystal structure of The crystal structure of netrin-1 in complex with DCC reveals the bifunctionality of netrin-1 as a guidance cue. Neuron *83*, 839–849.

Fitamant, J., Guenebeaud, C., Coissieux, M., Guix, C., Treilleux, I., Scoazec, J., Bachelot, T., Bernard, A., and Mehlen, P. (2008). Netrin-1 expression confers a selective advantage for tumor cell survival in metastatic breast cancer. Proc. Natl. Acad. Sci. U. S. A. *105*, 4850–4855.

Forcet, C., Ye, X., Granger, L., Corset, V., Shin, H., Bredesen, D.E., and Mehlen, P. (2001). The dependence receptor DCC (deleted in colorectal cancer) defines an alternative mechanism for caspase activation. Proc. Natl. Acad. Sci. U. S. A. *98*, 3416–3421.

Gao, X., Metzger, U., Panza, P., Mahalwar P., Alsheimer, S., Geiger H., Maischein H-M, Levesque M., Templin M., Söllner, C. (2015). A Floor Plate Extracellular Protein-Protein Interaction Screen Identifies Draxin as a Secreted Netrin-1 Antagonist, Cell Reports *12*, 694-708.

Geisbrecht, B. V, Dowd, K. a, Barfield, R.W., Longo, P. a, and Leahy, D.J. (2003). Netrin binds discrete subdomains of DCC and UNC5 and mediates interactions between DCC and heparin. J. Biol. Chem. *278*, 32561–32568.

Guan, K.-L., and Rao, Y. (2003). Signalling mechanisms mediating neuronal responses to guidance cues. Nat. Rev. Neurosci. *4*, 941–956.

Haddick, P.C.G., Tom, I., Luis, E., Quiñones, G., Wranik, B.J., Ramani, S.R., Stephan, J.-P., Tessier-Lavigne, M., and Gonzalez, L.C. (2014). Defining the ligand specificity of the deleted in colorectal cancer (DCC) receptor. PLoS One *9*, e84823.

Hedgecock, E.M., Culotti, J., and Hall, D.H. (1990). The unc-5, unc-6, and unc-40 Genes Guide Circumferential Migrations of Pioneer Axons and Mesodermal Cells on the Epidermis in C. elegans. Neuron *2*, 61–85.

Holzman, L.B., Marks, R.M., and Dixit, V.M. (1990). A Novel Immediate-Early Response Gene of Endothelium Is Induced by Cytokines and Encodes a Secreted Protein. Mol. Cell. Biol. *10*, 5830–5838.

Hong, K., Hinck, L., Nishiyama, M., Poo, M., Tessier-Lavigne, M., and Stein, E. (1999). A ligand-gated association between cytoplasmic domains of UNC5 and DCC family receptors converts netrin- induced growth cone attraction to repulsion.

Huber, A.B., Kolodkin, A.L., Ginty, D.D., and Cloutier, J.-F. (2003). Signaling at the growth cone: ligand-receptor complexes and the control of axon growth and guidance. Annu. Rev. Neurosci. *26*, 509–563.

Islam, S.M., Shinmyo, Y., Okafuji, T., Su, Y., Naser, I. Bin, Ahmed, G., Zhang, S., Chen, S., Ohta, K., Kiyonari, H., et al. (2009). Draxin, a repulsive guidance protein for spinal cord and forebrain commissures. Science *323*, 388–393.

Kappler, J., Franken, S., Junghans, U., Hoffmann, R., Linke, T., Müller, H.W., and Koch, K.W. (2000). Glycosaminoglycan-binding properties and secondary

structure of the C-terminus of netrin-1. Biochem. Biophys. Res. Commun. *271*, 287–291.

Kastenhuber, E., Kern, U., Bonkowsky, J.L., Chien, C.B., Driever, W., and Schweitzer, J. (2009). Netrin-DCC, Robo-Slit, and heparan sulfate proteoglycans coordinate lateral positioning of longitudinal dopaminergic diencephalospinal axons. J Neurosci 29, 8914-8926.

Keino-Masu, K., Masu, M., Hinck, L., Leonardo, E.D., Chan, S.S., Culotti, J.G., and Tessier-Lavigne, M. (1996). Deleted in Colorectal Cancer (DCC) encodes a netrin receptor. Cell *87*, 175–185.

Keleman, K., and Dickson, B.J. (2001). Short- and long-range repulsion by the Drosophila Unc5 netrin receptor. Neuron *32*, 605–617.

Kennedy, T.E., Serafini, T., de la Torre, J.R., and Tessier-Lavigne, M. (1994). Netrins are diffusible chemotropic factors for commissural axons in the embryonic spinal cord. Cell *78*, 425–435.

Kennedy, T.E., Wang, H., Marshall, W., and Tessier-Lavigne, M. (2006). Axon guidance by diffusible chemoattractants: a gradient of netrin protein in the developing spinal cord. J. Neurosci. *26*, 8866–8874.

Kerr, J.S., and Wright, G.J. (2012). Avidity-based extracellular interaction screening (AVEXIS) for the scalable detection of low-affinity extracellular receptor-ligand interactions. J. Vis. Exp. e3881.

Kettleborough, R.N.W., Busch-Nentwich, E.M., Harvey, S. a, Dooley, C.M., de Bruijn, E., van Eeden, F., Sealy, I., White, R.J., Herd, C., Nijman, I.J., et al. (2013). A systematic genome-wide analysis of zebrafish protein-coding gene function. Nature *496*, 494–497.

Kidd, T., Brose, K., Mitchell, K.J., Fetter, R.D., Tessier-lavigne, M., Goodman, C.S., and Tear, G. (1998). Roundabout Controls Axon Crossing of the CNS Midline and Defines a Novel Subfamily of Evolutionarily Conserved Guidance Receptors. Cell *92*, 205–215.

Kidd, T., Bland, K.S., and Goodman, C.S. (1999). Slit Is the Midline Repellent for the Robo Receptor in Drosophila. Cell *96*, 785–794.

Kimmel, C.B. (1993). Patterning the brain of the zebrafish embryo. Annu. Rev. Neurosci. *16*, 707–732.

Koch, M., Murrell, J.R., Hunter, D.D., Olson, P.F., Jin, W., Keene, D.R., Brunken, W.J., and Burgeson, R.E. (2000). A novel member of the netrin family, beta-netrin, shares homology with the beta chain of laminin: identification, expression, and functional characterization. J. Cell Biol. *151*, 221–234.

Kolodkin, A., Matthes, D.J., O'Connor, T.P., Patel, N.H., Admon, A., Bentley, D., and Goodman, C.S. (1992). Fasciclin IV : Sequence , Expression , and Function during G rowth Cone Guidance in the G rasshopper Embryo. Neuron *9*, 831–845.

Kolodkin, A.L., Tessier-lavigne, M., Chédotal, A., Richards, L.J., Dent, E.W., Gupton, S.L., Frank, B., Adams, R.H., Eichmann, A., Engle, E.C., et al. (2011). Mechanisms and Molecules of Neuronal Wiring: A Primer. Cold Spring Harb. Perspect. Biol. *3*.

Kolodziej, P. a, Timpe, L.C., Mitchell, K.J., Fried, S.R., Goodman, C.S., Jan, L.Y., and Jan, Y.N. (1996). *frazzled* encodes a Drosophila member of the DCC immunoglobulin subfamily and is required for CNS and motor axon guidance. Cell *87*, 197–204.

Kruger, R.P., Lee, J., Li, W., and Guan, K. (2004). Mapping Netrin Receptor Binding Reveals Domains of Unc5 Regulating Its Tyrosine Phosphorylation. J. Neurosci. *24*, 10826–10834.

Kwan, K.M., Fujimoto, E., Grabher, C., Mangum, B.D., Hardy, M.E., Campbell, D.S., Parant, J.M., Yost, H.J., Kanki, J.P., and Chien, C.-B. (2007). The Tol2kit: a multisite gateway-based construction kit for Tol2 transposon transgenesis constructs. Dev. Dyn. *236*, 3088–3099.

Lakhina, V., Marcaccio, C.L., Shao, X., Lush, M.E., Jain, R. a, Fujimoto, E., Bonkowsky, J.L., Granato, M., and Raper, J. a (2012). Netrin/DCC Signaling Guides Olfactory Sensory Axons to Their Correct Location in the Olfactory Bulb. J. Neurosci. *32*, 4440–4456.

Lauderdale, J.D., Davis, N.M., and Kuwada, J.Y. (1997). Axon Tracts Correlate with Netrin-1a Expression. Mol. Cell. Neurosci. *9*, 293–313.

Lauderdale, J.D., Pasquali, S.K., Fazel, R., Haffter, P., and Kuwada, J.Y. (1998). Regulation of netrin-1a Expression by Hedgehog Proteins. Mol. Cell. Neurosci. *11*, 194–205.

Leclère, L., and Rentzsch, F. (2012). Repeated evolution of identical domain architecture in metazoan netrin domain-containing proteins. Genome Biol. Evol. *4*, 883–899.

Lee, H.X., Ambrosio, A.L., Reversade, B., and De Robertis, E.M. (2006). Embryonic Dorsal-Ventral Signaling: Secreted Frizzled-Related Proteins as Inhibitors of Tolloid Proteinases. Cell *124*, 147–159.

Leonardo, E.D., Hinck, L., Masu, M., Keino-Masu, K., Ackerman, S.L., and Tessier-Lavigne, M. (1997). Vertebrate homologues of c.elegans UNC-5 are candidate netrin receptors.

Li, H., Chen, J., Wu, W., Fagaly, T., Zhou, L., Yuan, W., Dupuis, S., Jiang, Z., Nash, W., Gick, C., et al. (1999). Vertebrate Slit, a Secreted Ligand for the Transmembrane Protein Roundabout, Is a Repellent for Olfactory Bulb Axons. Cell *96*, 807–818.

Lin, J.C., Ho, W.-H., Gurney, A., and Rosenthal, A. (2003). The netrin-G1 ligand NGL-1 promotes the outgrowth of thalamocortical axons. Nat. Neurosci. *6*, 1270–1276.

Liu, J., and Rost, B. (2001). Comparing function and structure between entire proteomes. Protein Sci. *10*, 1970–1979.

Llambi, F., Causeret, F., Bloch-gallego, E., and Mehlen, P. (2001). Netrin-1 acts as a survival factor via its receptors UNC5H and DCC. EMBO J. *20*, 2715–2722.

Lumsden, A.G.S., and Davies, A.M. (1983). Earlist sensory nerve fibres are guided to peripheral targets by attractants other than nerve growth factor. 786–788.

Luo, Y., Raible, D., and Raper, J.A. (1993). Collapsin : A Protein in Brain That Induces the Collapse and Paralysis of Neuronal Growth Cones. Cell *75*, 217–227.

Mann, H.H., Ozbek, S., Engel, J., Paulsson, M., and Wagener, R. (2004). Interactions between the cartilage oligomeric matrix protein and matrilins. Implications for

matrix assembly and the pathogenesis of chondrodysplasias. J. Biol. Chem. *279*, 25294–25298.

Matsumoto, Y., Irie, F., Inatani, M., Tessier-Lavigne, M., and Yamaguchi, Y. (2007). Netrin-1/DCC signaling in commissural axon guidance requires cell-autonomous expression of heparan sulfate. J. Neurosci. *27*, 4342–4350.

Meeker, N.D., Hutchinson, S.A., Ho, L., and Trede, N.S. (2007). Benchmarks Method for isolation of PCR-ready genomic DNA from zebrafish tissues. *43*, 4–6.

Mehlen, P., Rabizadeh, S., Snipas, S.J., Assa-munt, N., Salvesen, G.S., and Bredesen, D.E. (1998). The DCC gene product induces apoptosis by a mechanism requiring receptor proteolysis. Nature *395*, 801–804.

Mehlen, P., Delloye-Bourgeois, C., and Chédotal, A. (2011). Novel roles for Slits and netrins: axon guidance cues as anticancer targets? Nat. Rev. Cancer *11*, 188–197.

Miner, J.H., and Yurchenco, P.D. (2004). Laminin functions in tissue morphogenesis. Annu. Rev. Cell Dev. Biol. *20*, 255–284.

Miyake, A., Takahashi, Y., Miwa, H., Shimada, A., Konishi, M., and Itoh, N. (2009). Neucrin is a novel neural-specific secreted antagonist to canonical Wnt signaling. Biochem. Biophys. Res. Commun. *390*, 1051–1055.

Miyake, A., Nihno, S., Murakoshi, Y., Satsuka, A., Nakayama, Y., and Itoh, N. (2012). Neucrin, a novel secreted antagonist of canonical Wnt signaling, plays roles in developing neural tissues in zebrafish. Mech. Dev. *128*, 577–590.

Moore, S.W., and Kennedy, T.E. (2006). Protein kinase A regulates the sensitivity of spinal commissural axon turning to netrin-1 but does not switch between chemoattraction and chemorepulsion. J. Neurosci. *26*, 2419–2423.

Moore, S.W., Tessier-Lavigne, M., and Kennedy, T.E. (2007). Netrins and their receptors. Adv. Exp. Med. Biol. *621*, 17–31.

Nüsslein-Volhard, C. and Dahm, R., 2002. Zebrafish - A Practical Approach. Oxford University Press.

Özkan, E., Carrillo, R. a, Eastman, C.L., Weiszmann, R., Waghray, D., Johnson, K.G., Zinn, K., Celniker, S.E., and Garcia, K.C. (2013). An extracellular interactome of

immunoglobulin and LRR proteins reveals receptor-ligand networks. Cell *154*, 228–239.

Park, K.W., Urness, L.D., Senchuk, M.M., Colvin, C.J., Joshua, D., Chien, C., and Li, D.Y. (2005). Identification of New Netrin Family Members in Zebrafish: Developmental Expression of netrin2 and netrin4. Dev. Dyn. *234*, 726–731.

Pasterkamp, R.J., and Kolodkin, A.L. (2003). Semaphorin junction: making tracks toward neural connectivity. Curr. Opin. Neurobiol. *13*, 79–89.

Placzek, M., and Briscoe, J. (2005). The floor plate: multiple cells, multiple signals. Nat. Rev. Neurosci. *6*, 230–240.

Rajagopalan, S., Deitinghoff, L., Davis, D., Conrad, S., Skutella, T., Chedotal, A., Mueller, B.K., and Strittmatter, S.M. (2004). Neogenin mediates the action of repulsive guidance molecule. *6*, 756–763.

Ramani, S.R., Tom, I., Lewin-Koh, N., Wranik, B., Depalatis, L., Zhang, J., Eaton, D., and Gonzalez, L.C. (2012). A secreted protein microarray platform for extracellular protein interaction discovery. Anal. Biochem. *420*, 127–138.

Raper, J., and Mason, C. (2010). Cellular Strategies of Axonal Pathfinding. Cold Spring Harb. Perspect. Biol. 1–21.

Reversade, B., and De Robertis, E.M. (2005). Regulation of ADMP and BMP2/4/7 at Opposite Embryonic Poles Generates a Self-Regulating Morphogenetic Field. Cell *123*, 1147–1160.

Ries, J., Yu, S.R., Burkhardt, M., Brand, M., and Schwille, P. (2009). Modular scanning FCS quantifies receptor-ligand interactions in living multicellular organisms. Nat. Methods *6*, 643–645.

Ross, L.S., Parrett, T., and Easter, S.S. (1992). Axonogenesis and Morphogenesis in the Embryonic Zebrafish Brain. J. Neurosci. *12*, 467–482.

Rothberg, J.M., Hartley, D.A., Walther, Z., and Artavanis-tsakonas, S. (1988). Slit: An EGF-Homologous Locus of D . melanogaster Involved in the Development of the Embryonic Central Nervous System. Cell *55*, 1047–1059.

Schatz, P.J. (1993). Use of peptide libraries to map the substrate specificity of a peptide-modifying enzyme. Nature.

Schneiders, F.I., Maertens, B., Böse, K., Li, Y., Brunken, W.J., Paulsson, M., Smyth, N., and Koch, M. (2007). Binding of netrin-4 to laminin short arms regulates basement membrane assembly. J. Biol. Chem. *282*, 23750–23758.

Serafini, T., Kennedy, T.E., Galko, M.J., Mirzayan, C., Jessell, T.M., and Tessier-Lavigne, M. (1994). The netrins define a family of axon outgrowth-promoting proteins homologous to C. elegans UNC-6. Cell *78*, 409–424.

Serafini, T., Colamarino, S. a, Leonardo, E.D., Wang, H., Beddington, R., Skarnes, W.C., and Tessier-Lavigne, M. (1996). Netrin-1 is required for commissural axon guidance in the developing vertebrate nervous system. Cell *87*, 1001–1014.

Shirozu, M., Tada, H., Tashiro, K., Nakamura, T., Lopez, N.D., Nazarea, M., Hamada, T., Sato, T., Nakano, T., and Honjo, T. (1996). Characterization of novel secreted and membrane proteins isolated by the signal sequence trap method. Genomics *37*, 273–280.

Söllner, C., and Wright, G.J. (2009). A cell surface interaction network of neural leucine-rich repeat receptors. Genome Biol. *10*, R99.

Sotelo, C. (2004). The Neurotropic Theory of Santiago Ramón y Cajal. IBRO, Hist. Neurosci.

Sperry, R.W. (1963). Chemoaffinity in the orderly growth of nerve. Proc. Natl. Acad. Sci. U. S. A. 703–710.

Stein, E., and Tessier-Lavigne, M. (2001). Hierarchical organization of guidance receptors: silencing of netrin attraction by slit through a Robo/DCC receptor complex. Science *291*, 1928–1938.

Strähle, U., Fischer, N., and Blader, P. (1997). Expression and regulation of a netrin homologue in the zebrafish embryo. Mech. Dev. *62*, 147–160.

Suárez, R., Gobius, I., and Richards, L.J. (2014). Evolution and development of interhemispheric connections in the vertebrate forebrain. Front. Hum. Neurosci. *8*.

Suli, A., Mortimer, N., Shepherd, I., and Chien, C.B. (2006). Netrin/DCC signaling controls contralateral dendrites of octavolateralis efferent neurons. J Neurosci *26*, 13328-13337.

Sun, K., Correia, J.P., and Kennedy, T.E. (2011). Netrins: versatile extracellular cues with diverse functions. Development *138*, 2153–2169.

Takahashi, T., Fournier, A., Nakamura, F., Wang, L., Murakami, Y., Kalb, R.G., Fujisawa, H., Strittmatter, S.M., and Haven, N. (1999). Plexin-Neuropilin-1 Complexes Form Functional Semaphorin-3A Receptors. Cell *99*, 59–69.

Tamagnone, L., Artigiani, S., Chen, H., He, Z., Ming, G., Song, H., Chedotal, A., Winberg, M.L., Goodman, C.S., Poo, M., et al. (1999). Plexins Are a Large Family of Receptors for Transmembrane , Secreted , and GPI-Anchored Semaphorins in Vertebrates. Cell *99*, 71–80.

Tessier-lavigne, M., and Goodman, C.S. (1996). The Molecular Biology of Axon Guidance. Science (80). *274*, 1123–1132.

Tessier-Lavigne, M., Placzek, M., Lumsden, A.G., Dodd, J., and Jessell, T.M. (1988). Chemotropic guidance of developing axons in the mammalian central nervous system. Nature *336*, 775–778.

Tomschy, a, Fauser, C., Landwehr, R., and Engel, J. (1996). Homophilic adhesion of E-cadherin occurs by a co-operative two-step interaction of N-terminal domains. EMBO J. *15*, 3507–3514.

Wang, H., Copeland, N.G., Gilbert, D.J., Jenkins, N. a, and Tessier-Lavigne, M. (1999). Netrin-3, a mouse homolog of human NTN2L, is highly expressed in sensory ganglia and shows differential binding to netrin receptors. J. Neurosci. *19*, 4938–4947.

Wang, K.H., Brose, K., Arnott, D., Kidd, T., Goodman, C.S., Henzel, W., Tessier-lavigne, M., and Francisco, S.S. (1999). Biochemical Purification of a Mammalian Slit Protein as a Positive Regulator of Sensory Axon Elongation and Branching. Cell *96*, 771–784.

Wojtowicz, W.M., Wu, W., Andre, I., Qian, B., Baker, D., and Zipursky, S.L. (2007). A vast repertoire of Dscam binding specificities arises from modular interactions of variable Ig domains. Cell *130*, 1134–1145.

Xu, K., Wu, Z., Renier, N., and Antipenko, A. (2014). Structures of netrin-1 bound to two receptors provide insight into its axon guidance mechanism. Science. *344*, 1275–1279.

Yebra, M., Montgomery, A.M.P., Diaferia, G.R., Kaido, T., Silletti, S., Perez, B., Just, M.L., Hildbrand, S., Hurford, R., Florkiewicz, E., et al. (2003). Recognition of the Neural Chemoattractant Netrin-1 by Integrins a6b4 and a3b1 Regulates Epithelial Cell Adhesion and Migration. Development *5*, 695–707.

Yu, S.R., Burkhardt, M., Nowak, M., Ries, J., Petrásek, Z., Scholpp, S., Schwille, P., and Brand, M. (2009). Fgf8 morphogen gradient forms by a source-sink mechanism with freely diffusing molecules. Nature *461*, 533–536.

Contributions

The work described in this dissertation was performed at the Max Planck Institute for Developmental Biology in Tübingen in the Department of Prof. Dr. Christiane Nüsslein-Volhard under the supervision of Dr. Christian Söllner.

Dr. Christian Söllner initiated the project, designed and performed the initial screen, which discovered the interaction between zebrafish Draxin and Netrin. He cloned the human genes encoding *DRAXIN*, *NETRIN* and Netrin receptors and initiated the Fc fusion protein *in situ* binding experiments. DNA maxi preparations and expression of recombinant proteins in HEK cells was majorly done with the helped of Hans-Martin Maischein. Hans-Martin and Paolo Panza helped with the optimization of experimental conditions for the Fc *in situ* detection assay as well as in setting up the gateway cloning platform. Paolo also helped with image acquisition. Horst Geiger helped with genotyping and fish line maintenance. The SPR experiments were done by Dr. Markus Templin and Dr. Ute Metzger at NMI (Naturwissenschaftliches und Medizinisches Institute an der Unviversität Tübingen) in Reutlingen.

Xuefan Gao designed and performed the experiments and wrote this dissertation.

Curriculum Vitae

General Information

Name: Xuefan Gao

Address: Max Planck Institute for Developmental Biology
                 Spemannstraße 35, 72076 Tübingen, Germany.

Date of birth: 19. 01.1983

Place of birth: Beijing, China

Education

2011-2015   Ph.D dissertation in Department of genetics, Max Planck Institute for Developmental Biology, and University of Tübingen, Tübingen, Germany
             Supervised by Dr. Christian Söllner, Prof. Dr. Christiane Nüsslein-Volhard and Prof. Dr. Alfred Nordheim

2001-2005   B.Sc. Degree, Biological Science, China Agricultural University, Beijing, China

1995-2001   Beijing 101 High school, Beijing, China

Working experience

2006-2010   Research Assistant, Laboratory of Yi Rao
             (Cellular mechanisms underlying social behaviors and social cognition), National Institute of Biological Sciences, Beijing, and Peking University, Beijing, China

Honors and Awards

2011-2012   Doctoral scholarship in Max Planck Society

2002-2004   Academic Excellent Scholarship, China Agricultural University

2000   First class Award in China High School Biology Olympiad (CHSBO)

Conference (selective)

2008 Gordon Research Conference: Molecular and Cellular Neurobiology,
     Hong Kong, China

2009 HHMI Janelia Farm Conference: Neural Circuits Controlling Sexual
     Behavior, VA, USA

2013 EMBO practical course, Developmental neurobiology: from worms to
     mammals, London, UK; poster presentation.

2014 EMBO workshop, Decoding neural circuits, Istanbul, TR; poster
     presentation.

2015 GfE and SFDB: Joint meeting of the German and French societies of
     developmental biologists. Nuremberg, Germany; poster presentations;
     travel award.

Publication

Christian Söllner, **Xuefan Gao** and Christiane Nüsslein-Volhard. "Interaction of Draxin and γ-Netrins", 2014, Patent application Number: 57261P EP, 57261P US (PATENT)

Xuefan Gao, Ute Metzger, Paolo Panza, Prateek Mahalwar, Sören Alsheimer, Horst Geiger, Hans-Martin Maischein, Mitchell P. Levesque, Markus Templin and Christian Söllner (2015). "A Floor Plate Extracellular Protein-Protein Interaction Screen Identifies Draxin as a Secreted Netrin-1 Antagonist", Cell Reports, 12 (4), 694-708. DOI: http://dx.doi.org/10.1016/j.celrep.2015.06.047

Acknowledgement

I would like to express my deep thanks to Prof. Dr. Christiane Nüsslein-Volhard. Without her support, my dissertation would not be able to carry out. Thanks to her push at important time points along the journey! Besides, I enjoy the cooking traditions a lot! I would like to thank Prof. Dr. Alfred Nordheim, for helping me at the university and for evaluating this work.

I would like to express my gratefulness to my supervisor Dr. Christian Söllner. I was hooked on the interesting project he initiated, from the very beginning. My deep thanks to his day to day discussion and endlessness support on this work! I do appreciate the scientific freedom he gave to me! ☺ This shaped me as an independent researcher. Very special thanks to PD. Dr. Andrea Wizenmann. With her warm support, I was able to pass the most difficult period with hope inside my heart. Thanks to my Ph.D advisory committee member Prof. Dr. Andrei Lupas, Dr. Gáspár Jékely, Dr. Michael Hothorn and Dr. Andrea Wizenmann for given valuable inputs along the development of the work and their taken care of the finishing! I would like to also thank Dr. Heinz Schwarz and Dr. Matthias Floetenmeyer for pointed out the right direction on sailing through political clouds for finishing the scientific work.

Many thanks to people who had given great help on improving my scientific English writing skill! I would like to thank Dr. Dagmar Sigurdardottir for the initial helping, Christian, Andrea, Dr. April Dinwiddie, Dr. Stefan Uwe Irion and Paolo Panza for their time, patient and effort on editing. It's a great experience to see how the text became smooth and my sense of good writing became sharpen. I would also like to thank all the members of department III for scientific and technical support during these years.

Also, I would like to give a special thank to the ladies in the foreigners' office (Ausländerbehörde, Tübingen), Frau Aouidet and Frau Kilic, for given enough time of the residency permit enabling me to finish the dissertation with calm mind. I would also like to thank J.S. Bach and his Goldberg Variations, for great company and for helping me concentrated on inner peace and strength while practicing.